Structural mechanical analysis of injection molds

Bc. Zdeněk Václavík

Master's thesis
2021/2022

Tomas Bata University in Zlín
Faculty of Technology

Univerzita Tomáše Bati ve Zlíně
Fakulta technologická
Ústav výrobního inženýrství

Akademický rok: 2021/2022

ZADÁNÍ DIPLOMOVÉ PRÁCE

(projektu, uměleckého díla, uměleckého výkonu)

Jméno a příjmení:	**Bc. Zdeněk Václavík**
Osobní číslo:	**T20123**
Studijní program:	**N3909 Procesní inženýrství**
Studijní obor:	**Konstrukce technologických zařízení**
Forma studia:	**Prezenční**
Téma práce:	**Strukturální mechanické analýzy vstřikovacích forem**

Zásady pro vypracování

1. Vypracujte literární studii na dané téma.
2. Proveďte konstrukci zadaného plastového dílu.
3. Navrhněte 3D sestavu vstřikovací formy pro výrobu zadaného dílu.
4. Nakreslete 2D výkres sestavy a příslušných řezů.
5. Návrh ověřte pomocí analýz.

Forma zpracování diplomové práce: **tištěná/elektronická**
Jazyk zpracování: **Angličtina**

Seznam doporučené literatury:

WANG, Maw-Ling, Rong-Yeu CHANG a Chia-Hsiang HSU. *Molding simulation: theory and practice*. Cincinnati: Hanser Publications, [2018], xviii, 513 s. ISBN 978-1-56990-619-4
BEAUMONT, John P. *Runner and gating design handbook: tools for successful injection molding*. 2nd ed. Munich: Hanser Publishers, c2007, xvi, 308 s. ISBN 978-1-56990-421-3
OSSWALD, Tim A., Lih-Sheng TURNG a Paul J. GRAMANN. *Injection molding handbook*. 2nd ed. Munich: Carl Hanser Publishers, c2008, xvii, 764 s. ISBN 978-1-56990-420-6
SCHILLER, Gary F. *A practical approach to scientific molding*. Munich: Hanser Publishers, [2018], xiv, 176 s. ISBN 9781569906866

Vedoucí diplomové práce: **prof. Ing. Michal Staněk, Ph.D.**
Ústav výrobního inženýrství

Datum zadání diplomové práce: **3. ledna 2022**
Termín odevzdání diplomové práce: **13. května 2022**

L.S.

prof. Ing. Roman Čermák, Ph.D. v.r.
děkan

prof. Ing. Berenika Hausnerová, Ph.D. v.r.
ředitel ústavu

Ve Zlíně dne 18. února 2022

PROHLÁŠENÍ AUTORA
DIPLOMOVÉ PRÁCE

Beru na vědomí, že:

- diplomová práce bude uložena v elektronické podobě v univerzitním informačním systému a dostupná k nahlédnutí;
- na moji diplomovou práci se plně vztahuje zákon č. 121/2000 Sb. o právu autorském, o právech souvisejících s právem autorským a o změně některých zákonů (autorský zákon) ve znění pozdějších právních předpisů, zejm. § 35 odst. 3;
- podle § 60 odst. 1 autorského zákona má Univerzita Tomáše Bati ve Zlíně právo na uzavření licenční smlouvy o užití školního díla v rozsahu § 12 odst. 4 autorského zákona;
- podle § 60 odst. 2 a 3 autorského zákona mohu užít své dílo – diplomovou práci nebo poskytnout licenci k jejímu využití jen s předchozím písemným souhlasem Univerzity Tomáše Bati ve Zlíně, která je oprávněna v takovém případě ode mne požadovat přiměřený příspěvek na úhradu nákladů, které byly Univerzitou Tomáše Bati ve Zlíně na vytvoření díla vynaloženy (až do jejich skutečné výše);
- pokud bylo k vypracování diplomové práce využito softwaru poskytnutého Univerzitou Tomáše Bati ve Zlíně nebo jinými subjekty pouze ke studijním a výzkumným účelům (tj. k nekomerčnímu využití), nelze výsledky diplomové práce využít ke komerčním účelům;
- pokud je výstupem diplomové práce jakýkoliv softwarový produkt, považují se za součást práce rovněž i zdrojové kódy, popř. soubory, ze kterých se projekt skládá. Neodevzdání této součásti může být důvodem k neobhájení práce.

Prohlašuji,

- že jsem diplomové práci pracoval samostatně a použitou literaturu jsem citoval. V případě publikace výsledků budu uveden jako spoluautor.
- že odevzdaná verze diplomové práce a verze elektronická nahraná do IS/STAG jsou obsahově totožné.

Ve Zlíně dne:

Jméno a příjmení studenta:

.....
podpis studenta

ABSTRAKT

Diplomová práce se zaměřuje na systematický přístup, kdy se v počátečních fázích konstrukcí vstřikovacích forem využívají informace a doporučení ze strukturálně mechanických analýz, které jsou zaměřeny na deformaci vstřikovacích forem způsobené tlakem během vstřikovacího cyklu a zároveň pomocí simulačních výsledků ušetření následných oprav spojených s přetoky. Diplomová práce je rozdělena na teoretickou a praktickou část.

Teoretická část je zaměřena na problematiku vstřikovacích forem, která zahrnuje vysvětlení vstřikovacího procesu, druhy vstřikovacích strojů, seznámení s typy vstřikovacích forem a jejich konstrukčních řešení. Významným obsahem teoretické části je obeznámení s mechanickým chováním vstřikovacích forem, které je zaměřeno na napětí a deformaci během vstřikovacího procesu a dále informace spojené s reologickým chováním polymeru v dutině formy během plnění a využití vtokových simulací při počátečním vývoji vstřikovacích forem.

Obsahem praktické části diplomové práce je provedení konstrukce plastového dílu. Na tento plastový díl je následně navrhnuta vstřikovací forma, která obsahuje konstrukční řešení pro studený vtokový systém a násobnost formy je zvolena jako čtyřnásobná. Součásti návrhu je i implementace vysokotlakových senzorů do jednotlivých dutin vstřikovací formy a speciální konstrukční řešení vtokového systému neboli možnost libovolně měnit počet dutin, které budou naplněny v průběhu vstřikovacího cyklu.

S konstrukčním návrhem vstřikovací formy je spojena i experimentální část. Experimentální část je zaměřena na použití návrhu vstřikovací formy na dvou odlišných vstřikovacích strojích při speciálních vstřikovacích parametrech jako je uzavírací síla, velikost dotlaku, násobnost vstřikovací formy, které jsou nastaveny tak, aby v některých případech docházelo k překročení uzavírací síly. Experimentální část je provedena v jednotlivých krocích od vytápění formy při přesně stanovených podmínkách pro materiál, se kterým je experiment proveden přes plnící studii pro tři kombinace násobnosti vstřikovací formy až po měření otevírání formy v dělící rovině během vstřikovací fáze a hmotnosti výstřiků na jeden zdvih. Součásti experimentu jsou i výpočty sil a predikce v jednotlivých krocích a pokusech, ve kterých by mohlo docházet k otevírání vstřikovací formy v dělící rovině. Následné hodnoty z experimentální části jsou využity pro porovnání vstřikovacích strojů a stanovení parametrů, které mají největší vliv na otevírání vstřikovací formy (přetoky) během vstřikovací fáze.

Jedním z bodů praktické části je i využití speciálního softwaru na vtokové simulace a ověření návrhu vstřikovací formy na průběh plnění, vytvoření tlakové křivky a plnící studie, které jsou následně porovnány s experimentální částí diplomové práce.
Hlavní bod praktické části tvoří ověření vstřikovací formy pomocí strukturálních mechanických analýz. Během simulace ve speciálním softwaru je navrhnut celkový postup, který zahrnuje okrajové podmínky a výsledky mechanického chování vstřikovací formy. Mezi tyto výsledky patří například von-Misesovo napětí na jednotlivých stranách formy a velikost otevírání vstřikovací formy v dělící rovině způsobené vstřikovacím tlakem a dotlakovou fází.
Závěr tvoří porovnání experimentálních a simulačních výsledku a stanovení tuhosti vstřikovacích strojů použitých při experimentální části.

Klíčová slova: vstřikovací formy, konstrukce forem, strukturální mechanické analýzy, vtokové analýzy

ABSTRACT

The diploma thesis focuses on a systematic approach where in the initial stages of injection mold construction use information and recommendations from structural mechanical analyzes focused on mold deformation caused by pressure during the injection cycle and simulation results of subsequent repairs associated with burrs. The diploma thesis is divided into a theoretical and practical part.

The theoretical part focuses on the issue of injection molds which includes an explanation of the injection molding process, types of injection molding machines, introduction to the types of injection molds and their design solutions. An important content of the theoretical part is the introduction to the mechanical behavior of injection molds focusing on stress and strain during the injection process and information related to the rheological behavior of the polymer in the mold cavity during filling and use of inlet simulations in the initial development of injection molds.

The content of the practical part of this diploma thesis is the construction of a plastic part. An injection mold is then designed for this plastic part which contains a design solution for

a cold inlet system, and the multiplicity of the mold is chosen to be fourfold. Part of the design is the implementation of high-pressure sensors in the individual cavities of the injection mold and a special design solution of the inlet system, or the ability to arbitrarily alter the number of cavities filled during the injection cycle.

The experimental part is also connected with the construction design of the injection mold. The experimental part places the emphasis on the use of injection mold design on two different injection molding machines with special injection parameters, such as the closing force, pressure of the injection mold, which are set so that in some cases the closing force is exceeded. The experimental part is performed in individual steps from heating the mold under the precisely determined conditions for the material with which the experiment is performed through the filling study for three injection mold multiplicity combinations to measuring mold opening in the parting plane during the injection phase and weight per cycle. The experiment also includes force calculations and predictions in individual steps and experiments, in which the injection mold could be opened in the parting plane. Subsequent values from the experimental part are used to compare injection molding machines and determine the parameters with the greatest influence on the opening of the injection mold (burrs) during the injection phase.

One of the points of the practical part is the use of special software for inlet simulations and verification of the design of the injection mold for the filling process, the creation of the pressure curve and the filling study which are then compared with the experimental part of the thesis.

The main point of the practical part is the verification of the injection mold using structural mechanical analyzes. During the simulation in special software, an overall procedure is designed that includes the boundary conditions and the results of the mechanical behavior of the injection mold. These results include, for example, the von-Mises stress on the individual sides of the mold and the amount of opening of the injection mold in the parting plane caused by the injection pressure and pressure phase.

The conclusion offers a comparison of experimental and simulation results and determination of the stiffness of injection molding machines used in the experimental part.

Keywords: injection molds, molds design, structural mechanical analysis, moldflow analysis

In this thesis I would like to thank my colleague and friend Dipl. Ing. Jens Held for his help and valuable advice. At the same time, I would like to thank Hirschmann Automotive GmbH for the opportunity to collaborate on the thesis. Many thanks also to the people from the University of Tomas Bata. I am grateful to Prof. Ing. Michal Staněk Ph.D. for supervising the thesis and Mgr. Jana Orsávová Ph.D. for her help in maintaining correct English grammar.

I hereby declare that the print version of my Master's thesis and the electronic version of my thesis deposited in the IS/STAG system are identical.

CONTENTS

INTRODUCTION

In the course of constantly growing competitive pressure, maintenance-oriented injection mold design has become increasingly important as it facilitates the control of mold maintenance cost. One of its decisive advantages is the avoidance of repairs of the mold part and thus reducing the cost of additional work and subsequent replacement of the mold part and simultaneously increases the production productivity.

Nowadays, we often encounter a situation where the designer or design department do not consider the mechanical deformation that might occur during the final production and the mold is designed based only on the designers' experience.

The aim of this master thesis is to create a systematic approach to possible analyzes of mold deformation and to provide acquired information to the mold designer to avoid unacceptable deformations whilst achieving the ideal product for the customer.

To accomplish this task and consider mechanical deformation during the injection molding cycles, it is essential to perform a simulation (FEA) of a test mold and compare obtained data with the particular experimental data from the production. The most comprehensive experimental data are gained by altering the process parameters and injection molding machine.

I. THEORY

1 INTRODUCTION TO INJECTION MOLDING

Over the past century, there has been significant progress in diffusion of polymers and plastics. Plastic material is considered as a composite polymer with one or more additives. Polymers and plastics have penetrated all markets worldwide, including the automotive, construction, medical, and many further industries and their use exceeds that of steel, aluminum, copper, or zinc.

Injection molding comprises the largest part of plastics production and is perceived as the most important manufacturing process. That explains why more than one third of plastics are produced by injection molding and more than half of all plastics processed are used in the injection molds production [1].

Figure 1 – Development of mold products [2]

1.1 Injection molding process

Injection molding process as a major polymer processing technology plays one of the most significant roles in the plastics industry due to its cost-effectiveness, high production speed, and ability to produce complex parts with high precision in a single highly automated operation. It manufactures a great variety of shapes, from simple to intricate three dimensional ones, from extremely small to large ones. These products are produced in high precision in the order of milligrams. Characteristic injection molded products can be found ubiquitously, including automotive parts, consumer electronics components, toys and household items [2].

Injection molding process is a cyclic process based on the heating and melting of the polymer.

Injection molding process involves five stages:

I. Plasticization

II. Injection

III. Packing

IV. Cooling

V. Ejection

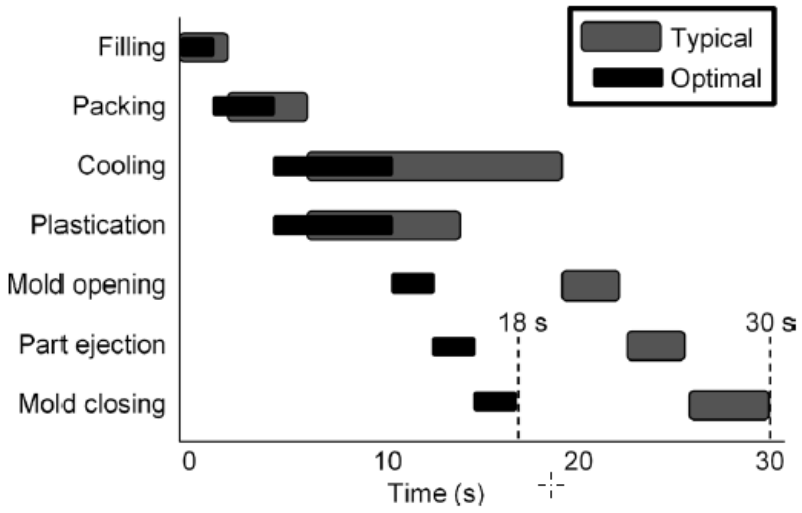

Figure 2 – Timing of injection molding process [2]

In the plasticization phase, the screw rotates and conveys plastic granules to form a shot of polymer melt. Subsequently, the molten polymer is forced out of the injection molding machine barrel through the nozzle into the mold. The polymer melt travels through the sprue bushing, sprue channel and gate location into the mold cavity, or various mold cavities. After the mold cavity is filled, the cooling phase commences and this phase lasts until the mold is cooled to the precise ejection temperature [1], [2], [3].

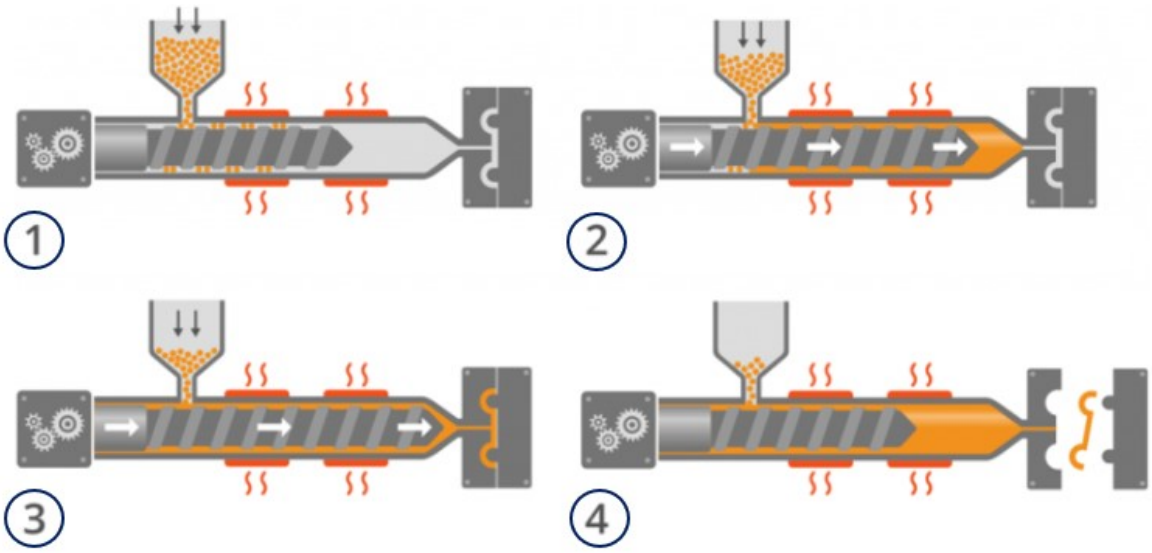

Figure 3 – Cycle of injection molding process [4]

1) Plastic granules fed via a hopper into the barrel and heated to a molten state

2) Heated plastic fills the barrel – a motorized screw pushes molten plastic to the mold

3) The screw injects molten plastic into the mold cavity via gates and hot runners under the pressure

4) The plastic product is allowed to being cooled and solidified before being ejected from the opened mold

2 INJECTION MOLDING MACHINE

The injection molding machine is an integral part of the injection molding process and one of the most important methods of plastic materials processing. It is divided into two main parts, the injection unit, the clamping unit, and also several secondary parts [2].

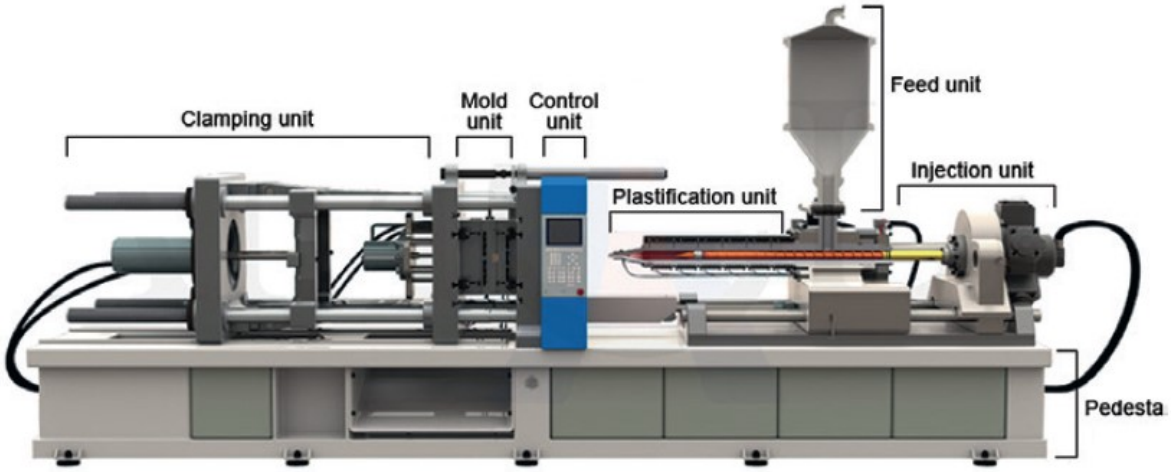

Figure 4 – Injection machine [2]

2.1 Injection unit

The injection unit is one of the main parts of the injection molding machine. It ensures the supply of plastic material (e.g. granules, as shown in Figure 5) to the plastification unit, which is a part of the injection unit. The most important elements of the injection unit on the polymer flow sequence include a hopper, screw, homogenizing elements on the screw (in some cases), non-return valve at the screw tip, nozzle, and heater bands in the last row.

Figure 5 – Plastic granules [2]

The solid plastic enters the screw channel though the inlet hopper. The high torque of the screw creates shear stress between the material and screw and between the material and

barrel. The plastic material is heated by two factors; by the heat from the heating bands and by dissipation caused by friction between the material, screw and barrel.

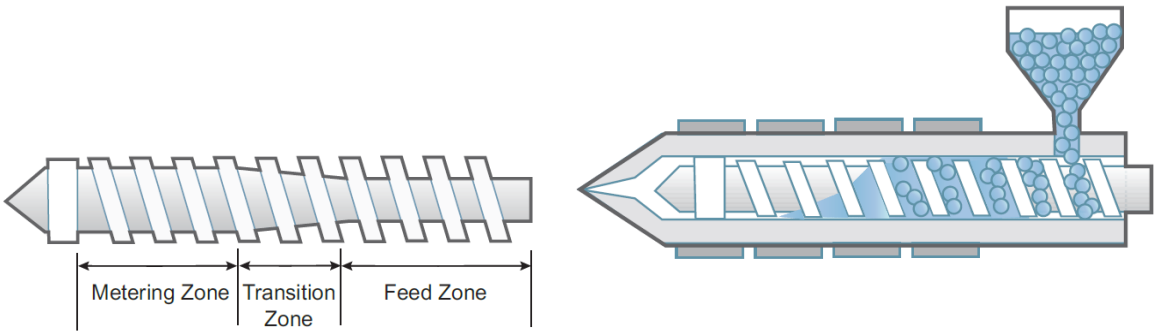

Figure 6 – Screw zones, barrel and plastification [2]

a) **Feed Zone**: The feed zone continuously doses the injection unit to ensure granulate dosage being constant in time.

b) **Transition Zone:** The transition zone presses the polymer against the heated cylinder wall (with a decreasing depth of the channel) causing melting and both solid granulate and semi-solid melt to enter the channel simultaneously.

c) **Metering Zone:** This zone ensures the transport and mixing of the melt. In some cases, the granulate is melted as well.

2.2 Clamping unit

The clamping unit is one of the most important parts of the injection molding machine. As the polymer is injected into the mold cavity under high pressure, the clamping unit must prevent the mold from opening during the injection cycle. It is also involved in the opening and closing of the mold and the ejection of the products. Various types of clamping units are available on the market, including hydraulic, mechanical, and hydraulic – mechanical types [1],[2].

2.3 Control unit

The control unit optimizes the individual steps of the injection molding machine. It coordinates the machine sequences and their initiation, as well as the timing of their progress. The temperature of the melt, barrel and mold is arranged by the control system with the implemented tempering equipment [1], [2].

Figure 7 – Control system [5]

2.4 Drive unit

Three conventional types of drives are commonly used. The most popular and traditional is the hydraulic drive. The hybrid hydraulic-electric drive and electric drive are recently invented drives [1], [2].

2.4.1 Hydraulic drive

A hydraulic drive system is particularly suitable for large, heavy parts where extensive clamping force is required. The hydraulic unit is preferred for controlling hydraulic cores and ejector systems. When compared to electric drives, the main advantages of hydraulic drives include a low purchase price and maintenance cost, high wear resistance and greater clamp force for large parts. However, its usage may be limited due to the nosier operation, higher power consumption and possible fluid leakage which is not ideal for clean spaces [6].

Figure 8 – Hydraulic injection molding machine [7]

2.4.2 Electric drive

An electric drive system first appeared on the market in 1980 and has promptly become popular. Energy efficiency is the main advantage of this drive; it requires energy only in the production mode. Since it does not use oil, as the hydraulic drive system, it does not include any filters which implies lower operating costs and significantly cleaner working area [6].

Figure 9 – Electric injection molding machine [8]

2.4.3 Hybrid hydraulic-electric drive

A hybrid drive system combines the advantages of hydraulic and electric drive systems. This type of drive has been on the market for several decades and provides excellent clamping force with energy savings and reduced noise. This method finds its application in the production of both thin-walled and thick-walled parts leading to its greater popularity and ease of use. Its main advantages include a continuous servo-pump adjustment and variety of product design. Furthermore, lower operating temperatures require less cooling and allow longer oil and machine life. These benefits enable fast investment return. As the disadvantage could be considered the fact that the supervisor must be educated and experienced for both hydraulic and electric drive systems [6].

Figure 10 – Hybrid injection molding machines [9]

3 INJECTION MOLD

The injection mold is a complex system that fulfils several requirements at any time. The main purpose of the mold is to form polymer into the final product shape. It also ensures a fast, safe production cycle including the product ejection. This process should be performed in the shortest possible time to guarantee the production efficiency.

Three main functions of the mold are to:

- contain the melt,
- transfer the heat,
- eject the molded parts.

Each of these functional steps contains sub-operations necessary for the proper functioning of the form. For example, conveying of the polymer melt requires the mold to be resistant to opening and the sprue system to provide a connection with the injection mold machine nozzle and mold cavity or cavities [3].

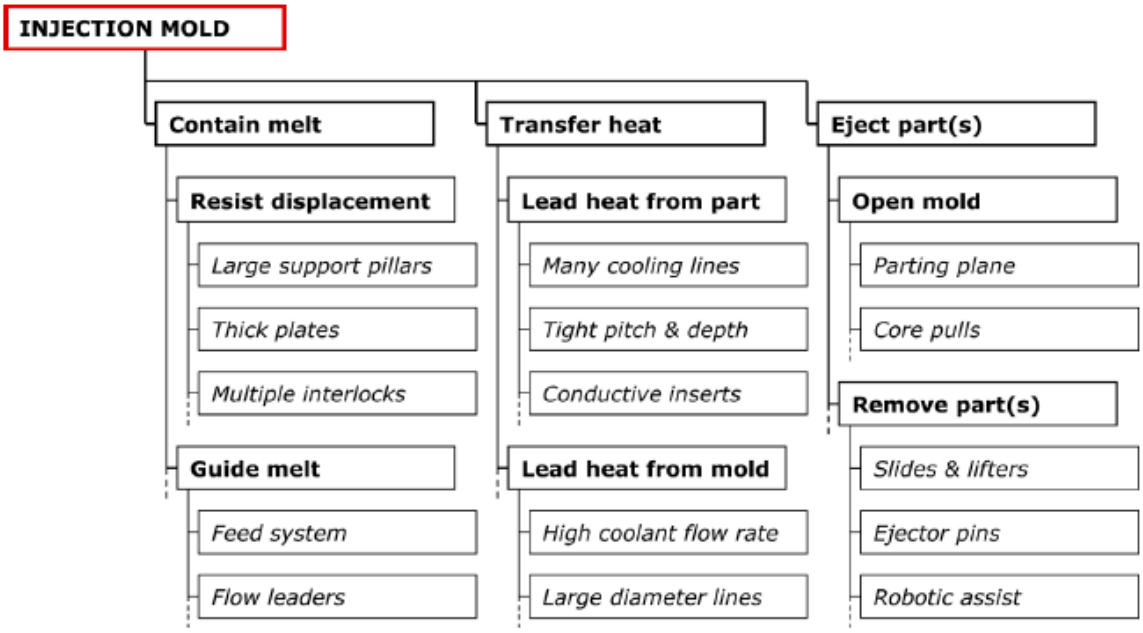

Figure 11 – Functional steps for injection molds [3]

Figure 11 shows only primary and secondary functional steps considered in the technical design of the injection mold [3].

3.1 Mold structures

The design of the injection mold must meet numerous requirements and functions in the production process. In the plastics industry, there are countless types of injection mold that meet these requirements. To introduce the topic, the “two-plate” mold will be described providing the technical terms of the mold component to facilitate understanding of the following text [3].

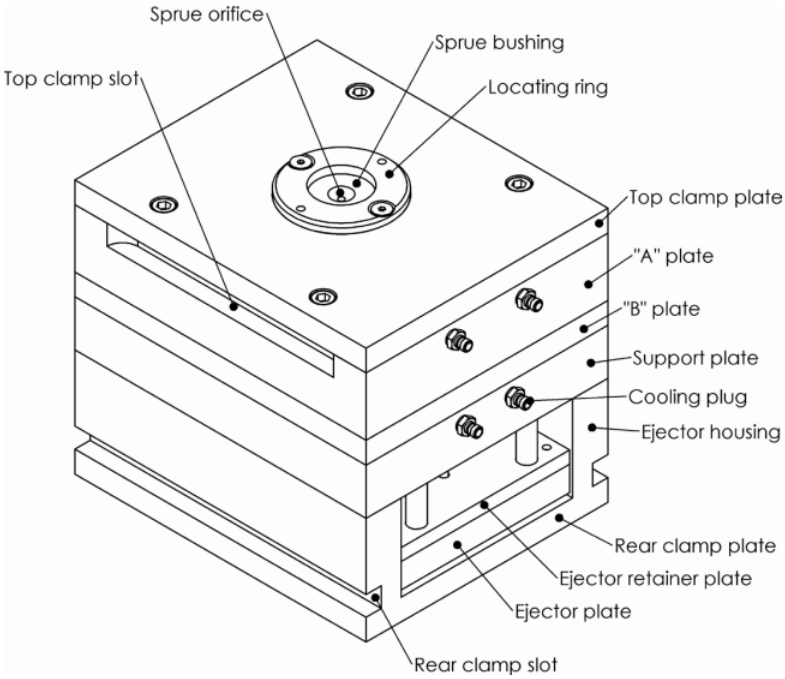

Figure 12 – Two-plate injection mold [3]

As Figure 12 depicts, injection molds are assembled from several different plates. These plates include the top clamping plate, “A” plate or cavity insert retainer plate, “B” plate or core insert retainer plate, rear clamp plate, ejector plate and ejector retainer plate. To transport melt, “A” and “B” plates are used to form a distribution channel for the polymer melt. In some cases, B plate is joined with the support plate to form one plate.

To facilitate compatibility, specific parameters of the positioning rings have been standardized. The most common variant is the positioning ring with 100 mm in diameter.

In the design and construction of the mold, any error or incorrect adjustment of “A” and “B” plates may result in the poor molding quality and faster mold wear [3], [10].

3.2 Mold layout design

Initially, a designer approves the mold type and determines dimensions and materials for the core, cavity inserts and mold base. The selection of the mold material is very important since the material influences the manufacturing time and cost of the mold and at the same time, structural and thermal performance of the injection mold. One of the main preliminary steps is the location of the parting plane, followed by determining dimensions of the core and cavity inserts. As a rule, the inserts are placed in the simplest and most compatible mold layout to save any later modifications that would be several times more expensive than the initial design [3], [11], [12].

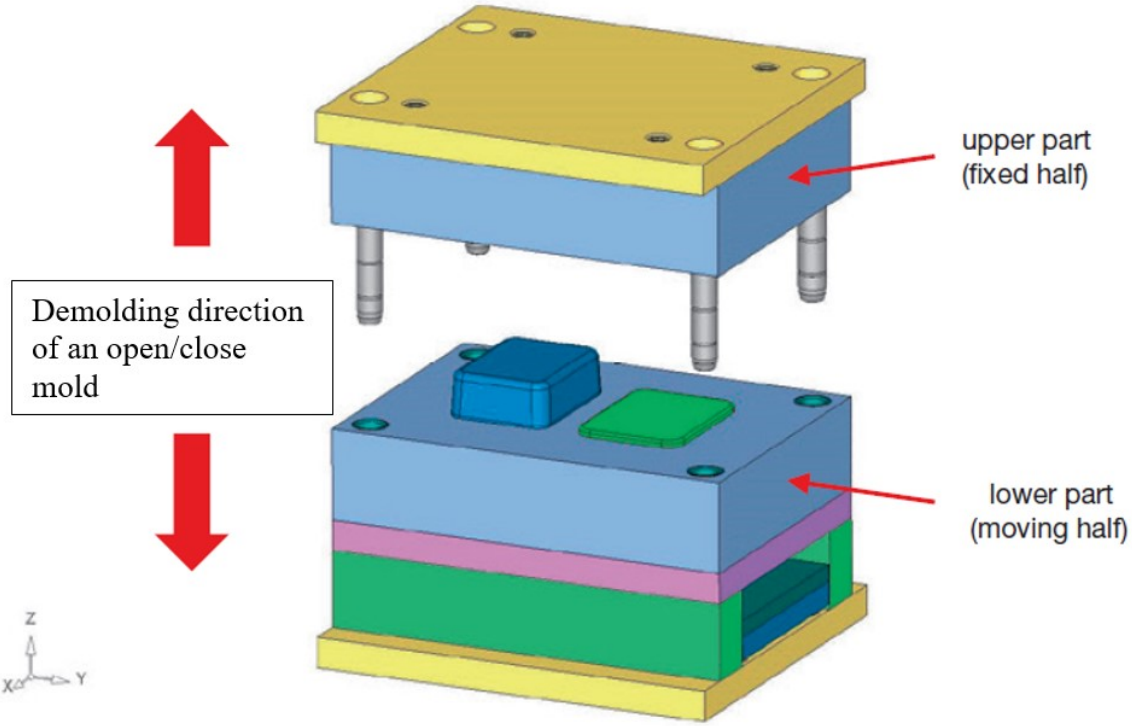

Figure 13 – Demolding direction of injection mold [11]

3.2.1 Parting plane

The parting plane is the contact surface between the fixed and moving part of the mold. Its main function is to close the mold cavity tightly to avoid any melt leakage. Most mold cores consist of two parts. Before determining the parting line and overall design of the parting plane, a designer must determine direction of the mold opening and whether the mold contains out-of-plane elements. Three-core and four-core molds are used when the part is very complex or has significant undercuts. The interface between these mold parts is called the parting plane. It can have any shape, however, to facilitate mold manufacturing, it is

more suitable to maintain it in one plane. The parting plane is always at the widest dimension of the product because it is more useful and efficient for the product ejection. If the parting line does not extend, the final product is adversely affected. Possible unsightly sharp edges or burrs result in the inadequate product quality. In the worst case, polymer may leak into the mold and damage it [12], [13].

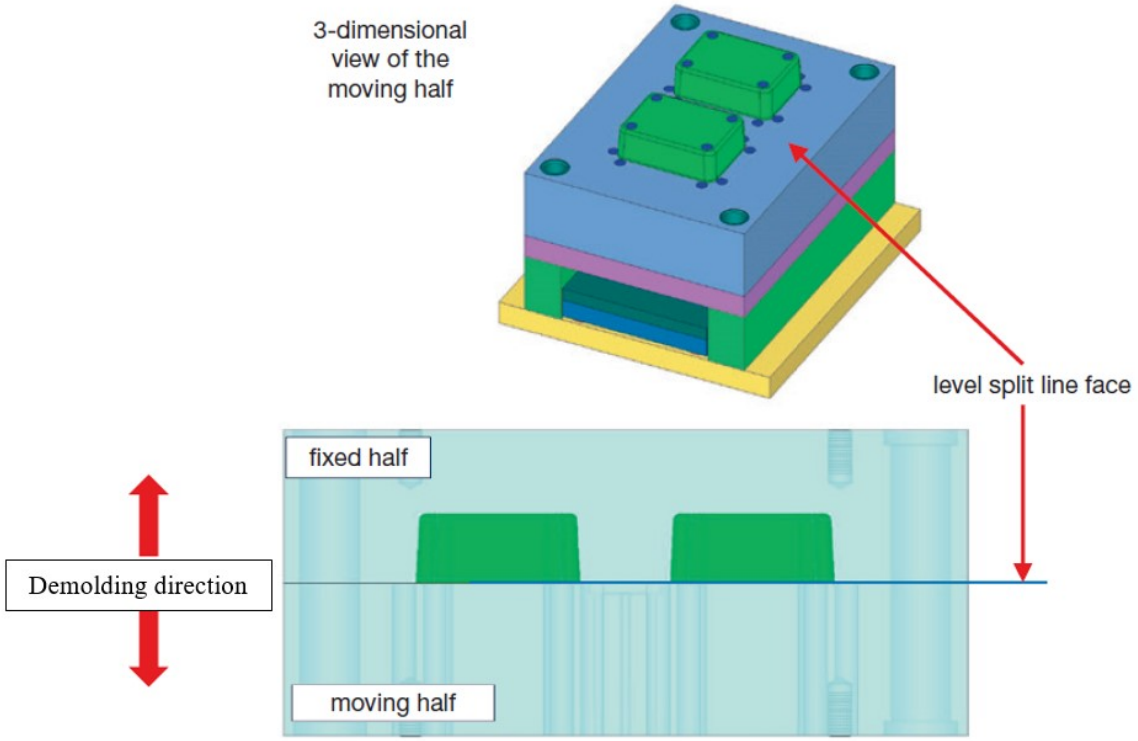

Figure 14 – Level split line face/Parting plane [9]

3.2.2 Cavity and core insert

For the design and construction of the core and cavity insert, it is necessary to define the length, width and height of the insert. The basic rules and conditions for the dimensioning of appropriately designed core inserts are as follows. The size of the core liners must withstand the forces resulting from the melt pressure acting on the cavity area. The core and cavity inserts must be of sufficient size to allow the design of the cooling system and the incorporation of the components, such as ejector pins or clamping screws. On the other hand, the cost of the product and the production of the liners grows with an increasing number of cavities and the size of the cavity and core inserts [3], [14].

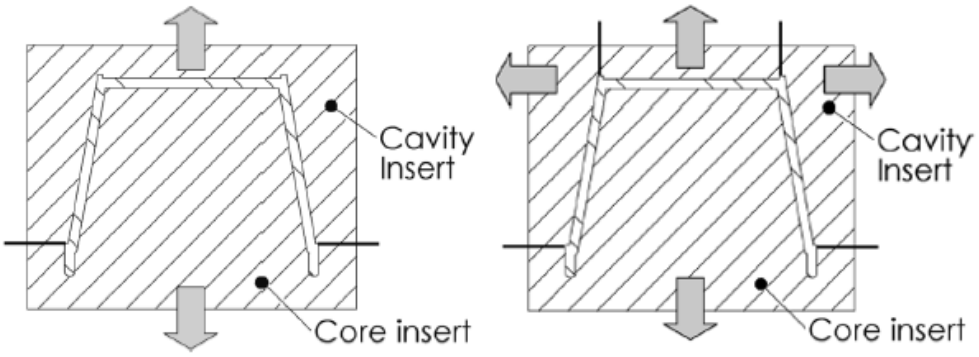

Figure 15 – Axial and radial mold opening directions [3]

Several factors must be considered when selecting the height as the core and cavity inserts should meet sufficient height above and below the product to design the cooling system properly. The diameter of the cooling system varies with the size of the mold. For large molds, the cooling diameter is usually up to 15.88 mm, while for smaller molds the diameter is selected from 4.76 mm. To ensure and prevent excessive stresses, the minimum height dimension between the bottom and top surface should be at least three times the diameter of the cooling line [3], [14].

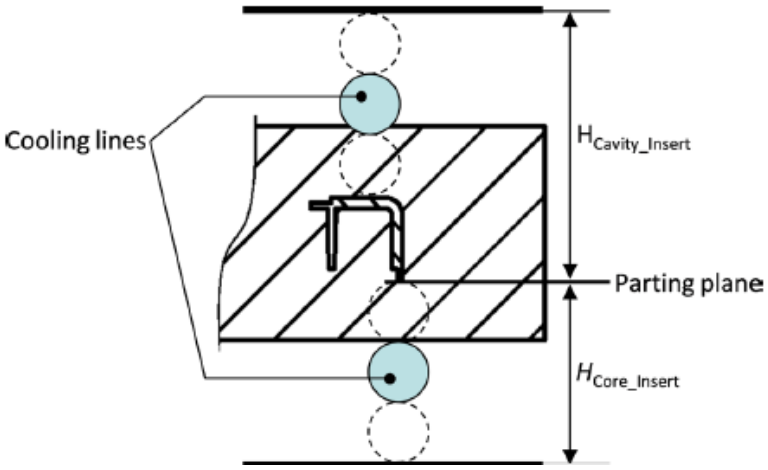

Figure 16 – Height of cores and cavities in proportion to the cooling system [3]

Secondly, the height of the core and cavity inserts should be equal to the height of the plates ("A" and "B" plates). Therefore, the cavities and cores should be designed to be levelled with the plane at the point of the parting plane or slightly elevated. When purchasing material for the cores and cavity inserts manufacture and estimating the cost, it is important to include an reserve for machining and finishing [3], [14].

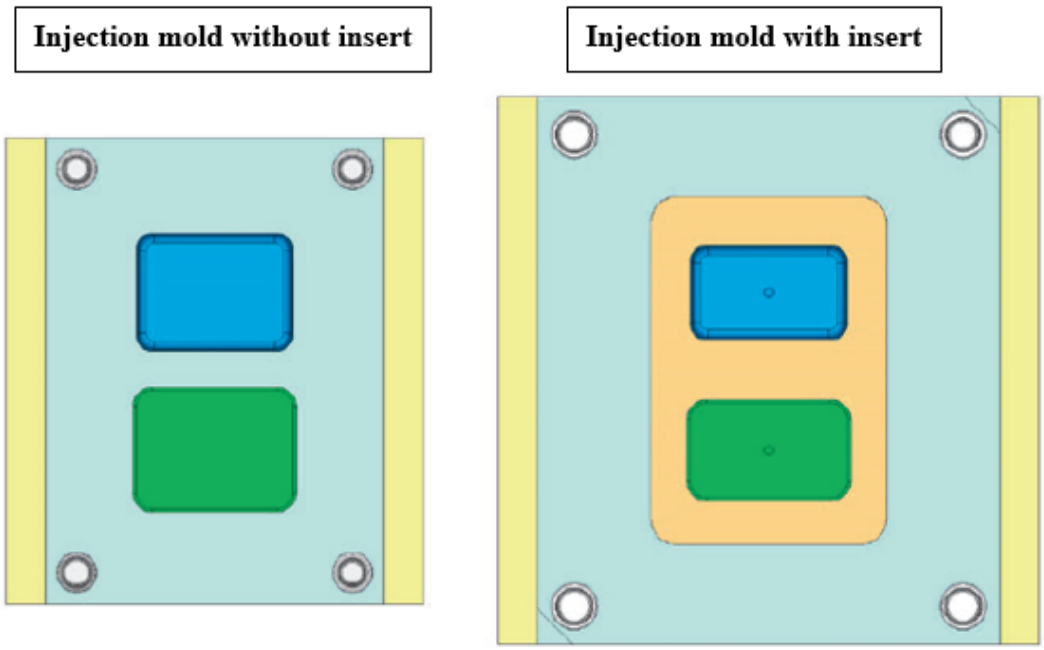

Figure 17 – Size comparison of the molds with or without inserts [11]

Mold Inserts

The mold contour for a plastic part can be placed in the injection mold in the cavity plate or insert installed in the cavity plate. The placement depends on several significant factors. [11]

1) Quantity of the parts

The first factor to consider is the quantity of produced parts and whether it is a serial form or for only a few test samples. Regarding the molds for samples, the mold cavity is integrated into the cavity plate. This step accelerates the production, provides easier design of the cooling system and eliminates the need to create pockets in cavity plates [11].

2) Hardening

Hardening is essential for serial molds ensuring the mold durability hence hardened inserts are used for the cavities of molds used in the series production. However, these inserts are more difficult to machine and finish due to the harder properties of the material [11].

3) Attaching

In most designs, a base used for the auxiliary installation in the cavity plate has a cubic shape. Hexagon socket head screws are used to connect the insert and plate according to DIN 912 (ISO 4762). The number of screws is defined by the geometry of the insert and its size. The

screw location is determined after the positioning mold cores, cooling and ejectors has been selected [11].

4) Cooling

A cooling system should be designed in each insert. However, it is not always possible to incorporate cooling channels into the design and there are several factors affecting it. The most common is a small insert that does not allow the incorporation of a cooling system or the fact it is not possible to transport cooling to the insert. In all cases, the cooling system contains the outlet and inlet of the circulation circuit. The inlet and outlet should be located on the bottom of the insert to provide upward circulation. An O-ring of rubber material is used to seal the space between the cavity plate and liner. Moreover, the connection and assembly of the components is easier and reliable when installed on the bottom surfaces of the insert and cavity plate [11].

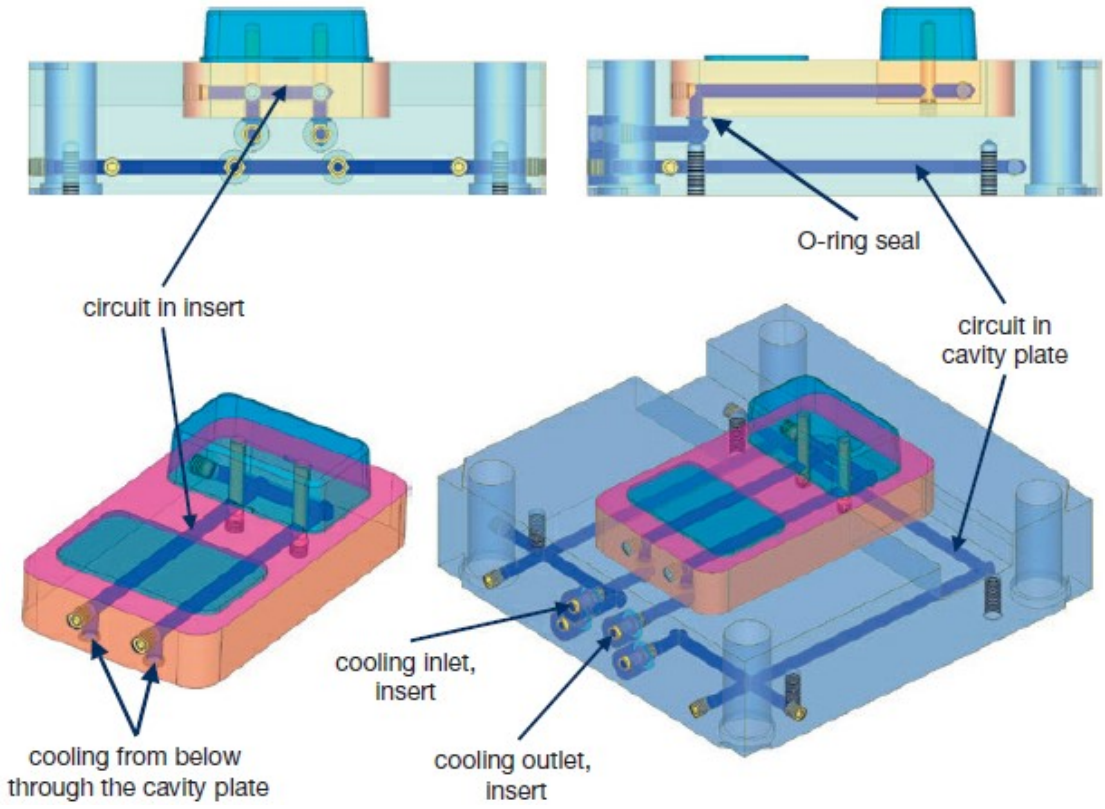

Figure 18 – Cooling system in the inserts [11]

5) Price, Maintenance, service, wear

The maintenance and service factor must be considered. If the areas of high wear and stress are included, it is recommendable to design them as separate inserts that are later easier to replace. What is more, better quality material could be employed specifically for these

individual components. Such an adjustment translates into a cheaper manufacturing process and overall time efficiency. Considering prices, injection molds with inserts are generally more expensive [11].

Mold cores

Mold cores are mostly located on a small area in the cavity. Their placement may be in both the moving and non-moving sides of the mold, however, it is difficult to determine the most common type as it reflects several factors, such as the type, appearance and technical use of the part [11].

Reasons for using mold cores

- A small protruding area in the mold insert: The insert contains the shape of a rectangle or circle, which, in order to save material and working time, is placed in the contour of the mold and acts as the core of the mold [11].

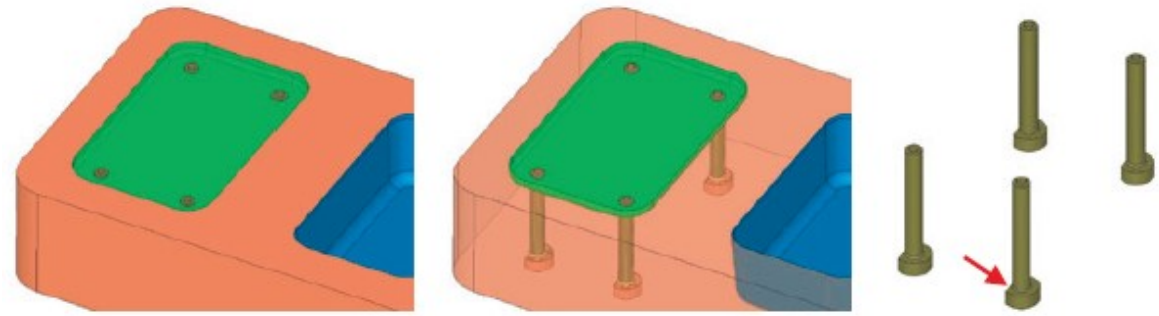

Insert with mold core for the holes	Insert with mold core for the holes	Mold cores with surface for fixing

Figure 19 – Round cores for hole pattern correction [11]

- Adjustment of the mold cavity due to changes in the product parameters: The product development process takes a long time. Therefore, it is less expensive and time consuming to modify the mold cavity or mold core than to undergo the development process from the beginning [11].

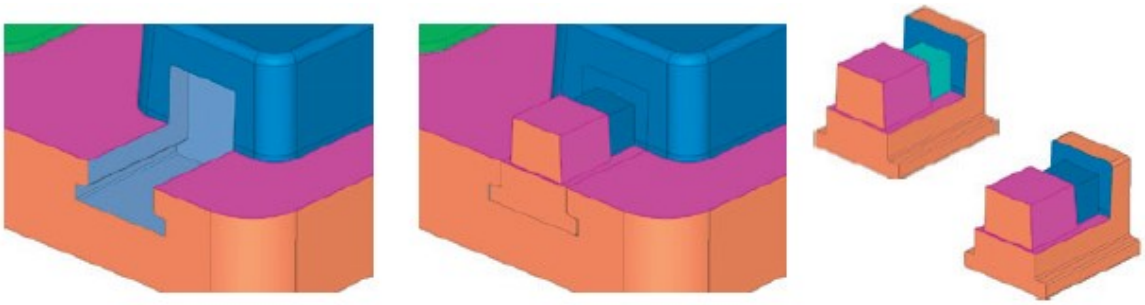

Insert without mold core | Insert with mold core | Mold cores to change

Figure 20 – Mold core for changing dimensions [11]

- As a thinner cooling core when no alternative cooling is possible: During the working cycle, the hot melt is in a direct contact with the thin domes which cannot be cooled and this generates extreme heating. Extreme heating prolongs the cooling time and overall duty cycle time. Changing the mold core material to copper alloy with better heat dissipation properties can solve this problem [11].

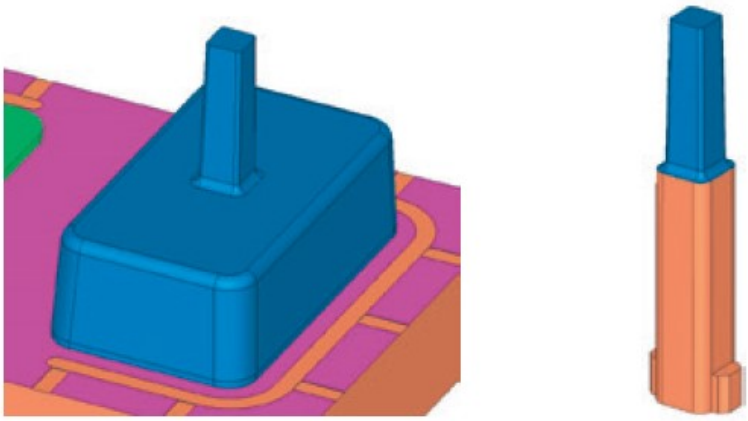

Insert with core | Mold core of copper alloy

Figure 21 – Mold core possibilities [11]

3.3 Selection of mold material

An essential part of the basic injection mold design is the selection of the material for inserts and components. Currently, we classify plastics suitable for the injection molding or further operations and also materials suitable for the individual injection molding operations. The most commonly used material with favorable properties and good availability is P20. In some specific cases, this material is replaced with cheaper materials and materials appropriate for different types of the injection molding. Such materials include, for example, high-strength clay alloys or 3D printed polymers used for inserts which of course do not achieve high durability.

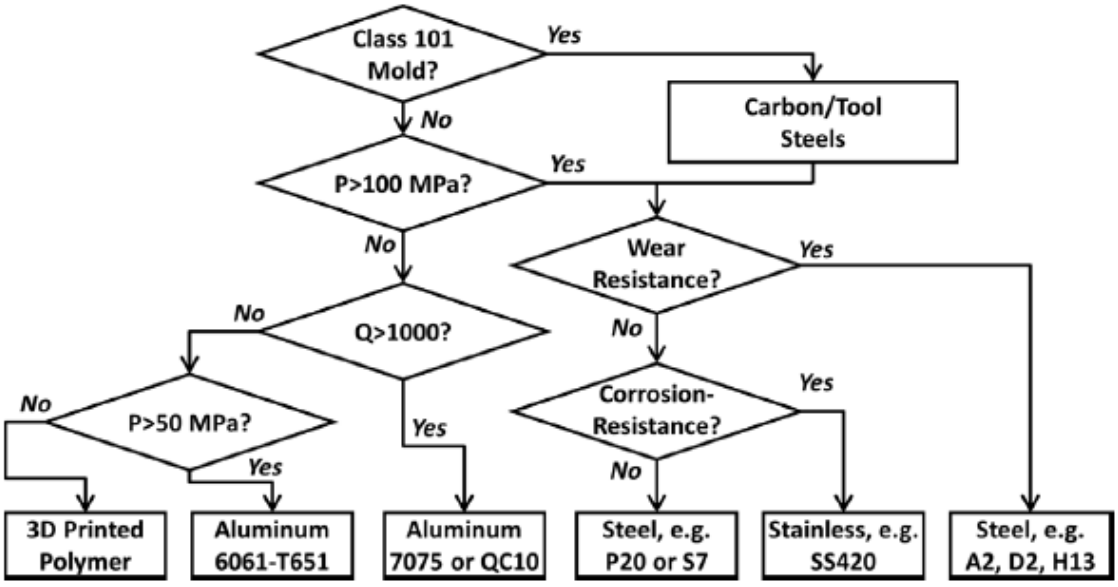

Figure 22 – Basic material selection [3]

Class 101 mold requires the use of tool/carbon steels which are also preferred for the high-pressure injection molding. This is followed by an evaluation of steel properties, such as wear and abrasion resistance. This is particularly important in manufacturing where resin-filled fibers are used. If the focus of the production is not on abrasion and wear properties, the main criterion is the corrosion resistance with SS420 grade steel as the main representative. Otherwise, the representative tool steels are P20 or S7 steels excelling in grinding and polishing. For short-run or intermediate production quantities where high pressure and wear requirements are not required, non-ferrous metals are preferred. The main representatives include aircraft aluminum 7075-T6 and special classes for mold development, such as Aleris Hokotl and Vista Duramold. These special classes provide high machining and pressing productivity with reasonable strength. For the lower cost production requirements, Commodity 6061-T6 steel is commonly applied. Despite its disadvantages of

a lower strength, it provides higher weldability and corrosion resistance. When rapid prototyping and small production quantities are required, poly-jet printing or fused deposition modelling processes are employed to produce the mold inserts [3], [12], [15].

3.3.1 Hardness vs. Machinability

In most cases, the properties of steels must include wear and abrasion resistance and great hardness. A number of instruments and methods evaluate them, such as the Brinell hardness test [16].

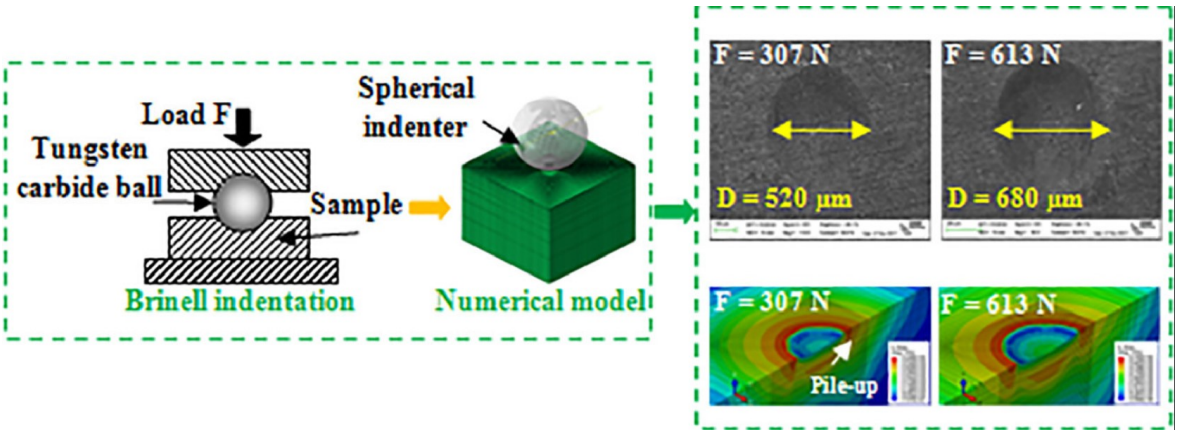

Figure 23 – The Brinell hardness test [17]

The Brinell hardness test expects pressing a carbide ball with a diameter D of 10 mm into the test material with a specific force. The diameter d resulting from the pressing is then measured and calculated according to the formula:

$$BHN = \frac{2F}{\pi D(D - \sqrt{D^2 - D^2})} \tag{3.1}$$

Further hardness measuring methods include the Rockwell and Vickers test. Their principle is almost identical to the Brinell hardness test, except for the fact that the load and geometry applied on the material differ. In general, material hardness is related to the modulus and compressive strength of the test material. Hardness values for different materials are listed in Appendix A.

As the hardness of the material declines, the difficulty of machinability also decreases. The ease of machinability allows to use less hard materials and to apply higher cutting speeds and feed rates. In Figure 24, the machining speed is expressed on X-axis as a function of Brinell hardness [3], [16].

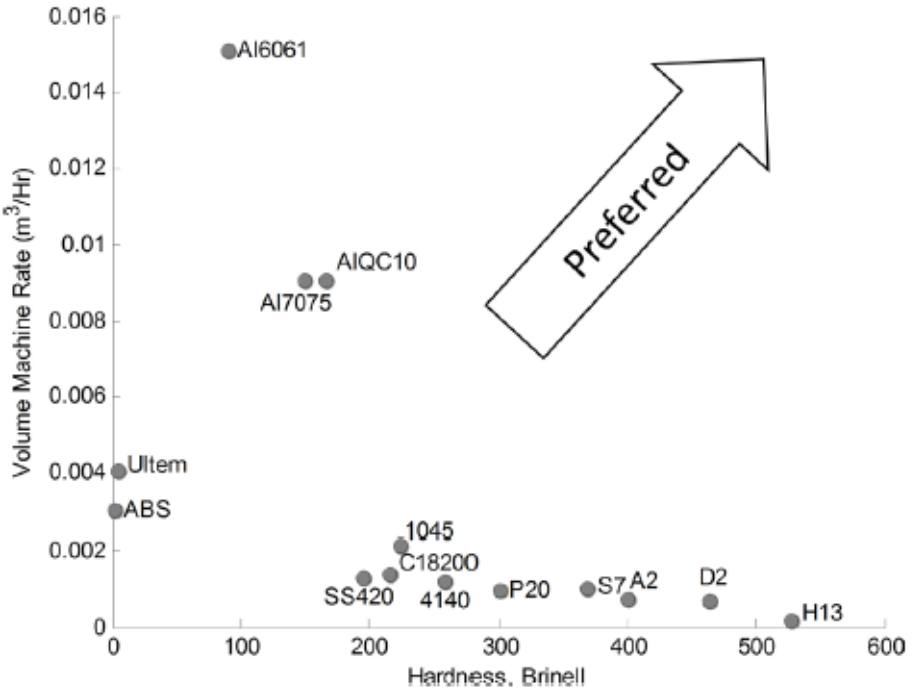

Figure 24 – Machining and wear performance of several mold materials [3]

Figure 24 shows the dependence of Brinell hardness on volume machine rate. Materials with high hardness perform low machining speeds. Because of the long machining time of hard materials, such as A2, S7, H13, and D2, they should be used only if abrasive materials are required otherwise rapid grinding could occur. It can also be seen that aluminum alloys perform high machining speeds and are, therefore, suitable for fast and economical mold manufacturing. Nevertheless, the disadvantage of these alloys is that they are used at the injection pressures smaller than 100 MPa [3], [18], [19].

3.3.2 Strength vs. Heat Transfer

Strength is commonly defined as the ultimate stress that a material can endure prior to its failure. In general, the yield strength characterizes stability because no permanent deformations in the yield strength occur when stresses are applied. These properties are not used in the injection molds and are replaced by the fatigue strength which is defined as the amount of stress that can be cyclically applied without causing a failure.

The choice of material plays a major role in the structural design which varies in many cases. Generally, most steels have a tensile strength specified as one half of the yield stress. For materials, such as aluminum, the ultimate strength cannot be determined and therefore, it is not possible to establish when permanent deformation occurs. This deformation often occurs after the continuous cyclic loading, regardless of whether the stress has been applied

to the material or not. For these reasons, the allowable stress is specified after a certain number of cycles. Requirements for the properties of the mold material vary in dependence on the subsequent use. Figure 25 shows the yield strength and thermal conductivity of several materials. As can be seen, the materials with high strength (H13, A2, D2 and P20) perform low thermal conductivity. The material with the best thermal conductivity is C18200. Unfortunately, it is not possible to identify a versatile material that can withstand significant ultimate stress and perform high thermal conductivity at the same time. The most common material used in mold manufacturing is P20, which has excellent fatigue strength but low thermal diffusivity [3], [16], [19], [20].

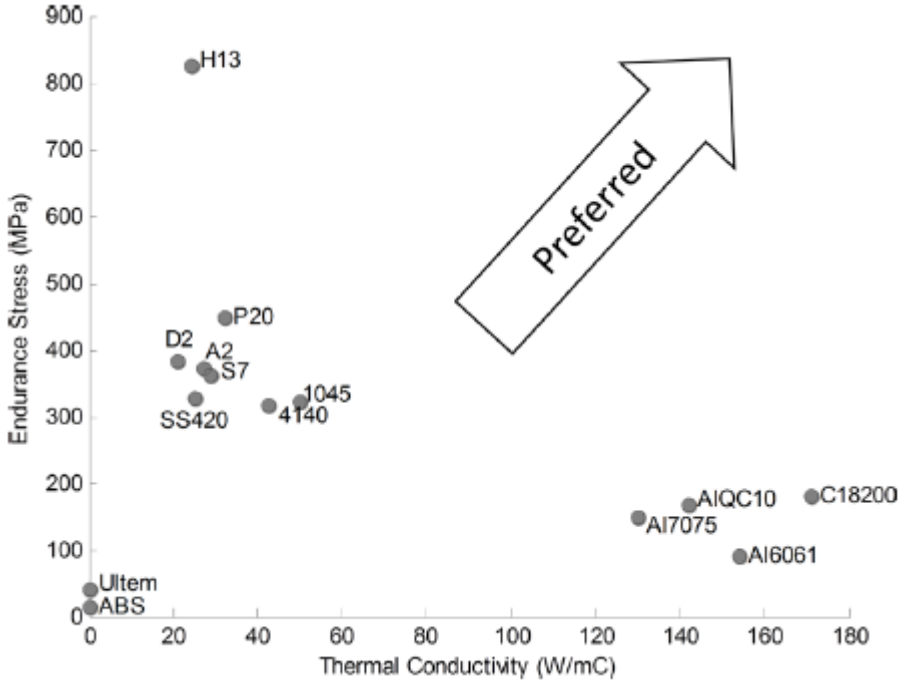

Figure 25 – Structural and thermal qualities of several mold materials [3]

3.4 Types of injection molds

The simple two-plate injection mold design is the simplest and most efficient. It is one of the most commonly used and can be encountered most often. However, a detailed analysis of this injection mold design reveals a number of limitations including:

- restricting the route of the feed system to the parting plane,
- limited possibilities of the flow from the feeding system into the mold cavity or cavities,

- extended cycle time associated with plasticization and cooling of the melt in the feed system,
- increased amount of material in the sprue residue,
- restriction on the tight spacing of cavities,
- additional forces due to flowing melt in the feed system.

For these reasons, the choice of two-plate mold is limited in some productions. These molds are replaced by molds with a more complex design, such as three-plate molds, hot runner molds, stack molds, and others. The most commonly used of these are hot runner and three-plate molds [3], [21].

Figure 26 – Stack mold [21]

3.4.1 Single cavity mold, multigated, hot runner

A significant percentage of mold produced today use hot runners. Although hot runners have several advantages if compared with cold runners, they also represent many limiting properties. This chapter discusses both the advantages and disadvantages that should be considered in the mold designing process. Due to the complexity of hot runners, their components are purchased within a special manufacturer either as an integrated system or components to be assembled [22].

One of the main benefits of a hot runner system is the fast cycle time. With this system, no cooling and filling of the sprue and cold runner system is required (unless it is a combination of cold and hot runner system). The filling time of the hot runner is generally only a fraction of a second which may be significant for high-speed applications. The hot runner system does not require a large clamp stroke as the mold opens only for the distance essential to eject the parts; the cold system and its sprue do not have to be considered. Therefore, the opening distance is shortened and the hot runner is expected to reduce the total energy consumption for the duty cycle. Obviously, it also saves runner filling and the use of granulate. On the other hand, more energy is required to ensure the heat transfer; to heat the heating elements and cool the mold. The hot runner system requires more investment to provide and control the hot runner temperature as it involves regular maintenance, parts replacement and what is more, operators' expertise. Another considerable disadvantage is the mold change time associated with purging the molds of a polymer melt, as it is unacceptable to allow traces of the previous material and its color in a different product. The main disadvantage and most significant error of a hot runner is usually a short-sighted buyer driving costs down by limiting engineering expertise and ignoring the need of employees for training. This could trigger problems and higher costs in long terms [3], [23].

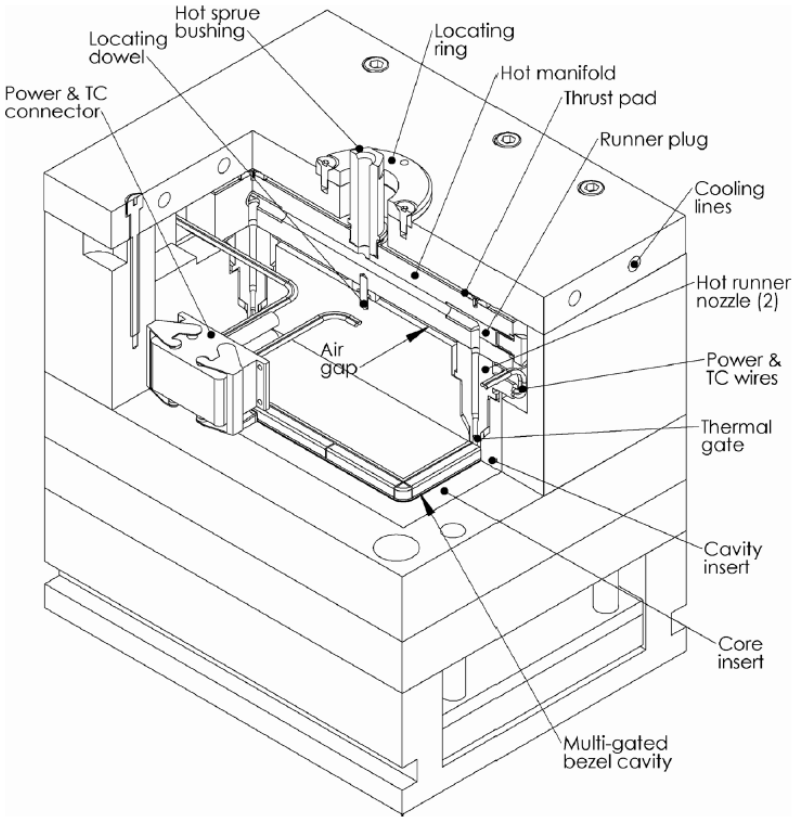

Figure 27 – Section of a multigated single-cavity mold [3]

3.4.2 Three-Plate mold, multi-cavity, family mold

The name of the three-plate mold was assigned on the basic of the third plate located between the two plates of the mold cavities and top clamp plate. During the injection cycle the plastic melt flows out of the nozzle of the molding machine, down the sprue bushing, across the primary runners, down the sprue, through the gates into the mold cavities. The feed system then freezes in place along with the molding.

The principle of the three-plate system is based on the opening of two parting planes. When the first parting plane is opened, the cold runner remains attached to the stripper plate by the sprue puller. The cold runner is then separated by a stripper bolt which pulls the stripper plate away from the top clamp plate and separates it from the sprue pullers. In the next step, the second parting plane is opened with additional molding stripper bolts and the product ejection follows.

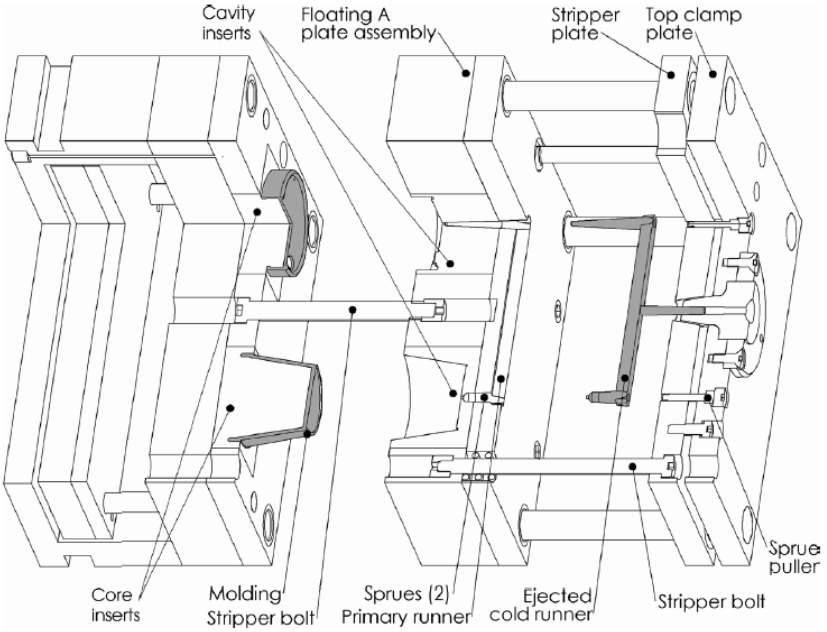

Figure 28 – Three-plate mold [3]

The advantages of three-plate mold include automatic separation of the cold runner from the injection molded product and flexible positioning of the gate in any location. These operations save additional adjustments and facilitate mold operation.

However, the existing design has a few significant potential problems. One of them is related to the cold runner. It is ejected every working cycle and if it is large compared to the product, it affects the cycle time and material consumption. As these parameters increase, the total price per piece grows as well.

The three-plate mold requires more plates and components for the formation and ejection of the cold runner which increases its cost. A large mold-opening stroke is essential to eject the cold runner; thus, a special injection molding machine with a larger mold opening height is required [3].

3.4.3 Stack mold

Stack mold differs from classic injection molds. Its design is special since it contains two parting planes in which one or more cavities may be placed. The lamination injection mold consists of a two-way ejection system, gating system and opening and closing clamping unit. Stack injection mold consists of a moving, middle and fixed part of the mold.

The fixed part of the mold is placed on the right side of the injection mold on the fixed plate of the injection machine. A heating element is in the solid part to heat the material and maintain it in a molten state. When the mold is closed, it is connected to the mold mouth of the injection molding machine. The extension part of the sprue channel must therefore be adequately long.

The middle part of the mold consists of a plate with a hot runner inside and cavity plate. Its feed system is equipped with a thermal nozzle on both sides. It is important to support the middle part on both sides. During the working cycle, the central part is located between the movable and fixed part of the mold and is opened evenly on both sides by means of the mechanisms described below. The hot runner system of these molds is almost identical to the conventional molds. It consists of nozzles, hot runner plates, and heating device. Moving part is on the left side and moves with the injection mold plate during the mold opening [21].

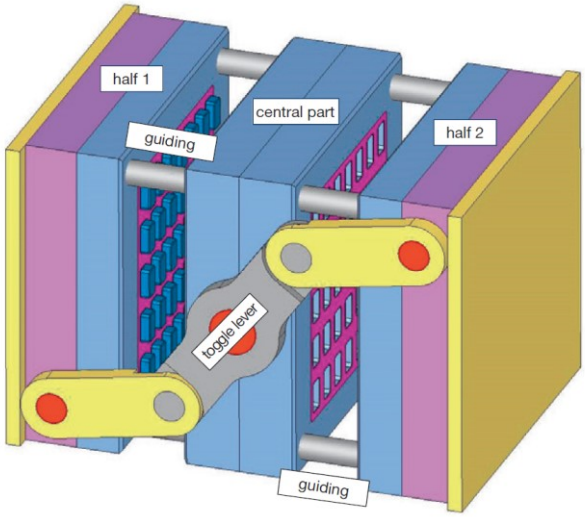

Figure 29 – Three-dimensional view with a toggle lever [10]

Stack mold design increases the production capacity twofold compared to a conventional mold. It reduces costs and enhances the quantity of parts produced per unit time. Stack injection mold does not require a special machine to function and can be mounted on the same machine as the single mold. When comparing the production of two single molds or a stack mold, the production of a stack mold would be 5-10 % shorter. Stack mold is suitable for small thin-walled plastic parts with multiple cavities and for the large-scale production of flat-shaped large plastic parts.

To ensure equal cooling and shrinkage of the product, the product should remain in the cavity on both sides for the same amount of time, hence it is important that the parting planes open at the same time [22].

Mold opening mechanism generally include three types of drives:

1) rack and pinion drive,
2) link drive/toggle lever,
3) hydraulic cylinder drive.

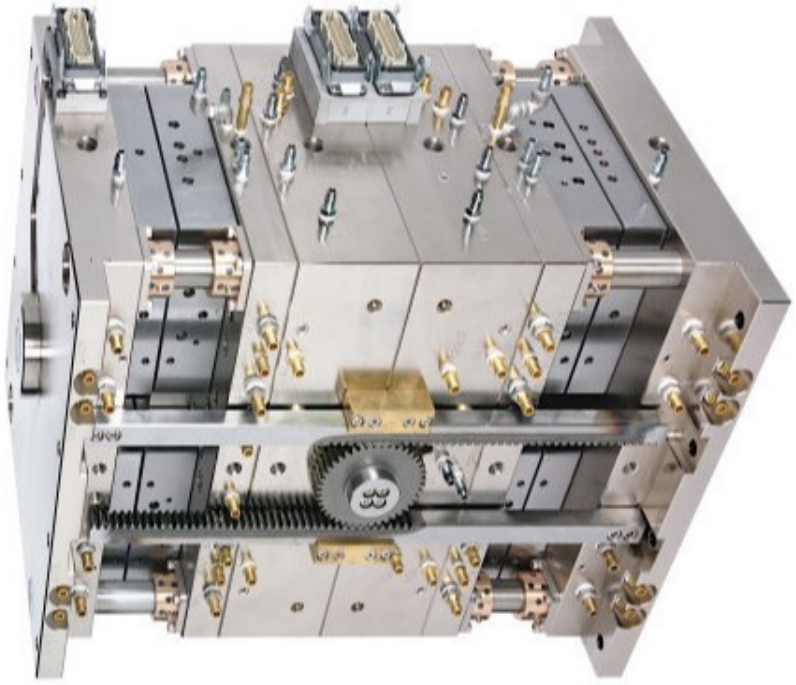

Figure 30 – Rack and pinion drive [21]

3.5 Comparison

The choice of the feed system plays one of the most important roles in the mold deign as it influences the mold design itself, choice of material, operation of the mold and its initiation in the production process. It is also a major factor for the cost and productivity.

Table 1 – Comparison of feed systems

Performance measure	Two- plate	Three-plate	Hot runner
Gating flexibility	Poor	Excellent	Excellent
Material consumption	Good	Poor	Excellent
Cycle times	Good	Poor	Excellent
Initial investment	Excellent	Good	Poor
Start-up times	Excellent	Good	Poor
Maintenance cost	Excellent	Good	Poor

4 PART DESIGN

Mold design is an important part of the product development process. The essential part of this process is the collaboration between the design and development department. Designers must consider several esthetic, functional and manufacturing related issues. The final design must satisfy the requirements of all these areas, which are often in conflict with one another. When developing a new product, there are a few different approaches to consider and many different processes to complete fabrication of a product. Most of them involve two fundamental attributes [3], [23].

1) **Structural development plan –** A coordination plan for concurrent design activities to ensure the complete design and production in the alignment with the schedule and requirements.
2) **Gated management process –** It attenuates the risk by allocating larger budgets after significant reviews during the project milestones [3].

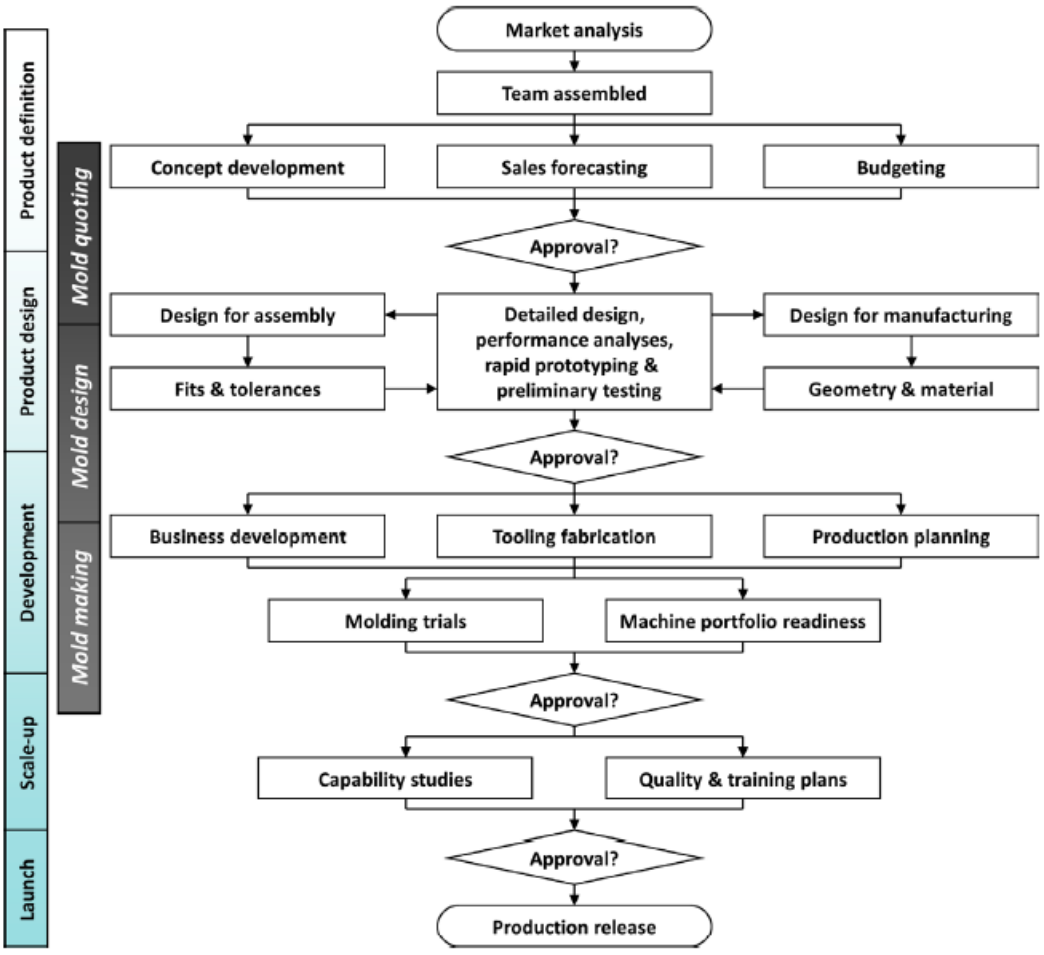

Figure 31 – A part of the development process [3]

4.1 Product definition

In most cases, the product development process commences with a product definition that includes a formal market analysis, definition of product specifications, comparative analysis of competitors, and an assessment of the potential profitability. Once the contract is approved by the management, a team is assembled to start the initial concept design and business development. An outline and prototype of the product are designed, along with the costs and features. During the initial development, the market study and analysis of associated cost of sales are conducted. Based on the obtained data, the budget and production time are determined and the sales forecast is provided to guarantee a successful profit [3].

4.2 Production planning

The main factors that determine and influence the production are:

- planned molds planned,
- cavities/mold,
- cycle time,
- production hours,
- annual production,
- target production.

All these factors are very important with respect to the selection of the mold layout and technology. The mold material, mold type and detailed design are related and play an important role in the overall production quantity and durability. Another factor affecting the economic aspect of the mold is its maintenance. With the need of frequent maintenance service and potential modification of parts, the mold price increases. Monthly production capacities depend on the production time, cycle time and number of the cavities in the mold. In most cases, the cycle time is known even before the mold starts as it is defined by numerical simulations in the preliminary analysis. If the customer cannot provide precise information, a preliminary design and analysis are performed to offer an efficient mold design. All these factors influence key decisions as they affect the total cost of the product. Any differences and alterations between the target and actual costs should be discussed during the revisions aiming for the continuous enhancement [3], [24].

4.3 Design for assembly and manufacturing

The collaboration between the mold designer, plastic product development department and customer is fundamental as it defines the product design and functionality. A promoted design is discussed and verified in several stages to ensure the best possible balance between the functionality, production and cost.

Unfortunately, such a collaboration is not always the priority and the mold designer could receive a completed plastic design. However, it often contains errors negatively affecting the mold. If such a design containing inaccuracies is processed, it may seem to be a fast and simple solution, nevertheless, in long terms it often leads to additional uneconomical operations and losses.

In all cases, a close collaboration with both the design development department and customer is important and beneficial [3], [25].

5 CAVITY FILLING ANALYSIS

Filling simulations in mold design help achieve the optimal design and avoid additional modifications. To complete the product, the polymer is required to fill the entire mold cavity. For this reason, the wall thickness of the product and placement of the sprue should be designed to allow the melt to pass from the sprue to the edge. In general, the analysis is not only used to determine the filling of the mold cavity at certain pressures, but also to assess the filling efficiency associated with achieving the desired quality without causing defects. Important points for calculation include mold filling, temperature, pressure, air pocket and flow lines. Computer programs with advanced software with more elaborated tools also show theoretical shrinkage and deformation of the plastic part.

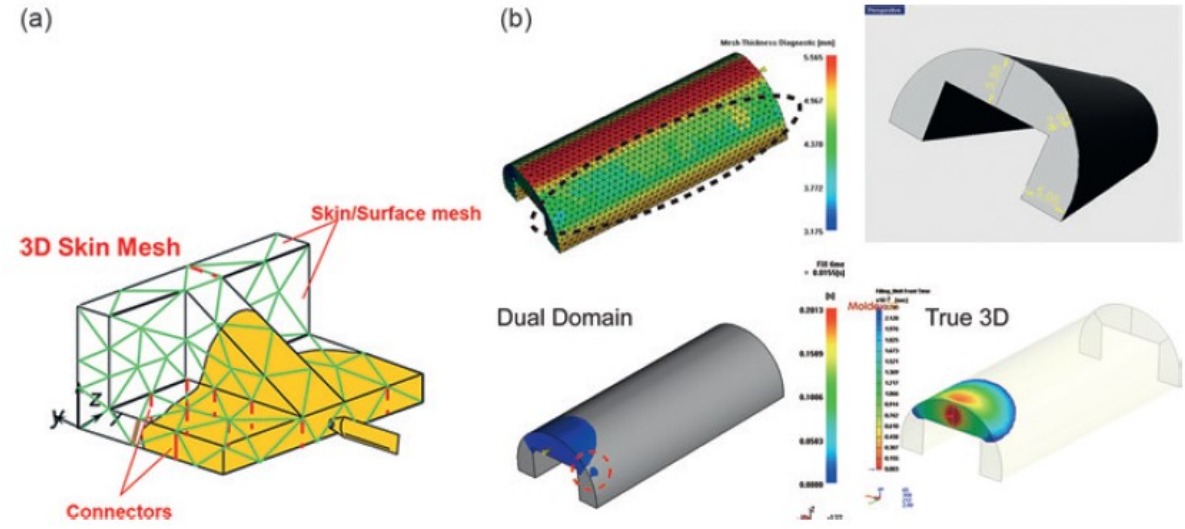

Figure 32 – a) dual domain model b) thickness determining issues of dual domain model [2]

5.1 Basic physics of the process

The filling phase is characterized by high flow rates associated with high shear rates. High heat and viscous dissipation can occur as a result of a high injection speed. Viscous dissipation depends on viscosity parameters and material deformation rates.

The viscous heating and highest flow rates appear most often in the areas of the runner channel and gates. However, viscous heating may also occur in the cavity if the flow rates are sufficiently high or the material has a high viscosity.

The purpose of the cooling system is to cool the mold cavity and to remove heat from the mold cavity caused by heat transfer from the melt material. Heat loss in the mold cavity results in a thin layer of solidified material. Thin layer can lead to swelling and thus

restricting the flow of the incoming melt. This influences shrinkage and deformation of the part as the pressure required to fill the mold is significantly affected.

During the injection process, conduction becomes the main heat transfer mechanism and the thickness of the frozen layer continues to increase until the gate freezes and the cavity is isolated from the applied pressure. The material solidifies, shrinks and can be torn away from the cavity wall of the mold. This negatively effects the temperature calculation of the material in the mold and is followed by the material solidifying to the ejection temperature.

To summarize the injection molding process, several mechanisms affect the process, including heat transfer, phase transformations, time boundary conditions in the frozen payer during the injection and cooling. Furthermore, material properties and geometry of the designed part significantly influence and complicate the simulation [26].

5.2 The filling phase

When the cooling cavity mold and plastic skin get into contact, plastic freezes while the central polymer core remains molten. As the polymer flows, further amount of the melt flows through the center of this core and displaces the material which is already there, so that a new flow front is created. The flow moves in the forward and outward direction. The outward flow is in contact with the cooled wall causing the formation of the frozen mantle. The forward shedding creates a new molten core. The new molten polymer passes through these frozen polymer walls as Figure 33 shows.

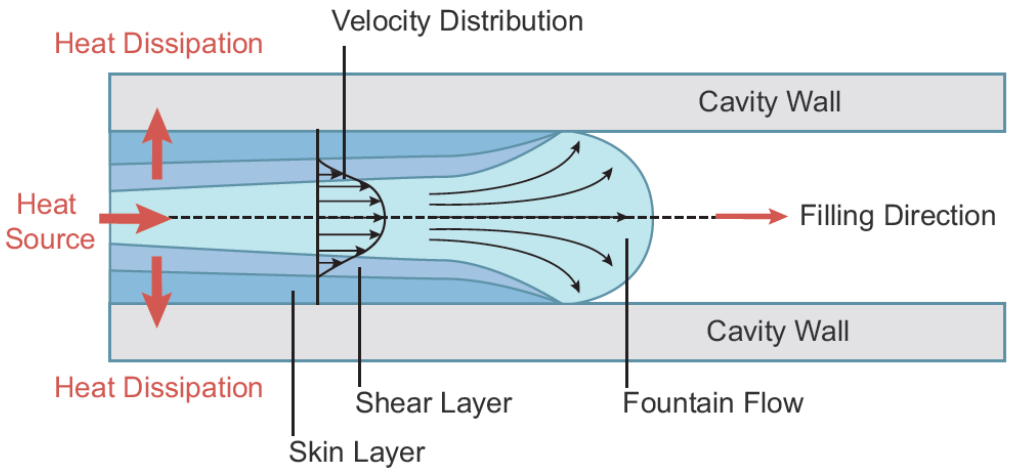

Figure 33 – Polymer melt filling progress [2]

The flow described above is called a fountain flow or bubble flow. The frozen layer is subjected to low shear stress and therefore, it has a very low level of molecular orientation [27].

5.3 Shear stress, shear rate, and viscosity

To understand polymer flow theory, it is important to understand the relationship between shear stress, shear rate and viscosity. The shear stress (τ) is defined as a direction of force applied to a cross section. The shear rate ($\dot{\gamma}$) expresses the rate at which the melt velocity changes. The viscosity is defined as the resistance of fluid to shear flow.

$$\tau=\eta\dot{\gamma} \tag{5.1}$$

Figure 34 shows the flow between a moving and stationary plate. It assumes that the melt flow is fully developed and there is no slip on the wall. A linear velocity profile is drawn across the fluid with zero velocity on the stationary wall and velocity v on the moving wall.

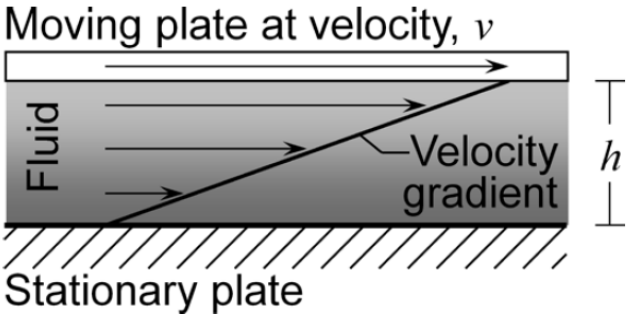

Figure 34 – Flow between two parallel plates [3]

Considering the melt flow between a stationary and one moving parallel plate, the shear rate is expressed as a change of the velocity through the thickness [3], [28].

$$\dot{\gamma} = \frac{dv}{dz} = \frac{v}{h} \tag{5.2}$$

5.4 Simulation

The guarantee of the product quality is one of the fundamental steps in the injection molding production process. In the initial sampling or series production, it is demanding to estimate the location of deformation, weld lines or burrs. On the other hand, the incorporation of CAE analysis may help avoid these issues. Figure 35 illustrates the simulation options that can be

included in the initial manufacturing process, such as the simulation of screw design, injection molding, and structure analysis including mold filling. The results obtained from the simulation could be applied in the initial stage of the design process for possible required design modification. This may help prevent potential problems in the injection molding even before the actual mold cavity is manufactured [2].

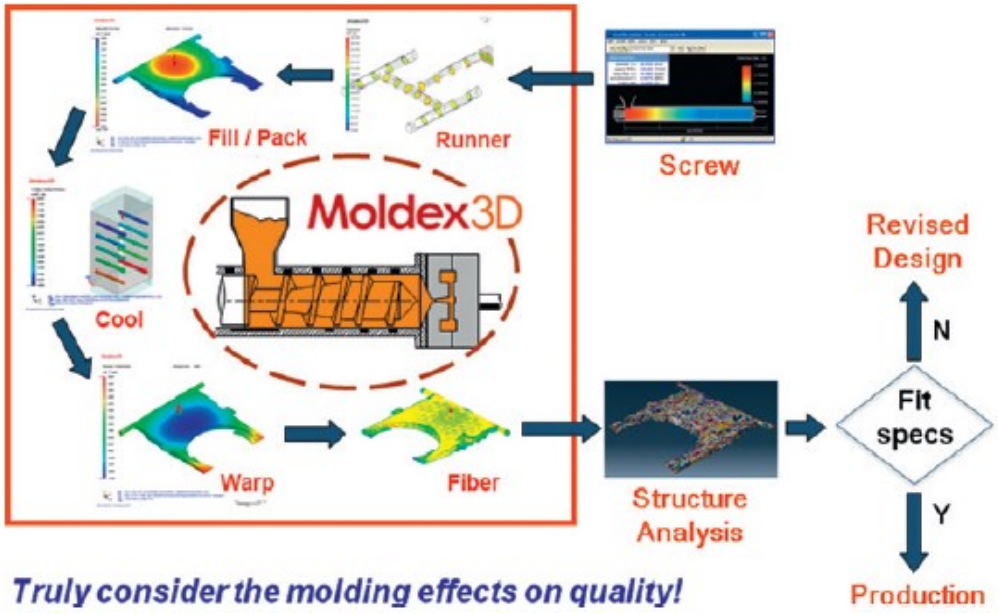

Figure 35 – CAE applications in design [2]

Fiber orientation plays an important role in the mold cavity filling study because fiber orientation is closely related to the mechanical response and strength of the product. Software that can be used to predict these properties, such as Moldex3D, Moldflow, transfers fiber orientation, stress and strain into precise and realistic structural simulations of these parameters [2].

Generally, simulations are nowadays simplified by user interfaces and various wizards for process conditions and parameters. Most of the validation studies have shown that common failure modes are related to the mold geometry, process conditions and material properties. Even though these studies provide useful data, they should be always verified before accepting into the operation and assessed whether they correlate with the previous knowledge and experience in the field.

An example of such a simulation can be seen in Figure 36. It shows the average melt flow rate of the polymer during the filling phase. At the filling time of 0.44 s, the average melt flow velocity is 50 cm/s. The simulation provides the information regarding melt flow which would be otherwise difficult to determine. The flow characteristics include a local flow

around the windows and bosses, radial flow out of the gate, melt flow convergence in the last region and flow stagnation on the side walls.

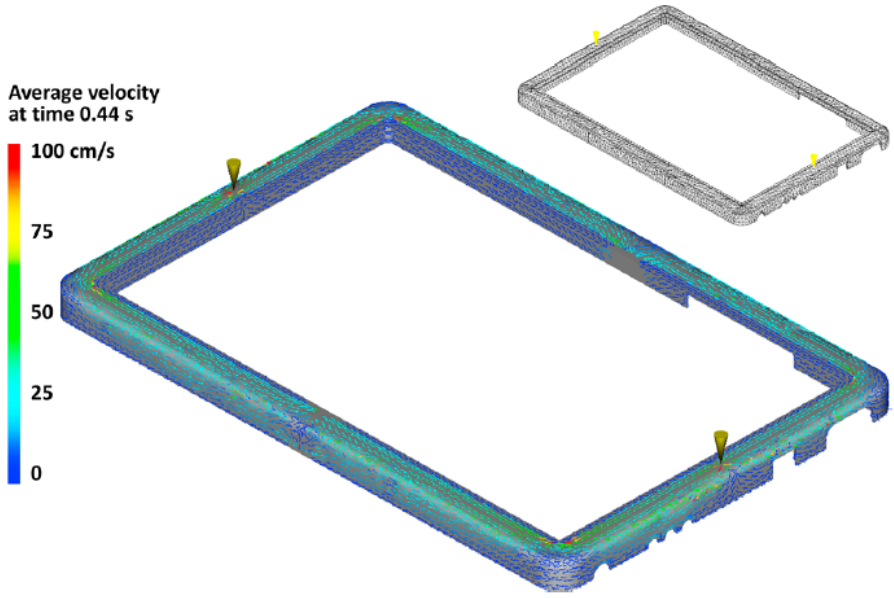

Figure 36 – Melt average velocity at time 0,44 s [3]

One of the main uses of simulation is to determine appropriate process conditions for the injection molding, including temperature, cooling, pack pressure, and injection time. Figure 37 displays a graph of the simulation from 0.05 s to 2s for Cyclocac MG47 material. It can be seen that the temperature for the 2-second injection time is 240 °C. If the injection time is reduced to 0.5 s, the temperature reaches more than 260 °C. This increase stems from the heating of the polymer melt at higher injection speeds together with smaller heat transfer of the conduction due to a shorter filling time [3].

In the real production, the injection time is set so that the melt volume temperature is the same throughout the filling process. Figure 37 shows the injection pressure along with the bulk temperature. The injection pressure is the lowest around the injection time of 0.2 s. This is owing to a higher bulk temperature and shear rate causing a lower viscosity and because of a thinner frozen layer of polymer melt in the defined injection time.

The injection time is recommended to be set to minimize the injection pressure as much as possible. Although the main objective is to minimize the injection pressure and maintain the uniform melt temperature, it is not possible to simulate these divergences the same way as they may occur in the real injection mold sampling. The most likely filling time to minimize this range is 0.1 – 0.5 s. After the optimal parameters are identified, it is important to

incorporate the runner system and cooling lines into the simulation to optimize the process to obtain the most ideal solution for the production [29].

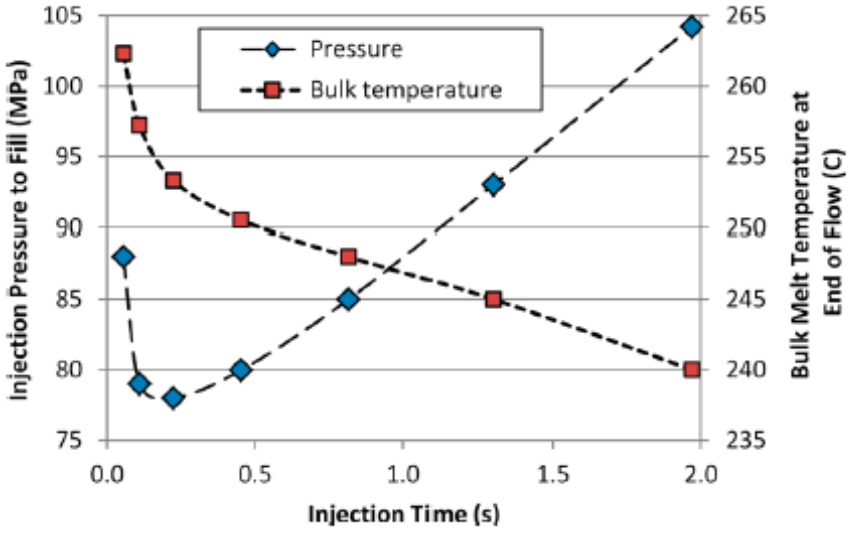

Figure 37 – Results of simulation during the injection time [3]

6 STRUCTURAL SYSTEM DESIGN

During the injection molding, a large amount of polymer melt is applied into the mold cavity. Forces that can be expected at these pressures range from tens to thousands of unit tons. As the mold itself must withstand the forces acting on the mold cavity while maintaining the product quality, the mold design plays a significant role in its robustness.

For a high-quality robust injection mold design, the relationships between the forces, pressures and stresses in the mold and the mold cavity itself must be considered.

Figure 38 shows a typical distribution of pressures across the injection mold plates, clamping plates and injection molding machine. The pressure on the injection mold cavity causes compressive and shear stresses on the core liners, cavity liners and backing plates [3], [30].

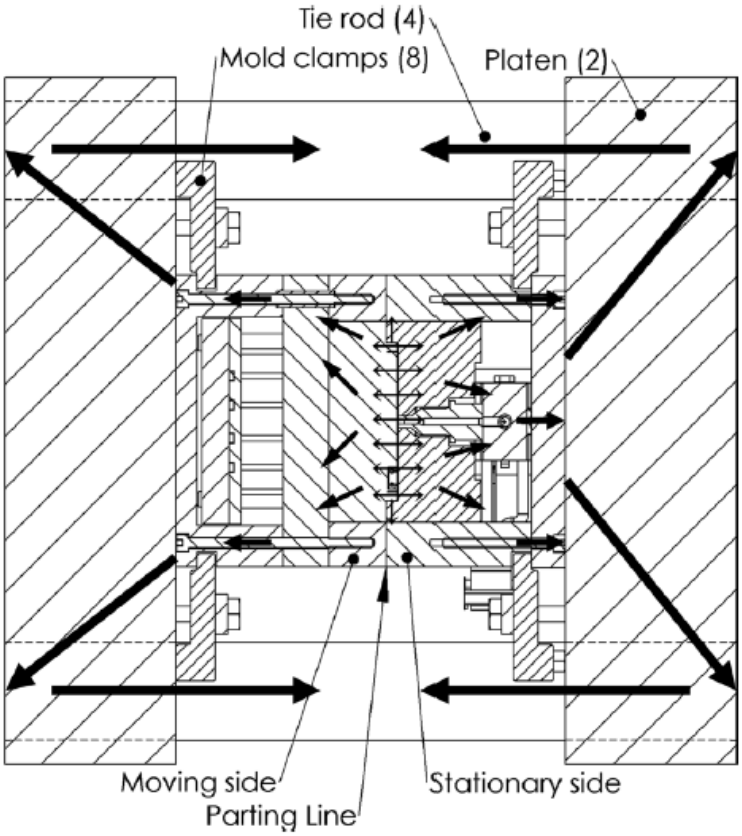

Figure 38 – Stress pathways in mold and molding machine during the injection molding cycle [3]

6.1 Injection pressure/cavity pressure

Especially during the injection process, injection pressure and cavity pressure should not be underestimated. It is important to emphasize that injection pressure is not a clamping force and does not act only in the axial direction but in all directions. The difference could be recognized in flat and thick parts, where the radial force is smaller than in thick parts.

$$F = A \times p \rightarrow \textit{closing force (N)} = \textit{projected area } (m^2) \times \textit{injection pressure (Pa)} \quad (6.1)$$

To guarantee the injection mold withstands such force, it is recommendable to base the injection pressure on the maximum pressure of the injection molding machine. Then it is possible to confirm that the injection mold does not break during the injection cycle, even in case of any possible machine error. The anchorage in the cavity plate during the injection plays an important role ensuring the absorption of the injection pressure.

Figure 39 shows the direction of the pressure. A large number of arrows indicates greater pressure applied [9].

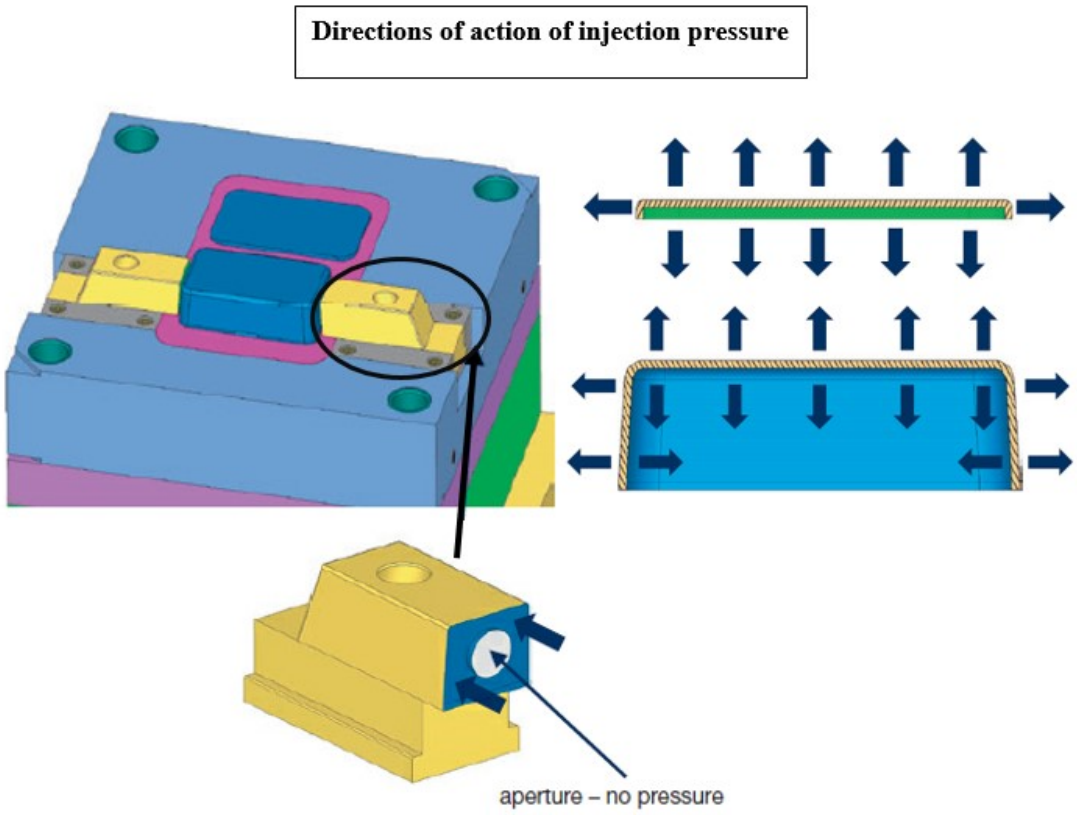

Figure 39 – Direction of injection pressures [9]

6.2 Objectives in the design of structural systems

The injection mold design should withstand as many working cycles as possible and should not deform excessively. It should be designed in a size that matches the structural requirements of the components in the mold ensuring the reasonable price of the injection mold.

The objectives of the initial development of the injection mold include minimizing stress, deflection and cost associated with the mold size.

6.2.1 Minimize stress of the mold

The tension between the individual sides of the injection mold varies considerably in the state of stress. Most mold designs allow cavity inserts to be supported by the stationary plate and top clamp plate. One of the main reasons of a different stress state between the sides of the injection mold is the pocket required to accommodate the ejection assembly and thus causing less support for the plates in which the core inserts are located. That is why, significant bending of the backing plate could be observed due to the load transfer owing to compressive and shear stresses.

An example of mold loading is shown in Figure 40. It includes a hot runner injection mold designed to produce a laptop frame. The injection mold cavity is subjected to a pressure of 150 MPa [3], [31], [32].

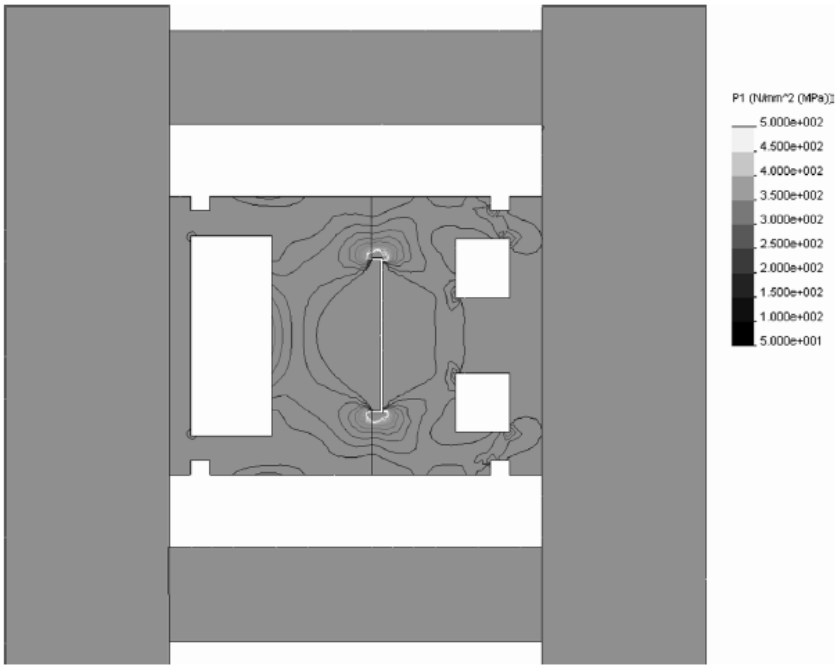

Figure 40 – Von Mises stresses caused by pressure during molding [3]

Von Mises stress is a criterion commonly used to predict failure and can be expressed as:

$$\sigma_{Mises} = \sqrt{\sigma_1^2 - \sigma_1\sigma_2 + \sigma_2^2} < \sigma_{limit} \tag{6.1}$$

where $\sigma_1$and σ_2 are the first and second principal stresses. To avoid failure, von Mises stress must be less than a selected stress limit value.

The limiting stress should satisfy various basic rules. One of them is to avoid high stresses that could plastically deform the mold. When a material is subjected to stress, either deformation or strain occurs. For most materials, the magnitude of the resulting deformation is proportional to the applied stress.

The relationship of stress and strain with the elastic modulus (*E*) can be defined as:

$$\varepsilon = \frac{\sigma}{E} \tag{6.2};$$

the formula expresses the deformation (ε) resulting from the application of stress (σ). The higher the elasticity of the material, the less it tends to deform when stress is applied. Another important factor is the yield strength. It can be defined as the stress at which the material deforms plastically or it does not return to its original state after the load is removed. The material deviates from the linear behavior. Subsequently, if the yield strength is exceeded, load transfer reaches the point of ultimate stress and the total failure occurs.

The initial steps of the mold design should ensure that the manufacturing stress is lower than the yield stress. To guarantee the mold withstands the load during the production, its design should include the analysis of the initial development to simulate the highest possible pressure the melt can apply.

Another option is to set the limit stress(σ_{limit}) equal to the yield stress (σ_{yield}) divided by a factor of safety (*f*).

$$\sigma_{limit} = \frac{\sigma_{yield}}{f} \tag{6.3}$$

In most cases, the mold design assumes the robustness of the mold if the yield strength and conservative safety factor are considered in the design, however, the growing number of pressing cycles may result in the mold failure due to cyclic stresses shown in Figure 41. Each cyclic cycle generates stresses that can lead to cracks in the mold. Over the course of several thousand cycles, these stresses may act like a clay hammer when the number and size of cracks increase. A critical crack size is reached and the concentration that develops around

the crack causes the mold to fail, even though the design has considered a stress limit well below the yield stress. This phenomenon is called fatigue [3], [31], [32].

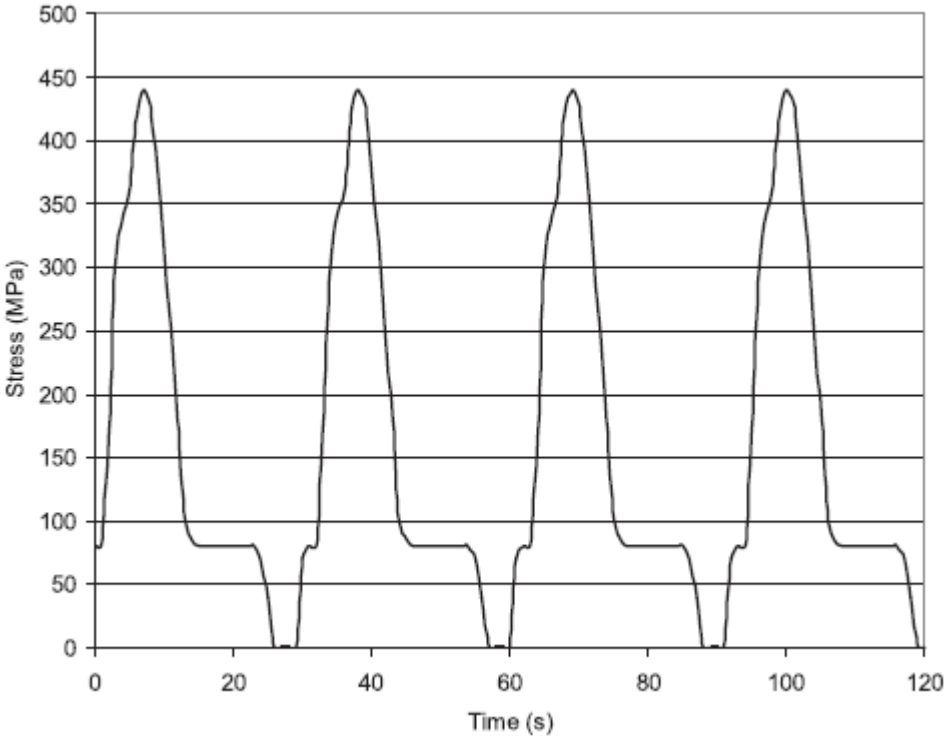

Figure 41 – Cyclic stresses during molding [3]

6.2.2 Minimize deflection of the mold

Excessive stress in the mold components can cause damage to mold components. However, what might be even more significant problem is the mold deflection. It causes the occurrence of the burrs influencing the final product quality which, in consequence, affects also the specifications and customers' requirements. Therefore, in practice, more emphasis is placed on minimizing deflection than stress.

Figure 42 shows deflection of the mold and plates under the same stress distribution as in Figure 40. The greatest deflection of the plates can be seen clearly in the center of the injection mold. The total deflection is 0.36 mm because the core surface deflects 0.24 mm to the left and the cavity deflects 0.12 mm to the right. The value of 0.36 mm is significantly higher than the venting value usually specified for the tool room separation of 0.02 mm. Thus, it can be easily predicted that burrs occur in this case and a solution to this deflection issue will have to be designed.

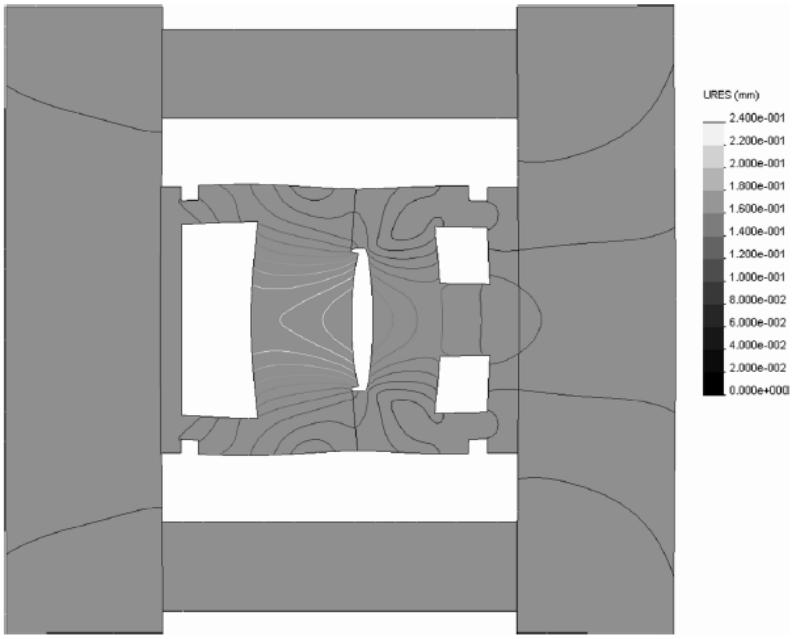

Figure 42 – Deflection caused by pressure during molding [3]

Mold designers and injection mold plate manufacturers often expect plates to be stiff without any deviations. Hence the plate deflection is also perceived as a considerable problem. As can be seen in Figure 42, the deflection of a stationary plate is approximately 0.04 mm which is the value twice higher than the deflection of a moving plate. The reason of this issue may be classified as the transfer of the force of the ejector body closer to the sides of the moving plate causing smaller applied load and deflection in the center of this plate if compared to the stationary plate deflection [3], [31].

6.2.3 Minimize size of the mold

In the mold design, various properties of different mold materials are investigated to ensure the reduction of stress and deflection. By examining the material properties of the Appendix – A, it can be concluded that materials, such as H13, perform significantly higher stress resistance than materials with softer properties, such as QC7. It could be also assumed that all steel materials have a similar modulus of elasticity and its value of 200 GPa does not differ significantly. That is why, the steel deflection may be influenced mainly by the mold geometry. To minimize deflection, the simplest solution seems to be a choice of a greater thickness of material. However, it considerably affects the final cost of the mold and it may limit the use of the individual injection molding machine. For these reasons, the appropriate analysis and structural components for support, such as support pillars and interlocks, appear to be a better solution [3], [31].

6.3 Plate compression

The half-load usually acts only on one side of the mold plate. Even though the sides of the plates are supported by the surrounding plates, the load is transmitted through the thickness and across the plate by compressive and shear stresses. Deflection that occurs during the compression does not cause problems in most cases because of two following factors. If the deflection extent is relatively small, it is not a problem. Moreover, deflection caused by compression is uniform throughout the mold; the compressive forces that arise during the mold clamping tend to cause uniform compressive stresses on the mold plates. The compressive stress (σ) is defined as the forces (F) acting per unit of an area compressed ($A_{compression}$) [3], [31]:

$$\sigma = \frac{F}{A_{compression}} \tag{6.4}$$

The strain deformation (ε) could be expressed as stress divided by the modulus of elasticity (E):

$$\varepsilon = \frac{\sigma}{E} \tag{6.5}$$

The amount of deflection is defined as the strain multiplied by the length across which the strain exists:

$$\delta_{compression} = \epsilon L \tag{6.6}$$

II. ANALYSIS

7 MASTER THESIS OBJECTIVES

The objectives of the thesis “Structural Mechanical Analysis of Injection Molds” are:

- literature research on the given topic,
- construction of the designed plastic part,
- design of a 3D injection mold assembly to produce the specified part,
- verify the design by the analysis.

The theoretical part explains the subject of this diploma thesis, the injection molding process including introducing the injection molds, product design, flow analysis and the structural design of the injection mold.

The diploma thesis has been developed in the cooperation with Hirchmann Automotive GmbH. One of the main objectives was to provide structural mechanical analyses.

The experimental part discusses the results and their subsequent verification by means of analysis. The results were processed using software, such as MiniTAB 20, Moldex 3D, Catia V5 R20, and ANSYS Mechanical 2021 R1.

8 CHARACTERISTICS OF THE INJECTION MOLDED PRODUCT

The plastic product was selected based on the injection mold used in the experimental part. The product contains an asymmetric differing mold cavity and is made of RADILON A RV250W 100 NT. It is PA66 material containing 25 % of glass fibers. This material is suitable for the products of medium stiffness, good mechanical resistance and excellent maintenance of the heat aging properties.

8.1 Material Handling and processing parameters

The material is supplied in the moisture-resistant skins ready to be processed. The maximum recommended water content for most processing is 0.15 %. The ideal drying conditions are at the temperature of 80 °C, dew point -20 °C or below, and for the duration between 2 – 4 h or even more. Specific information and material properties are attached in Appendix B.

Table 2 – Material processing parameters [33]

RADILON A RV250W 100NT		
Melt temperature	**Mold temperature**	**Injection speed**
280 – 300 °C	80 – 100 °C	medium – high

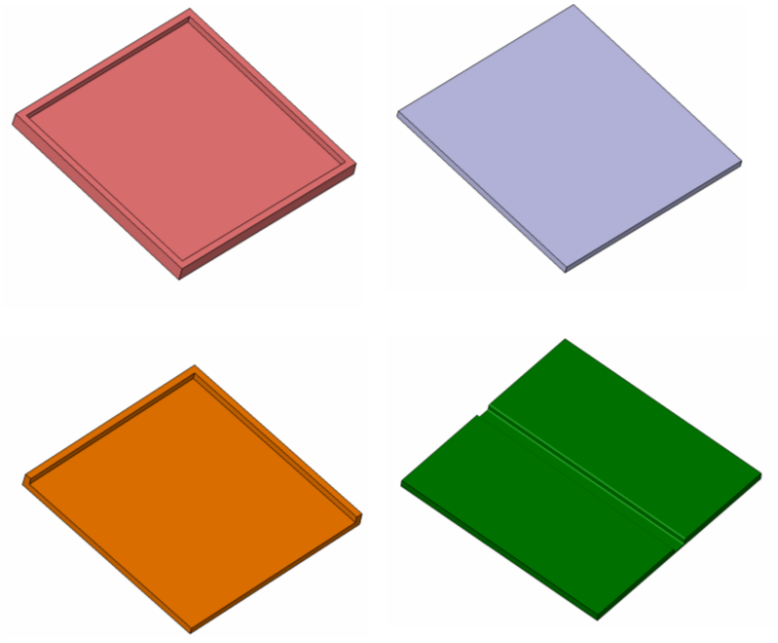

Figure 43 – 3D model of injection product

9 INJECTION MOLD

The mold design must consider the simplicity and cost – effectiveness of the injection mold. This thesis employs most of the parts from Meusburger company, some parts were from Kistler company specializing in the high-pressure sensors production. Standardized parts accelerate the injection mold development and eliminate laborious production and machining.

9.1 Injection mold multiplicity

The choice of multiplicity reflects the economy of the production, injection molding machine capacity, and accuracy. The mold design in this experimental part enables to alter the number of cavity fillings as the mold can be modified to fill one, two, three, or all four cavities and the multiplicity is not precisely determined.

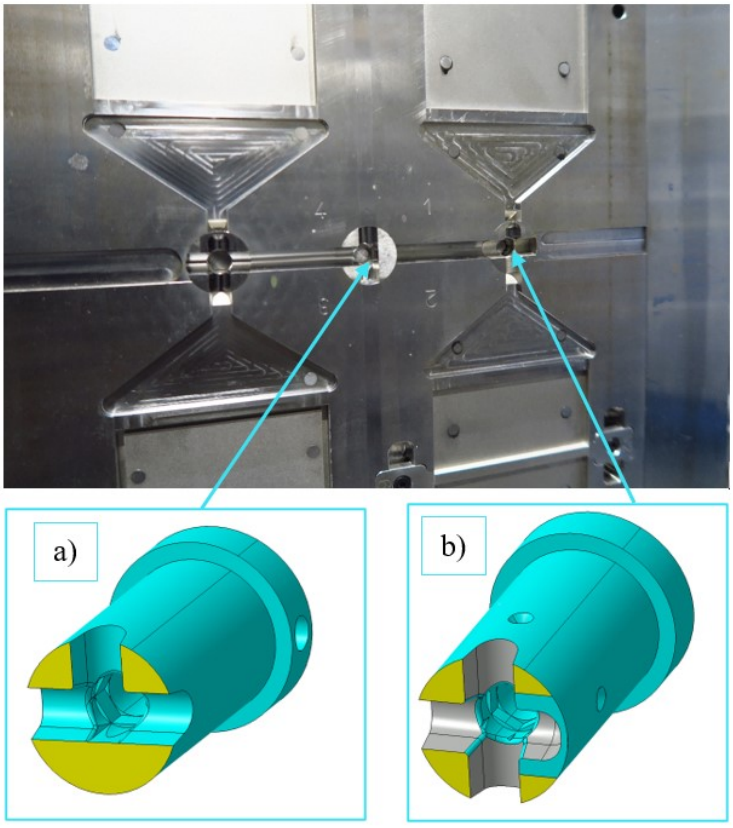

Figure 44 – Mold multiplicity a) middle insert b) outermost insert

The position of the inserts is arranged by ball-bearing compression tabs which prevent the insert from rotating during the working cycle. The inserts can be rotated by applying a greater force which can be exerted by a hammer and another tool.

9.2 Runner system

The runner system transports molten polymer into the mold cavity. This experiment applies a cold runner system. The sprue system consists of a sprue cone, primary runner and gate. The primary runner system has a semi–circular cross section and gate designed by film gate, also called flash gate. This gate type is generally used for flat parts, such as a mobile phone cap. Recommended thickness varies approximately from 0.2 mm to 0.6 mm, however, it depends on the product dimensions and weight. For larger parts, dimensions of 0.6 – 1 mm could be designed. The primary runner is held by inserts on the ejection side and is subsequently ejected by the ejector system.

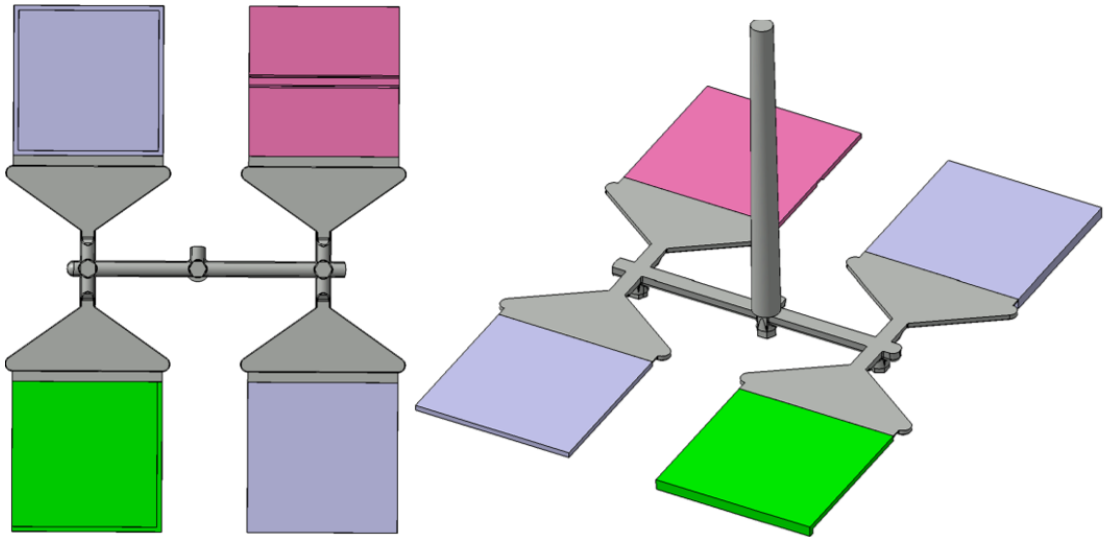

Figure 45 – Runner system

9.3 Mold cavity

In this experiment, the mold cavity is formed only by core and cavity determining the final product shape. The injection mold does not contain any subdivision planes and therefore, has only the main subdivision plane. The design of the mold cavity must take into account also the shrinkage of the material. In this experiment, the mold material and the geometry cavity have not been precisely defined as this mold is universal and multifunctional intended for diverse experiments.

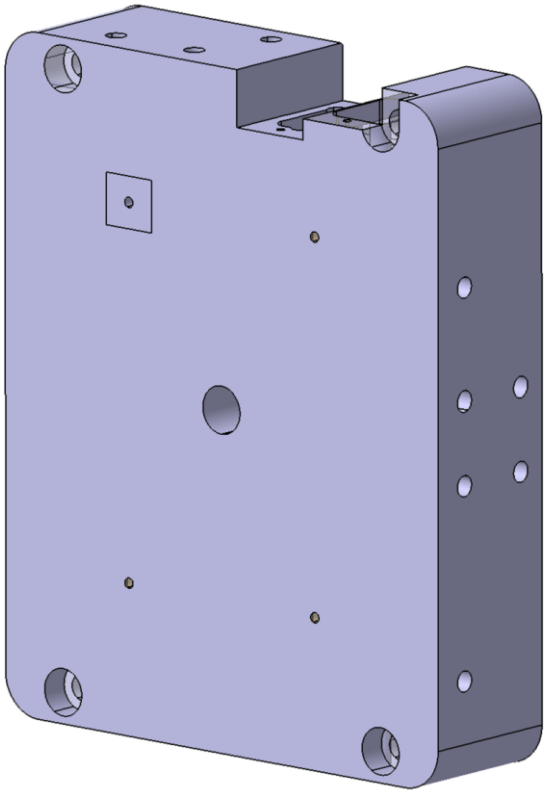

Figure 46 – Core insert

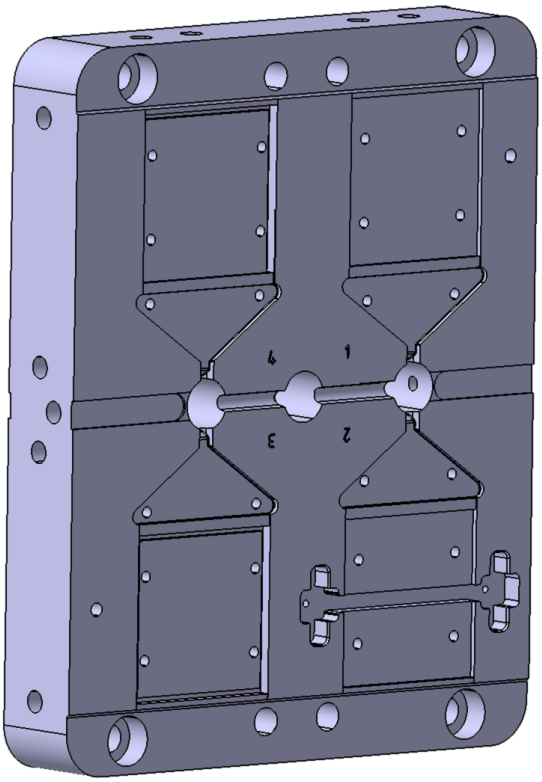

Figure 47 – Cavity insert

9.4 Cooling system

The cooling system provides cooling or heating of the mold to the temperature required for the injection molding cycle. Additionally, it equalizes the temperature field of the mold, which ensures uniform solidification of the material in the mold cavity. Various types of tempering media are used today, such as oil or water. In this experiment, water was used as the tempering medium. Based on the concept of the injection mold, the cooling circuit was adapted to the concept of the mold. Each side of the injection mold contains one cooling circuit of its own.

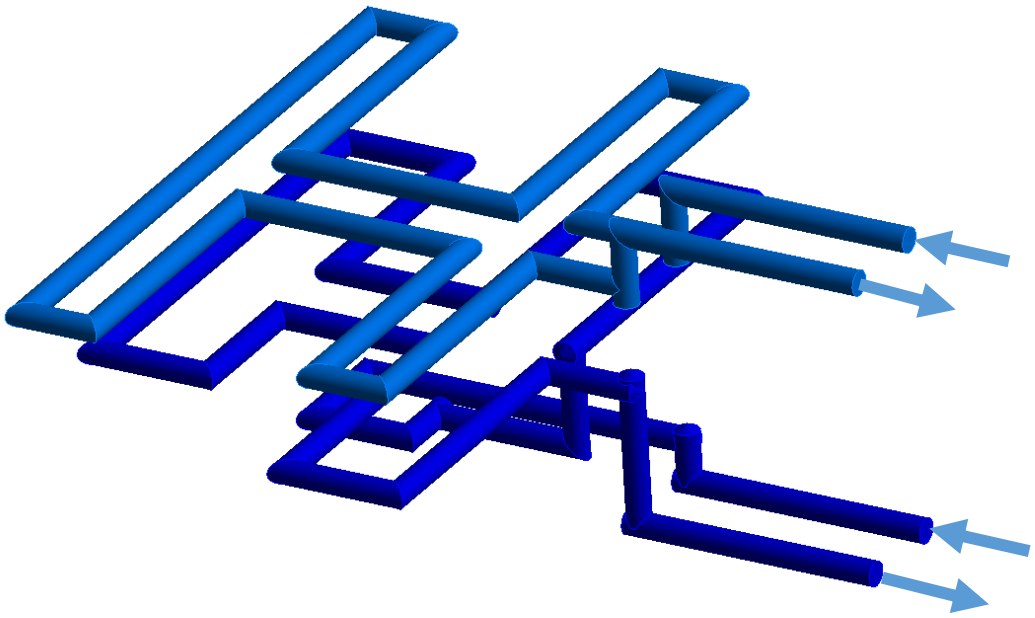

Figure 48 – Cooling system

9.5 Air venting

During the injection cycle, air is compressed and heated in the mold cavity which may negatively affect the final product. Adverse effect that can occur include the Diesel effect, where the injection material and mold cavities are burnt and degraded. Short shot is another negative effect on the process indicating incomplete filling of the mold cavity. To avoid this problem, the mold must be sufficiently vented, and venting must be of correct size as oversizing could cause burrs.

In this mold design, the venting is a small pocket of 0.015 mm at the beginning of the venting (Figure 49) located symmetrically at both ends of the runner system.

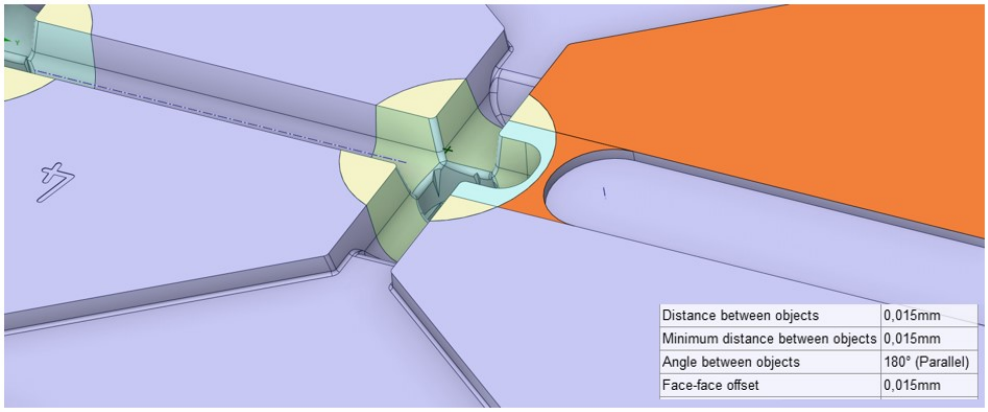

Figure 49 – Air venting

9.6 Ejection system

The main function of the ejector system is to eject the product that remains on the left side of the mold or ejection side when the parting plane is opened. As a rule, the ejection is designed so that the ejector pins do not press on the view side. The guide bolt fixed in the injection molding machine moves the ejector system. Twenty-four Ø4x160 ejector pins were chosen to eject the product and runner system. In addition, three Ø6x160 ejector pins were designed primarily for the ejection of the runner system. The pins Ø10x160 that lead into the parting plane were used to secure the initial position of the ejector system. The movable side of the mold, when the parting plane is closed, pushes the pins including the ejector system into the initial position. This is a mechanical safety device that is both inexpensive and highly effective. Another design element included the springs placed on the support rollers. The springs act as the ejection back action and the support rollers provide the opposing force during the injection molding cycle.

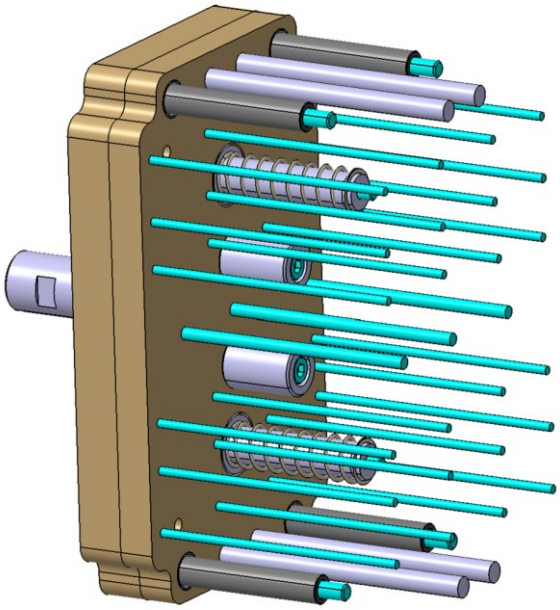

Figure 50 – Ejector system

9.7 Injection mold assembly

As Figure 51 shows, the injection mold assembly consists of two sub-assemblies. The first assembly is the mold core including the ejection system. It can be combined with different types of injection molding frames. The second assembly represents the injection mold body.

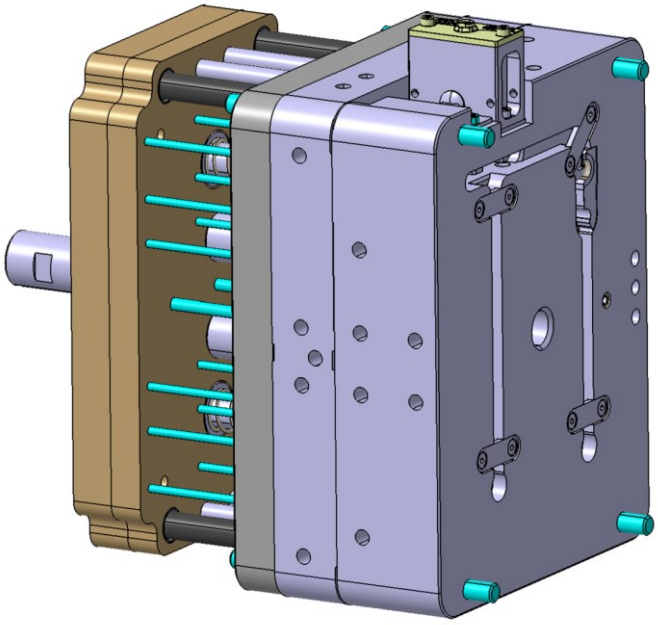

Figure 51 – Injection mold core

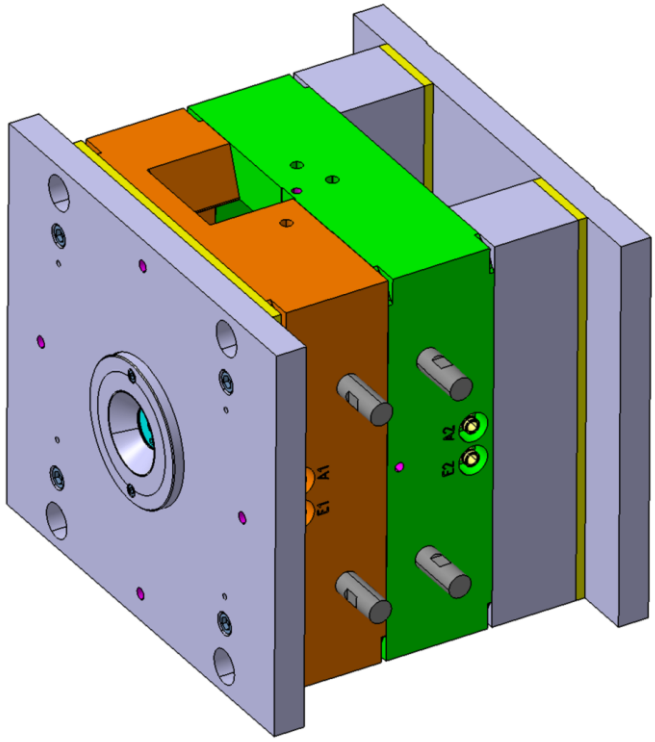

Figure 52 – Injection mold body

A special product (Figure 53) is used to connect these two sub-assemblies to facilitate the assembly of the two sub-assemblies and vice versa. The overall injection mold consists of several intercepted plates connected by various standardized components, for example Meusburger. The mold is divided into the ejection side and injection side or left and right side and is clamped by magnetic plates on the injection molding machine.

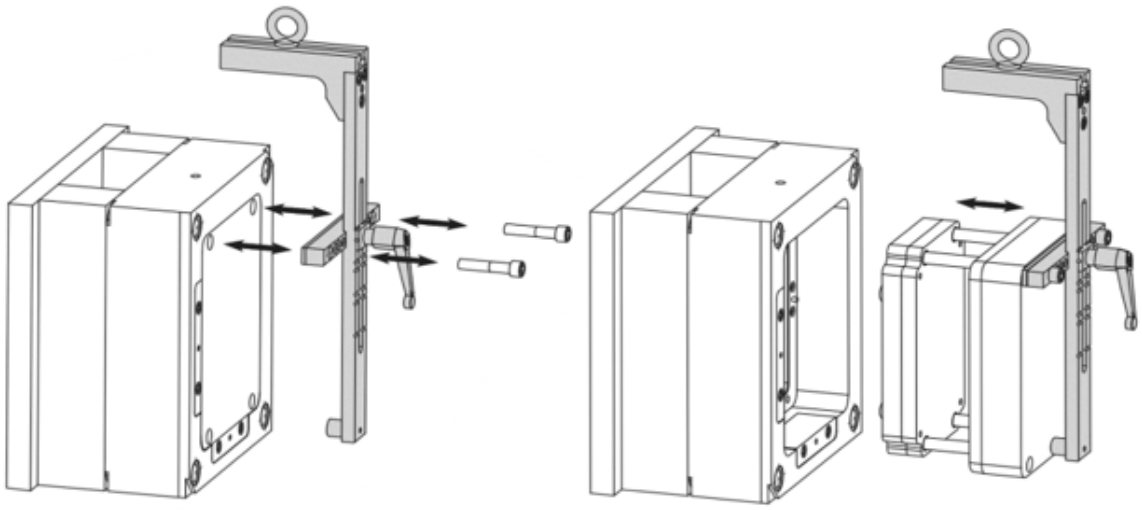

Figure 53 – Special product for injection mold connection assemblies

9.7.1 Ejection side

The moving part of the injection mold performs the movement allowing the product to be unmolded and ejected. To center the mold after clamping, the guide bush engages with the guide pillar from the injection side of the mold. The ejection side includes the ejection system ejecting the product after the main parting plane has been opened and the ejection side of the mold has departed. The ejection side also includes isolation plates located behind the clamping plate. The location of these plates ensures the magnetic clamping on the injection molding machine. The isolating plates prevent heat transfer from the mold to the machine. On the sides, support pillars are placed to center the mold when it is split into the ejection and injection sides. They facilitate handling and maintenance.

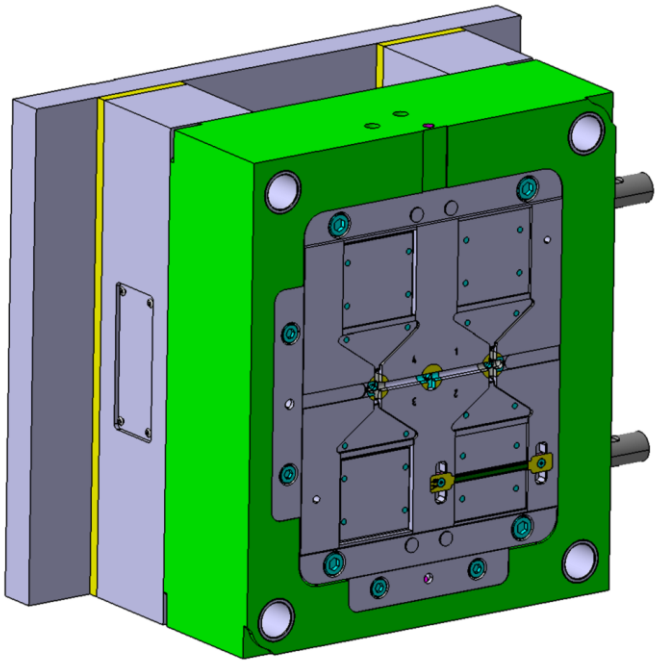

Figure 54 – Ejection side

9.7.2 Injection side

It is a non-movable part of the mold which contains a centering ring used to center the injection mold and injection molding machine. The molten material is injected into the mold through the sprue bushing located in the clamping plate and continues through the runner system into the mold cavity. The injection side also includes high-pressure sensors from Kistler company used to measure the injection pressure on the mold cavity during the injection cycle. Support pillars and isolation plate are designed in the ejection side. The purpose of these components is explained in Chapter 9.7.1.

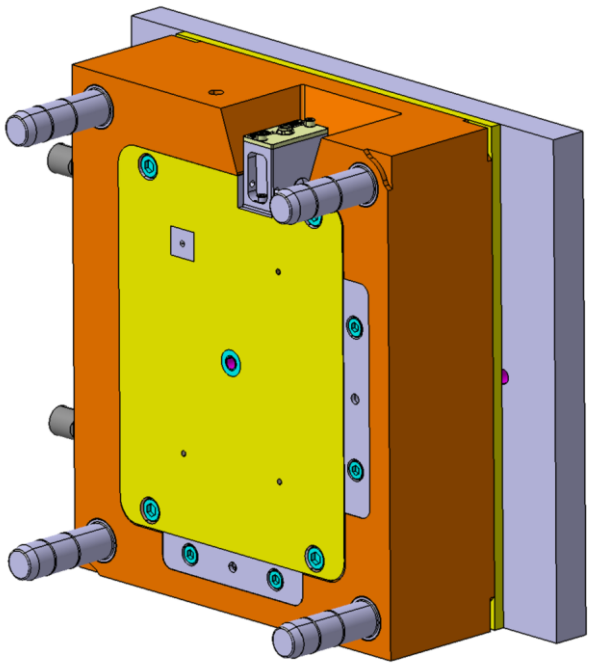

Figure 55 – Injection side

9.8 Transport equipment

Due to their size but especially the wight of the mold, transporting is difficult. For this reason, for example, forklift trucks with injection molds or cranes are used to move them. For transport and handling by cranes, a suspension device is required which must ensure safe handling of the mold. Mold handling involves camping the molds into the machine, moving the molds during production, and maintaining and storing the molds. For this mold, a transport traverse was designed for handling, which includes a hanging eye, screws to connect to the mold and the clamping block itself.

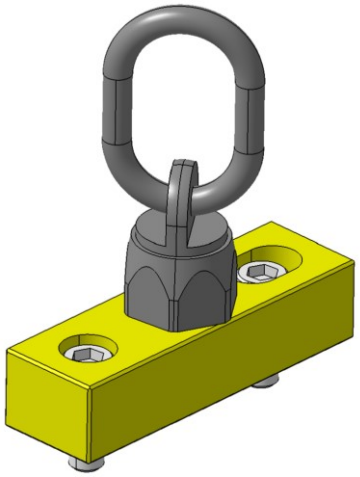

Figure 56 – Transportation traverse

10 DESIGN OF EXPERIMENT

The experimental part of the thesis investigates the machine stiffness and injection mold opening during the injection molding cycle. The experimental part was performed in the cooperation with Hirchmann automotive GmbH Rankweil, mainly with the departments of plastic technology and basic development.

The Demag and Ferromatik injection molding machines were used to determine the results. First, the process parameters, such as number of cavities of filling, mold clamping forces, packing pressure, were established. The injection mold in this experiment allows to adjust the number of cavities that are filled during the injection cycle by the flow sprue setting.

The opening of the injection mold was analyzed by a measuring device from TESA. It was placed on the injection mold with a magnetic device during so that the mold opening could be detected during the cycle.

Due to the design of experiment, it was required to use cavity number 1,3 and 4. Consequently, the lower, middle and upper point was specified. If all cavities were utilized, it would be impossible to establish the midpoint.

10.1 Testing on the Demag Injection Molding Machine

The Sumitomo Demag Intelect 180 – 450 was used for the first part of the experiment.

Table 3 – Demag Machine

Demag	
Type	180t/Ø40
Year of manufacture	2018

Table 3 describes the parameters of the Demag injection molding machine. The injection mold had to be heated to the required value according to the material sheet before the start of the experiment. This temperature was set to 90 °C and the mold was heated using HB-THERM THERMO-5. The process parameters (Table 4) were determined prior the

experiment which allows to identify all the parameters that will be subsequently included in the design of experiment created in MiniTab.

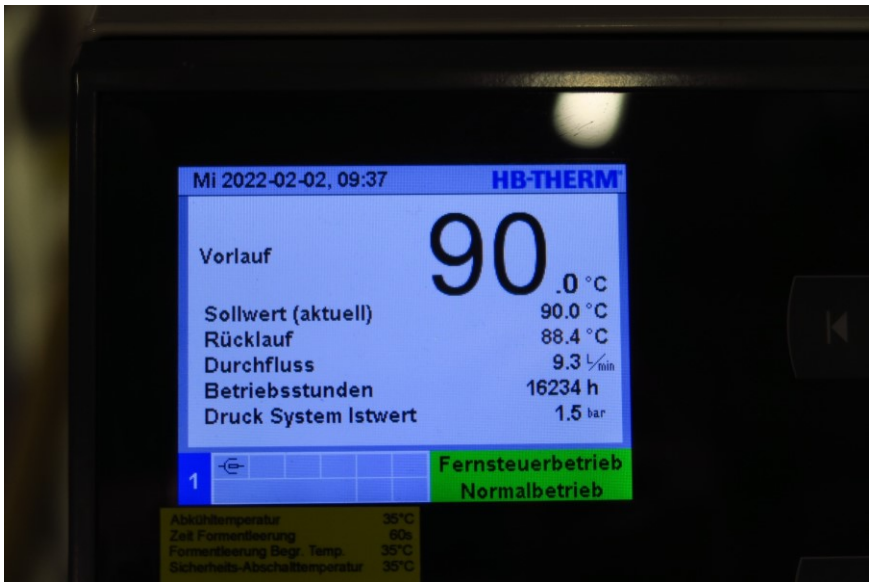

Figure 57 – Setting the tempering device (Demag)

Table 4 – Demag injection process parameters

Run order	Clamping force [kN]	Packing pressure [bar]	Number of cavities [-]	Machine type
1	35	250	2	Demag
2	10	100	1	Demag
3	60	100	1	Demag
4	10	400	1	Demag
5	60	400	1	Demag
6	10	100	3	Demag
7	60	100	3	Demag
8	10	400	3	Demag
9	60	400	3	Demag
10	35	250	2	Demag

Prior to the experiment, it was also necessary to set the injection parameters to perform the experimental measurements correctly.

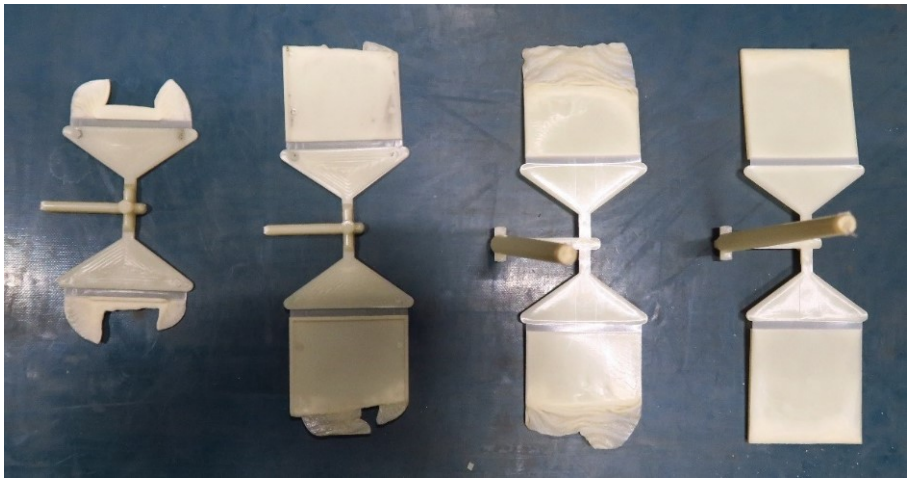

Figure 58 – Filling study of a two-cavity system (Demag)

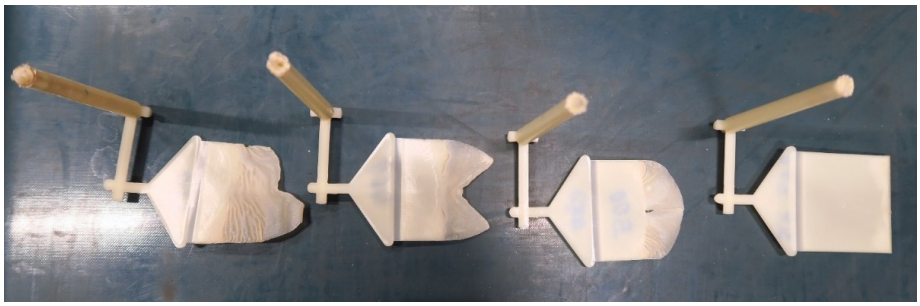

Figure 59 – Filling study of a one-cavity system (Demag)

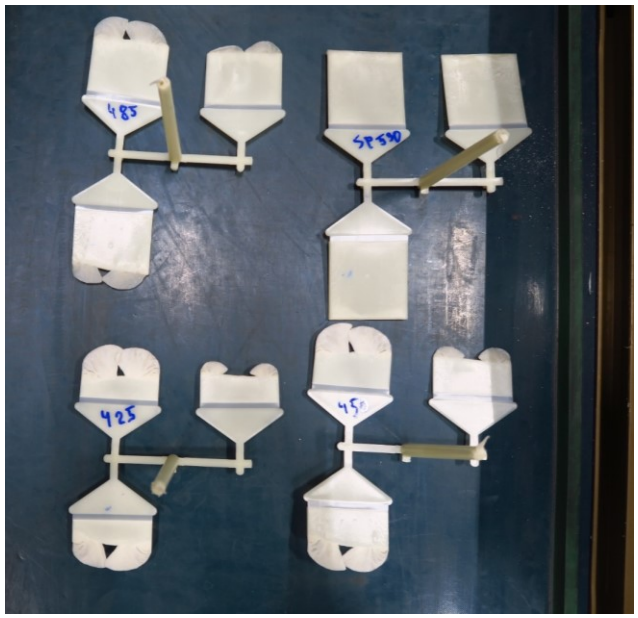

Figure 60 – Filling study of a three-cavity system (Demag)

To estimate the mold opening, formula 10.1 was used to calculate in which cases to predict it. First, it was necessary to convert the bars to MPa. Then, ANSYS software was used to establish the area of one cavity subjected to pressure during the mold opening. The area of one cavity subjected to pressure is 4630 mm^2.

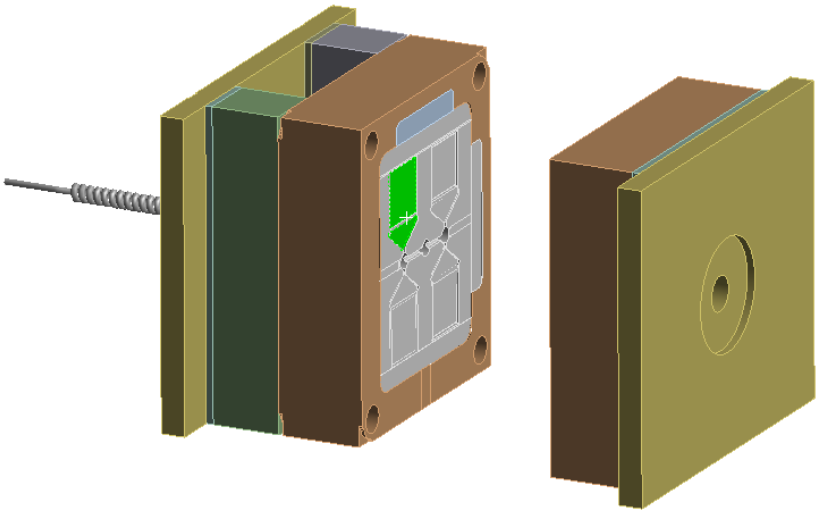

Figure 61 – Measured area of one cavity by ANSYS software

$$P = \frac{F}{S \cdot n} \rightarrow F = P \cdot S \cdot n \quad (10.1)$$

$F = 25\ MPa \cdot 4630\ mm^2 \cdot 2$ (numbers of cavities)

$F = 231\ 500\ N$

P…… Packing pressure [MPa]

F…….. Force [N]

n…….. Number of cavities [-]

S…….. Cavity area [mm²]

Using Excel, all remaining values were calculated. For round experiments 4, 6 and 8 it was found that large mold opening could be expected as the clamping force was exceeded.

Table 5 – The expected mold opening (Demag)

Run order	Clamping force [kN]	Packing pressure [bar]	Number of cavities [-]	Packing pressure [MPa]	F [N]	F [t]
1	35	250	2	25	231500	23.61
2	10	100	1	10	46300	4.72
3	60	100	1	10	46300	4.72
4	10	400	1	40	185200	18.89
5	60	400	1	40	185200	18.89
6	10	100	3	10	138900	14.17
7	60	100	3	10	138900	14.17
8	10	400	3	40	555600	56.67
9	60	400	3	40	555600	56.67
10	35	250	2	25	231500	23.61

10.2 Testing on the Ferromatik injection molding machine

The Ferromatik Milacron Elektra 155 evolution was employed in the second part of the experiment.

Table 6 – Ferromatik Machine

Ferromatik	
Type	EE 155l/Ø40
Year of manufacture	2013

Table 6 displays the parameters of the Ferromatik injection molding machine. The injection mold had to be heated to the required temperature according to the material sheet before the experiment. This temperature was set to 80 °C and the mold was heated with HB-THERM THERMO-5, the same equipment as in the Demag injection molding machine measurement.

Figure 62 – Setting the tempering device (Ferromatik)

Table 7 - Ferromatik injection process parameters

Run Order	Clamping force [kN]	Packing pressure [bar]	Number of cavities [-]	Machine type
1	35	250	2	Ferromatik
2	10	100	1	Ferromatik
3	60	100	1	Ferromatik
4	10	400	1	Ferromatik
5	60	400	1	Ferromatik
6	10	100	3	Ferromatik
7	60	100	3	Ferromatik
8	10	400	3	Ferromatik
9	60	400	3	Ferromatik
10	35	250	2	Ferromatik

Table 7 shows different injection process parameters for the experimental part using the Ferromatik machine.

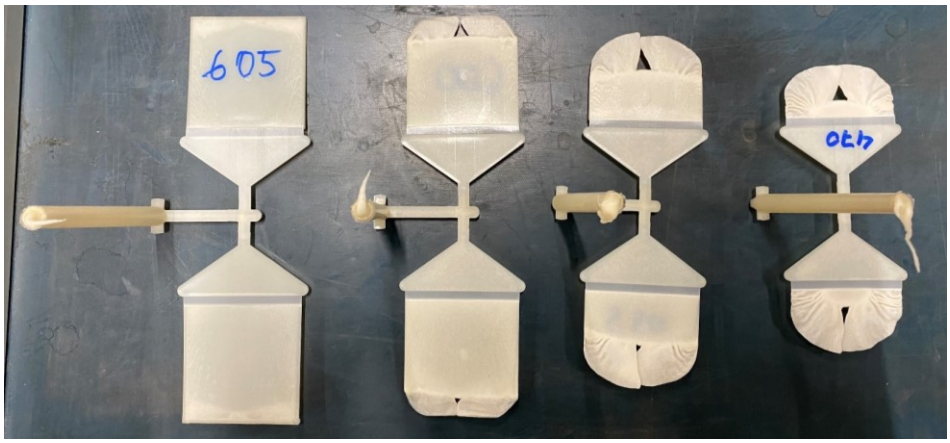

Figure 63 – Filling study of a two-cavity system (Ferromatik)

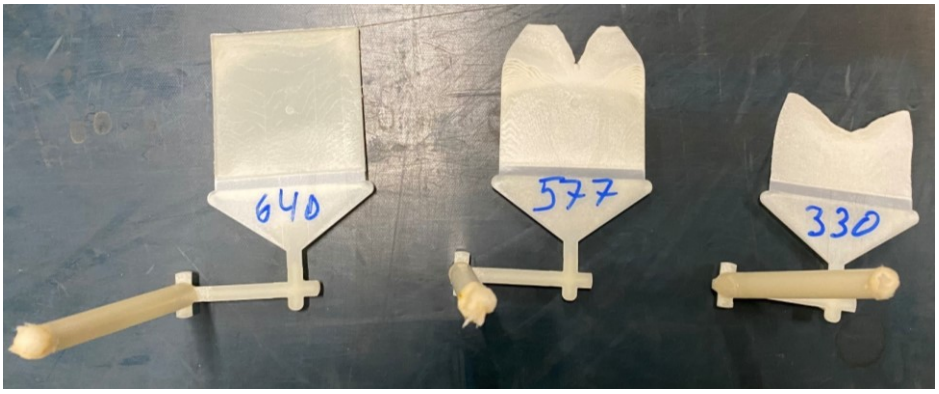

Figure 64 – Filling study of a one-cavity system (Ferromatik)

Figure 65 - Filling study of a three-cavity system (Ferromatik)

To identify the expected opening of the mold, formula (10.1) from Chapter 10.1. was used.

Table 8 - Expected mold opening (Ferromatik)

Run Order	Clamping force [kN]	Packing pressure [bar]	Number of cavities [-]	Packing pressure [MPa]	F [N]	F [Ton]
1	35	250	2	25	231500	23.61
2	10	100	1	10	46300	4.72
3	60	100	1	10	46300	4.72
4	10	400	1	40	185200	18.89
5	60	400	1	40	185200	18.89
6	10	100	3	10	138900	14.17
7	60	100	3	10	138900	14.17
8	10	400	3	40	555600	56.67
9	60	400	3	40	555600	56.67
10	35	250	2	25	231500	23.61

Table 8 shows significant forces in experiment 4, 6 and 8 using the Ferromatik machine which considerably influenced the mold opening; the same way as in Chapter 10.1 since the same process parameters were used.

10.3 Measured values of the experiment

The measurement of this experimental part evaluates the opening of the injection mold in the parting plane when the injection pressure is applied during the injection cycle. Subsequently, the mass of the injection parts has also been measured. TESA device with the accuracy of 0.01 mm was applied in monitoring the mold opening parameters. The device was fixed using a magnetic device clamped on the injection mold. Figure 6 shows the measurement weight tolerance of 0.001 g. The maximum load capacity of this weight is 320 g and minimum measurable value of 0.002 g.

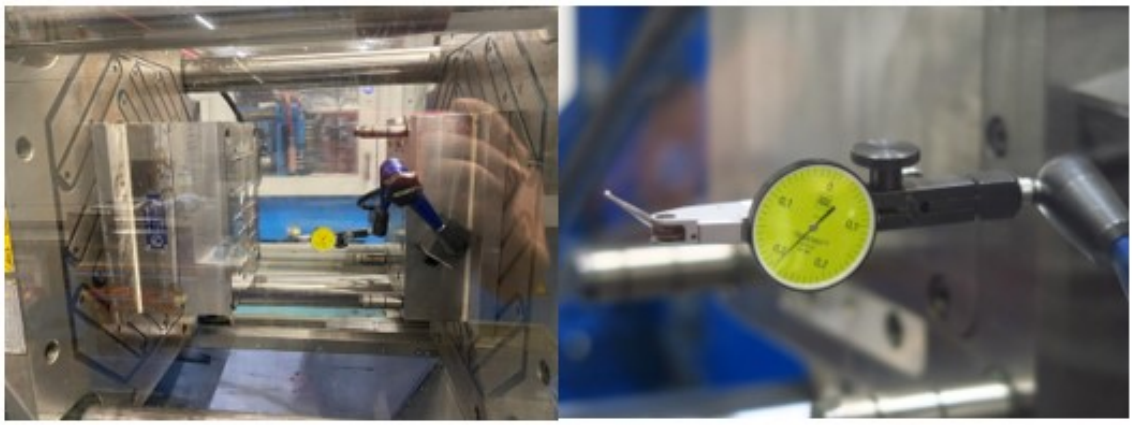

Figure 66 – Mold opening measuring device

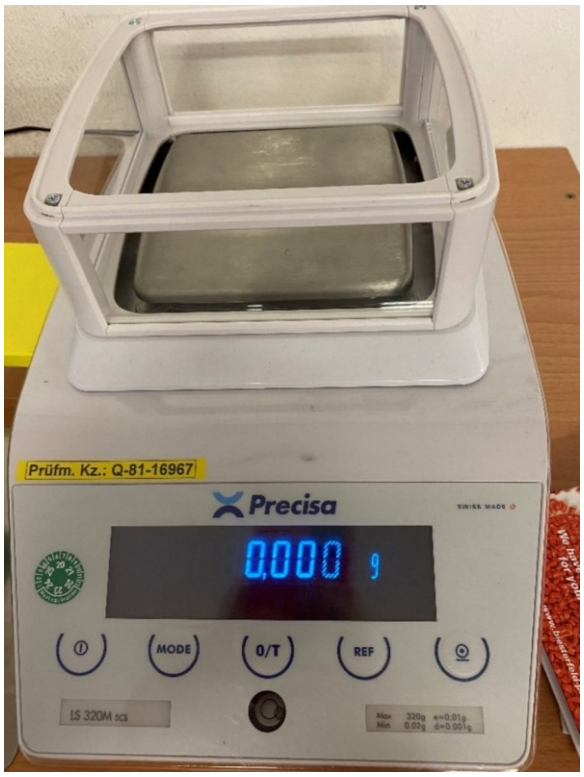

Figure 67 – Mass measuring device

The experiments were repeated 5 times following the filling study and determination of the injection parameters for a specified number of cavity fills. The measured mold opening values obtained using the Demag machine are shown in Table 9. The largest mold opening occurred in cycle 8 with the mold closing force of 10 kN and packing pressure 400 bar.

Table 9 – Mold opening (Demag)

Run Order	Mold opening 1 [mm]	Mold opening 2 [mm]	Mold opening 3 [mm]	Mold opening 4 [mm]	Mold opening 5 [mm]
1	0.005	0.005	0.005	0.005	0.005
2	0	0	0	0	0
3	0	0	0	0	0
4	0.15	0.15	0.15	0.14	0.14
5	0	0	0	0	0
6	0.08	0.08	0.09	0.1	0.11
7	0	0	0	0	0
8	0.5	0.4	0.4	0.5	0.45
9	0	0	0	0	0
10	0	0	0	0	0

The mass of the parts using the Demag machine is displayed in Table 10. All pieces ejected per cycle, including burrs, were measured. The largest value was recorded in experiment 8 where the largest injection opening was documented.

Table 10 – Mass of parts (Demag)

Run Order	Mass [g]	Mass [g]	Mass [g]	Mass [g]	Mass [g]
1	18.847	18.716	18.896	18.902	18.921
2	9.751	9.739	9.742	9.736	9.776
3	9.727	9.531	9.687	9.594	9.749
4	10.476	10.485	10.509	10.468	10.472
5	9.721	9.735	9.729	9.736	9.739
6	29.85	29.841	29.846	29.818	29.845
7	27.845	28.124	28.263	27.943	27.869
8	38.452	36.674	38.245	37.304	38.269
9	28.346	27.928	27.515	27.919	27.923
10	18.678	18.703	18.683	18.676	18.669

The measured mold opening values from the Ferromatik machine are shown in Table 11.

Table 11 – Mold opening (Ferromatik)

Run Order	Mold opening 1 [mm]	Mold opening 2 [mm]	Mold opening 3 [mm]	Mold opening 4 [mm]	Mold opening 5 [mm]
1	0.02	0.02	0.02	0.02	0.02
2	0.15	0.15	0.15	0.15	0.15
3	0	0	0	0	0
4	0.25	0.25	0.25	0.25	0.25
5	0	0	0	0	0
6	0.2	0.2	0.2	0.2	0.2
7	0	0	0	0	0
8	0.35	0.4	0.4	0.4	0.35
9	0	0	0	0	0
10	0	0	0	0	0

The mass of the parts gained using the Ferromatik machine is displayed in Table 12.

Table 12 – Mass of part (Ferromatik)

Run Order	Mass [g]	Mass [g]	Mass [g]	Mass [g]	Mass [g]
1	18.877	18.894	18.914	18.877	18.912
2	16.058	14.966	15.826	13.801	14.909
3	9.503	9.52	9.506	9.509	9.504
4	18.21				
5	9.766	9.751	9.755	9.763	9.767
6	33.622				
7	27.375	27.433	27.361	27.432	27.4
8	35.532	33.403	33.569	34.427	34.451
9	27.431	27.394	27.421	27.407	27.372
10	19.042	18.998	19.179	18.998	18.987

During the experiment with the Ferromatik machine, a problem occurred in run 4 and 6. The large mold opening caused sizable burrs in the parting plane. As can be seen in Figure 68, there was a burr of molten polymer melt into the parting plane in run 4. In this case, the mold may have been damaged as the molten polymer flowed into the screw locations connecting the mold core with the clamping plate. For this reason, the experiment had to be ended. In run 6, there were large burrs that did not allow the individual pieces to be measured accurately. For these reasons, the values could not be collected for run 4 and 6.

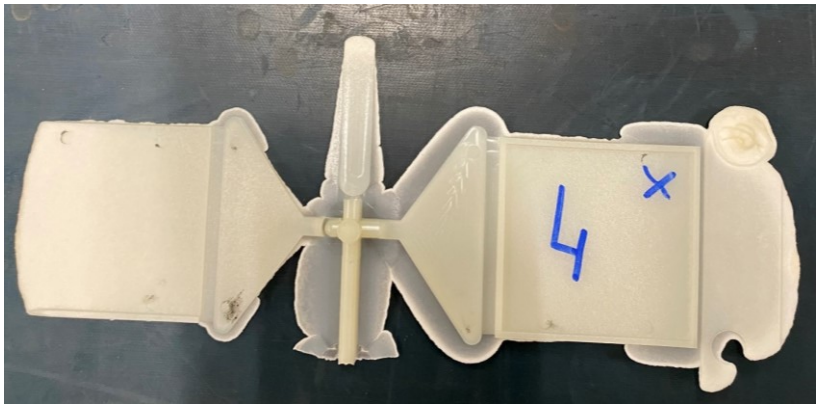

Figure 68 – An issue in run 4 using Ferromatik

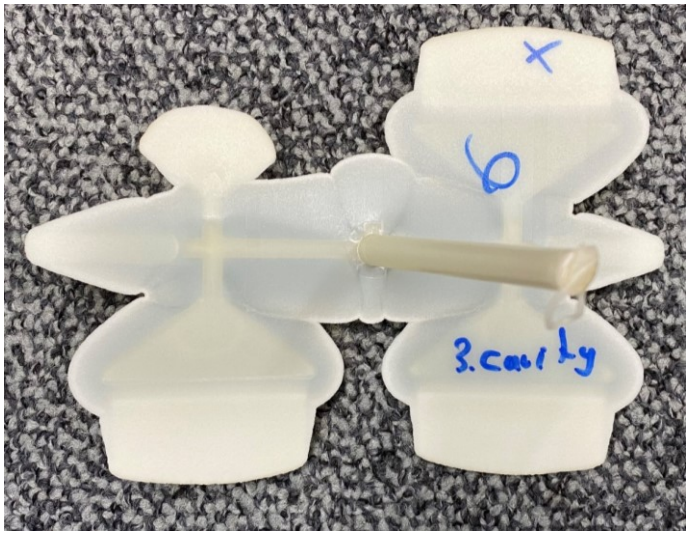

Figure 69 – An issue in run 6 using Ferromatik

10.4 Design of experimental results

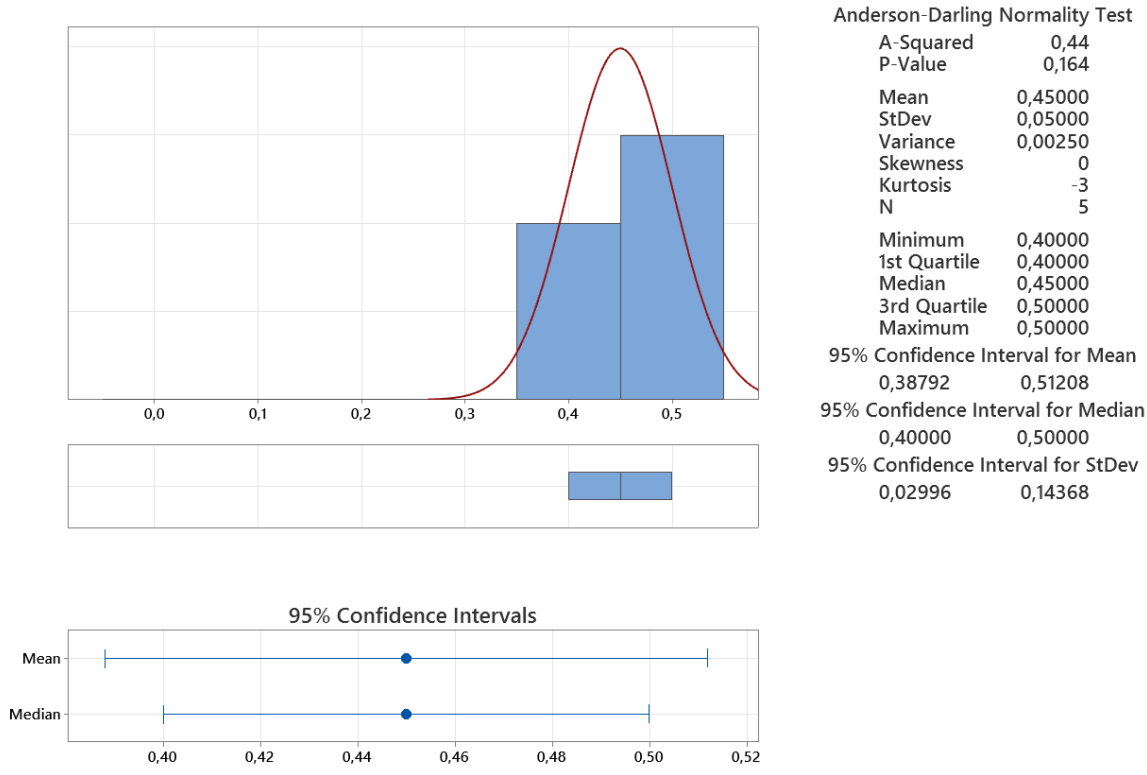

Figure 70 – Summary report of the opening in millimetres

Figure 70 shows the normal distribution obtained at the beginning of the data evaluation using MiniTAB software. It also presents that the P-Value of 0,164 is greater than $\alpha = 0,05$. Therefore, it may be summarized that a normal distribution has been achieved.

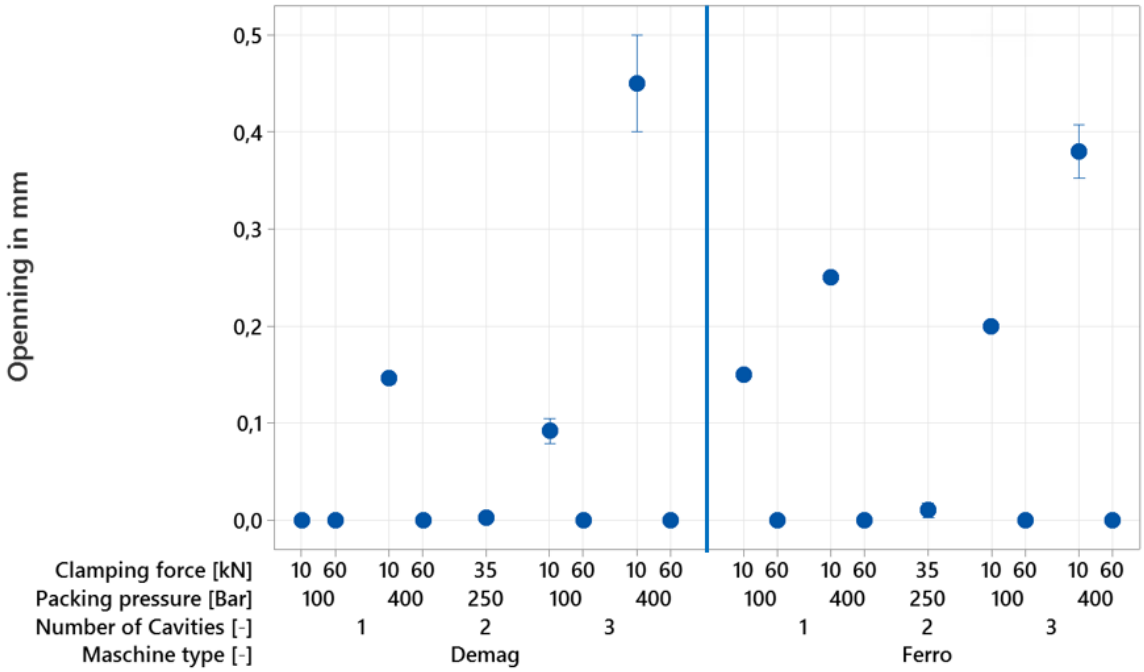

Figure 71 – Interval plot of the opening in mm

Figure 71 shows the dependence of mold opening on the clamping force, filling pressure, number of cavities and type of injection molding machine for both the Demag and Ferromatik machines. As can be seen, the Ferromatik machine provides more frequent opening during the injection cycle. On the other hand, the highest average measured mold opening value was recorded using the Demag machine. It is apparent that the most frequent mold opening occurs along with the clamping force of the injection mold of 10 kN. The injection pressure is an important factor as well as it plays a significant role in mold opening in the conditions of the high and low clamping force. For example, as the results show, the mold opening above 0.1 mm occurred in all cases at the clamping force of 10 kN and injection pressure 400 bar. Another significant factor is a number of cavities filled during the injection cycle. If only one of the cavities was filled, the Ferromatik machine had two mold openings, whereas Demag performed only one. The highest value was established with three filled cavities with the closing force of 10 kN.

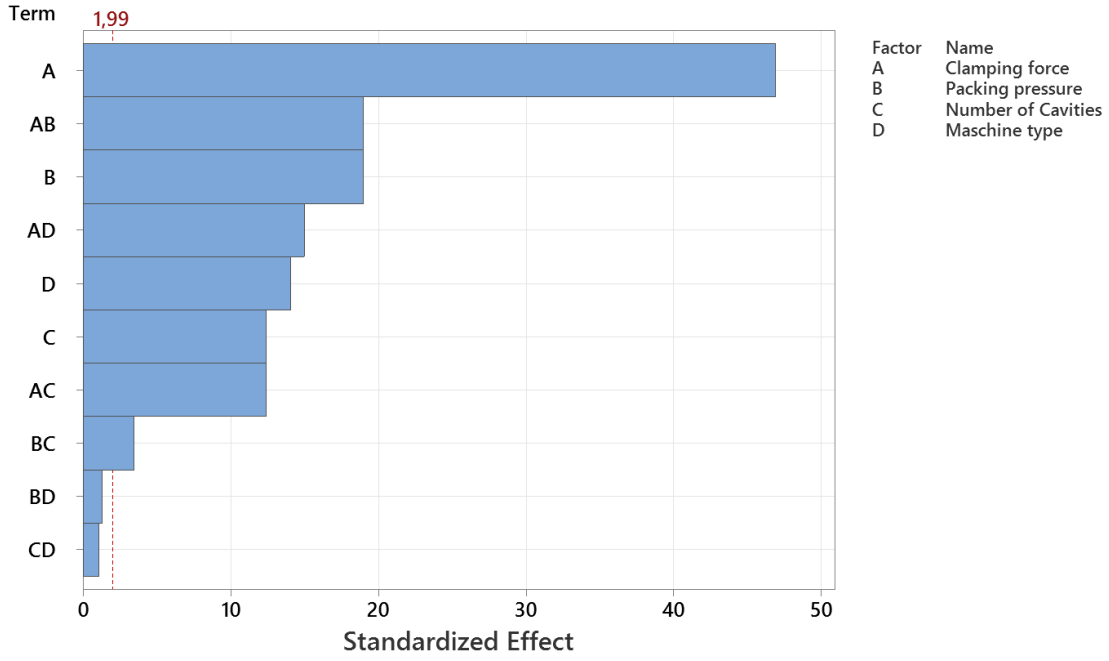

Figure 72 – Pareto chart of the standardized effects

Figure 72 is a Pareto chart showing the absolute values of the standardized effects in the scale from the largest to smallest effect. The chart also represents a reference line to indicate statistically significant effects. In this experiment, the parameters comprised in the Pareto diagram included the clamping force, packing pressure, number of cavities and type of injection molding machine. Furthermore, the Pareto diagram also contains possible combinations of these parameters.

As the Pareto diagram shows, the most significant value in this experiment is the clamping force followed by the filling pressure. It can also be concluded that all selected parameters included in the Pareto diagram are significant and the experiment could be considerably influenced by changing any of these parameters. As the least affecting factor in this experiment seems to be the combination of the filling pressure and type of injection machine including the combination of number of cavities and injection machine. However, the combination of the filling pressure and clamping force can affect the experiment as much as the filling pressure.

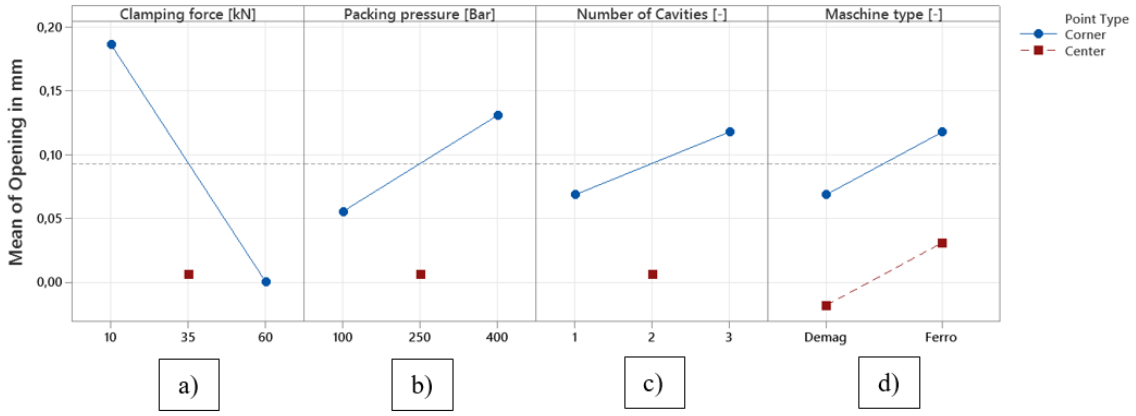

Figure 73 – The main effects for the opening in millimeters

Figure 73 shows the main effects influencing the opening of the injection mold. These graphs include a graph of the dependence of the mean of opening in mm on the clamping force, packing pressure, number of cavities and type of injection molding machine.

Graph a determines that there is no mold opening within the clamping force of 60 kN. At the same time, as the pressure increases, the probability of the mold opening grows. The curve in the graph shows that as the value of the clamping force increases, the probability of mold opening declines.

Graph b displays an increasing curve expressing that as the packing pressure increases, the tendency to open the mold rises. The mean of mold opening was slightly above 0.05 mm at 100 bar while it was above 0.1 mm at 400 bar.

From graph c can be seen that the number of the filled cavities affects the mold opening as the curve grows from one cavity to three cavities. The lowest mean of the opening ranged from 0.05 m to 0.1 mm while for three cavities this value varied between 0.1 mm and 0.15 mm.

Graph d depicts the dependence of the injection molding machine on mold opening and expresses that the Demag machine provided a smaller mold opening if compared with the Ferromatik machine.

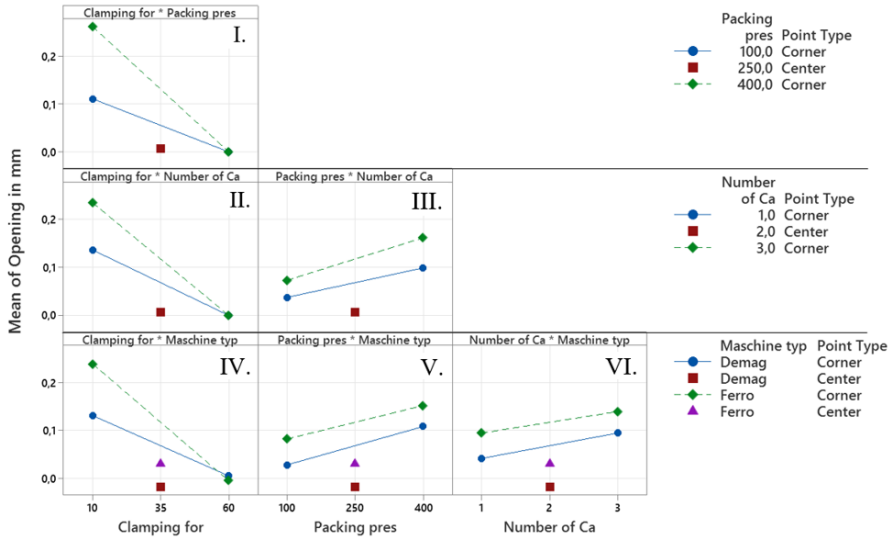

Figure 74 – Interactions for the opening in millimeters

Figure 74 shows the interactions of the mold opening. Graph I depicts the dependence of the clamping force, mean of opening and packing pressure. The green curve indicates the filling pressure of 400 bar and the blue curve 100 bar. It can be stated that there is no mold opening at the clamping force of 60 kN. Both curves express a linear decline; however, the 400 bar curve shows a steeper decline and it could be concluded that up to 1.5 times more mold opening occured at 400 bar than at 100 bar.

Graph II displays the dependence of clamping force and number of cavities on the mean of opening. It can be seen that no injection mold opening occurred at the clamping force of 60 kN and filling number of 3 cavities. At the clamping force of 10 kN, more injection mold openings were observed for 3 cavities than for 1 cavity.

Graph III, dealing with the filling pressure and number of cavities per diameter, shows two types of curves. The blue curve clearly shows that the maximum mean of opening to 0.1 mm occurs within the filling of a single cavity.

Graphs IV, V and VI express the dependence of the clamping force, packing pressure, number of cavities and type of injection machine on the mean of opening. All these relationships clearly establish that the Ferromatic machine provided more frequent injection mold opening during the experiment.

As can be seen in Figure 73 and 74, there was only a small opening of the injection mold with the pressure of 250 bar, filling number of 2 cavities and clamping force of 35 kN. This was due to the setting parameters of the experiment as the clamping force was not exceeded.

11 MOLDFLOW SIMULATION

The simulation was simplified to a full model because it was unnecessary to obtain deformation results. This step avoided errors that might have occurred during the simulation. The simulation primarily focused on the analysis of the filling study. The results from the filling studies were chosen to establish general parameters and were not specified for a special type.

11.1 Mesh preparation

The mesh around the corner of the gate system had to be refined to ensure a better-quality mesh in the area. Without modifying that area, the calculation would not have been possible because of possible errors during the calculation. The size of the main elements was set to 0.6 mm. Considering geometry, 5-layer BLM mesh type was used.

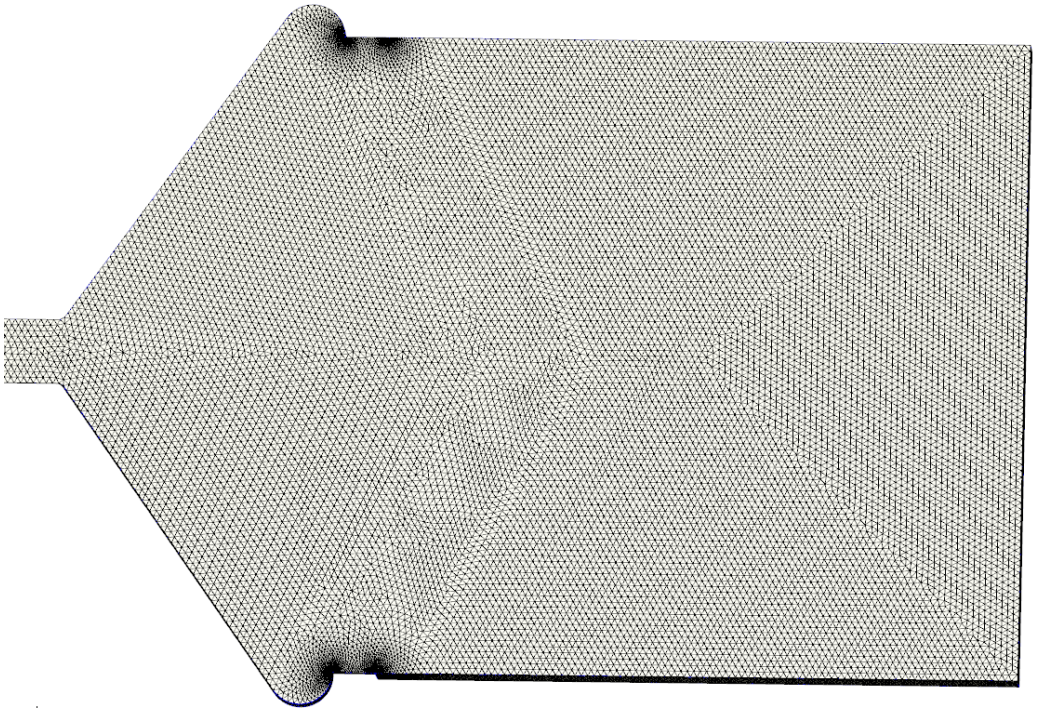

Figure 75 – Part Meshing

The mesh can be seen in detail in Figure 76 and 77. In both cases, the surface five-layer mesh was used. Regarding the detail of the gate system, the system selected only one tetra element between the two five-layer mesh.

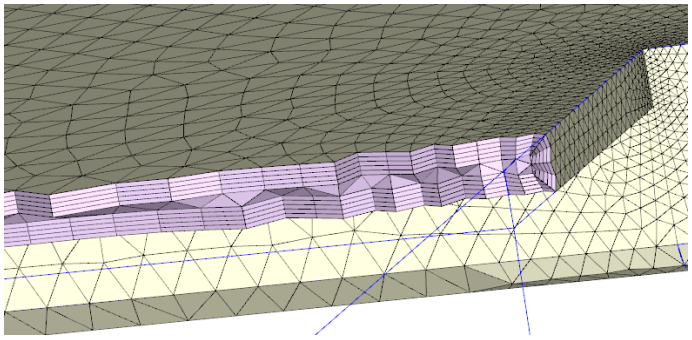

Figure 76 – Mesh detail of the gate system

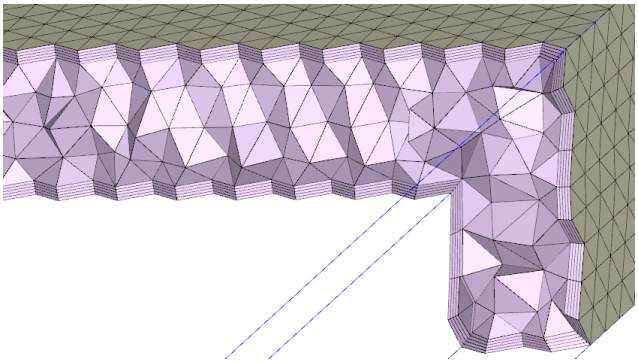

Figure 77 – Part mesh detail

```
Moldex3D MDE File Version = 21001
Moldex3D MDE File Type = Standard cool
Created by = Moldex3D-Designer Build 2021.1
Unit = mm

Sensor Node Count: 0
Fixed Node Count: 0
Coolant Entrance Node Count: 2
Coolant Exit Node Count: 2
Measure Node Count: 0

Cooling Channel Line Count: 0
Heating Rod Line Count: 0

Moldbase Count: 1

Melt Entrance : Yes
Symmetry Boundary Condition : No
User Define Boundary Condition : Yes

Cavity Solid Mesh Node Count: 955915
Cavity Solid Mesh Element Count: 2641749
Cavity Solid Mesh Volume: 41090.743521
Cold Runner Solid Mesh Node Count: 2410
Cold Runner Solid Mesh Element Count: 2016
Cold Runner Solid Mesh Volume:: 273.906818
Hot Runner Solid Mesh Node Count: 0
Hot Runner Solid Mesh Element Count: 0
Hot Runner Solid Mesh Volume:: 0.000000

Bad Orthognality Count: 0
Bad Jacobian Count: 0

Total Nodes of Solid Mesh: 958325
Total Elements of Solid Mesh: 2643765
```

Figure 78 – Mesh statistic

11.2 Setting of the process conditions

One – cavity		Two – cavity		Three – cavity	
Model Details		**Model Details**		**Model Details**	
Mesh Type	Solid	Mesh Type	Solid	Mesh Type	Solid
Solid Mesh Eleme...	**2,680,058**	**Solid Mesh Eleme...**	**2,260,151**	**Solid Mesh Eleme...**	**4,388,917**
Part	1,855,705	Part	1,440,859	Part	2,641,749
Cold Runner	2,016	Cold Runner	2,016	Cold Runner	2,016
Moldbase	631,621	Moldbase	626,560	Moldbase	1,639,168
Cooling Channel	190,716	Cooling Channel	190,716	Cooling Channel	105,984
Surface Mesh Ele...	**157,128**	**Surface Mesh Ele...**	**149,438**	**Surface Mesh Ele...**	**266,732**
Part	157,128	Part	149,438	Part	266,732
Dimension	**(mm)**	**Dimension**	**(mm)**	**Dimension**	**(mm)**
Part	114.00x81.93x130...	Part	210.00x81.93x130....	Part	210.00x160.00x13...
Mold	618.45x568.50x61...	Mold	618.45x568.50x61...	Mold	396.00x346.00x33...
Volume	**(cc)**	**Volume**	**(cc)**	**Volume**	**(cc)**
Part	19.93	Part	29.88	Part	41.09
Cold Runner	0.08	Cold Runner	0.08	Cold Runner	0.27
Material		**Material**		**Material**	
Part	PA66_RadilonARV...	Part	PA66_RadilonARV...	Part	PA66_RadilonARV...
Temperature	**°C**	**Temperature**	**°C**	**Temperature**	**°C**
Freeze	238.000	Freeze	238.000	Freeze	238.000
Process Condition		**Process Condition**		**Process Condition**	
Time	**sec**	**Time**	**sec**	**Time**	**sec**
Filling	1.000	Filling	1.000	Filling	1.000
Packing	5.000	Packing	5.000	Packing	5.300
Cooling	16.500	Cooling	16.500	Cooling	10.300
Mold Open	5.000	Mold Open	5.000	Mold Open	5.000
Cycle	27.500	Cycle	27.500	Cycle	21.600
Temperature	**°C**	**Temperature**	**°C**	**Temperature**	**°C**
Melt	300.000	Melt	300.000	Melt	290.000
Mold	100.000	Mold	100.000	Mold	90.000
Ejection	218.000	Ejection	218.000	Ejection	218.000
Air	25.000	Air	25.000	Air	25.000
VP Switch-Over	**%**	**VP Switch-Over**	**%**	**VP Switch-Over**	**%**
By Volume Filled	99.800	By Volume Filled	99.800	By Volume Filled	99.000

Figure 79 – Moldflow setting of the process simulation

11.3 Cooling system

The cooling system is used to cool the part to the ejection temperature more quickly. For the balance of the mold, in general, the greater mass of the injection molded product, the shorter working cycle and the greater difference between the melt and mold temperature, the more heat must be dissipated per unit time.

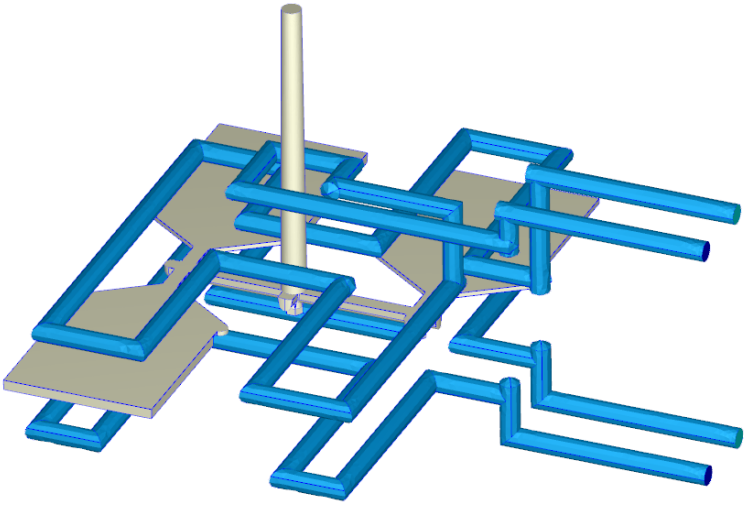

Figure 80 – Cooling system geometry

The designed cooling system is divided into upper and lower tempering systems in order to achieve tempering when the mold is opened on both sides, i.e., in particular in the core and cavity.

11.4 Characteristics of the cooling medium

Water was selected as the cooling medium. The channels are drilled to a diameter of 8 mm, and the flow rate is 120 cm^3/s bar. The inlet tempering medium temperature is 90 °C.

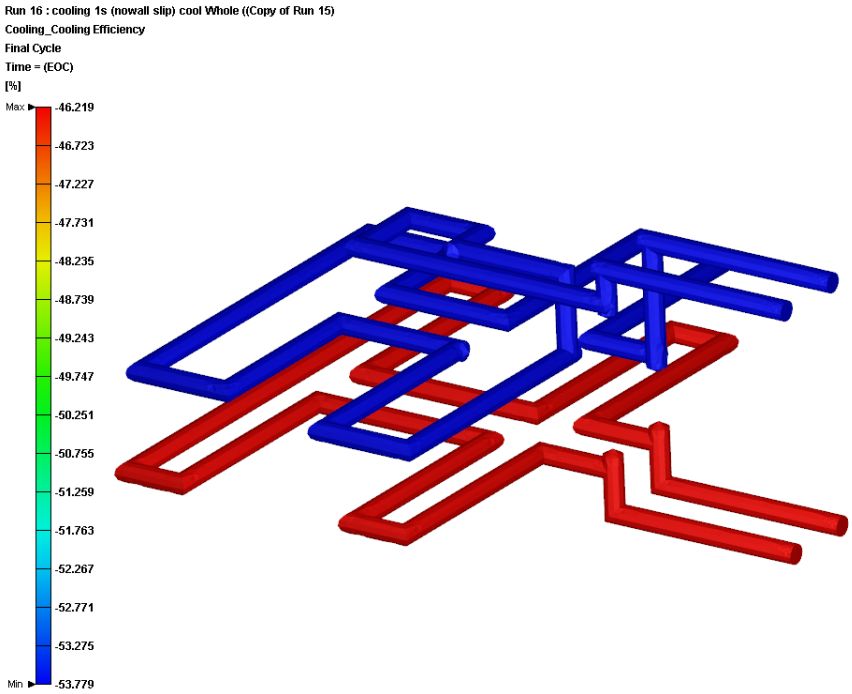

Figure 81 – Cooling efficiency

This is the cooling efficiency of the cooling channel. If Q2 is the total heat absorbed through one surface of the cooling channel and Qp is the heat released by the part during the pressing cycle, the cooling efficiency of the cooling channel is defined as Q2/Qp · 100 %. Figure 81 indicates the percentage of total heat removed by the cooling channel [34].

11.5 One–cavity filling

Figures 82, 83, 84 and 85 illustrate the filling of the mold cavity for a single cavity at 60 %, 65 %, 80 %, 99 %. At 60 % product filling, the injection pressure was 24,8 MPa in the simulation and the pressure was approximately 33 MPa in the area of this filling in the experimental part. At 65 % filling, the pressure in the simulation was 35.806 MPa and in the experiment it was approximately 35 MPa in this area. Considering 80 % filling, the pressure in the simulation was 42.504 MPa and in the experiment the pressure was 50 MPa in this area. At 99 % filling, the pressure in the simulation was 52.940 MPa and the pressure was 55 MPa in this area in the experiment. The inaccuracies may stem from different conditions; they were ideal in the simulation, while the real conditions may be influenced by the actual condition of the machine and its wear. Filling data obtained using both machines were compared with the simulation data.

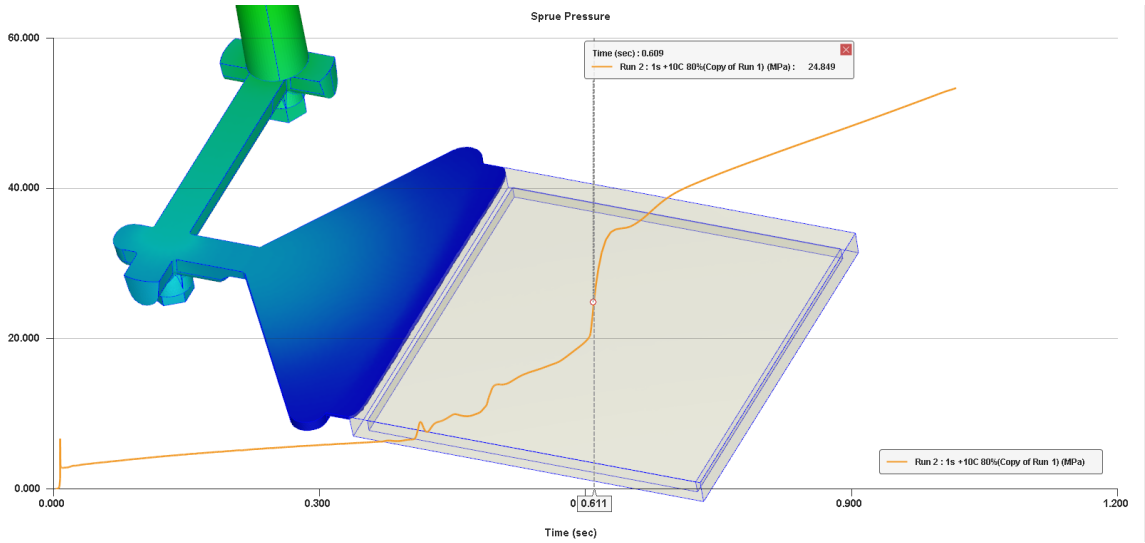

Figure 82 – One–cavity filling 60 %

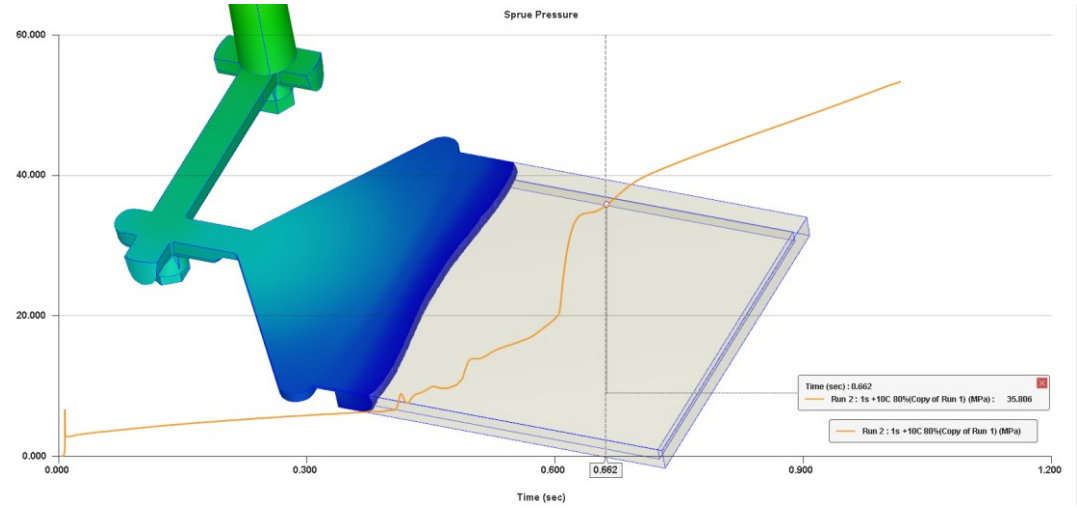

Figure 83 – One–cavity filling 65 %

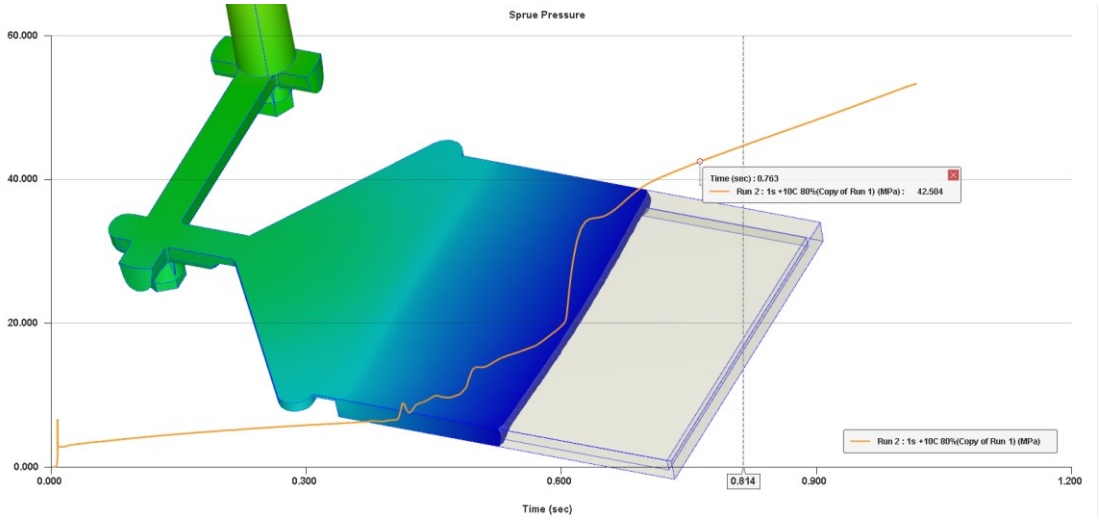

Figure 84 – One–cavity filling 80 %

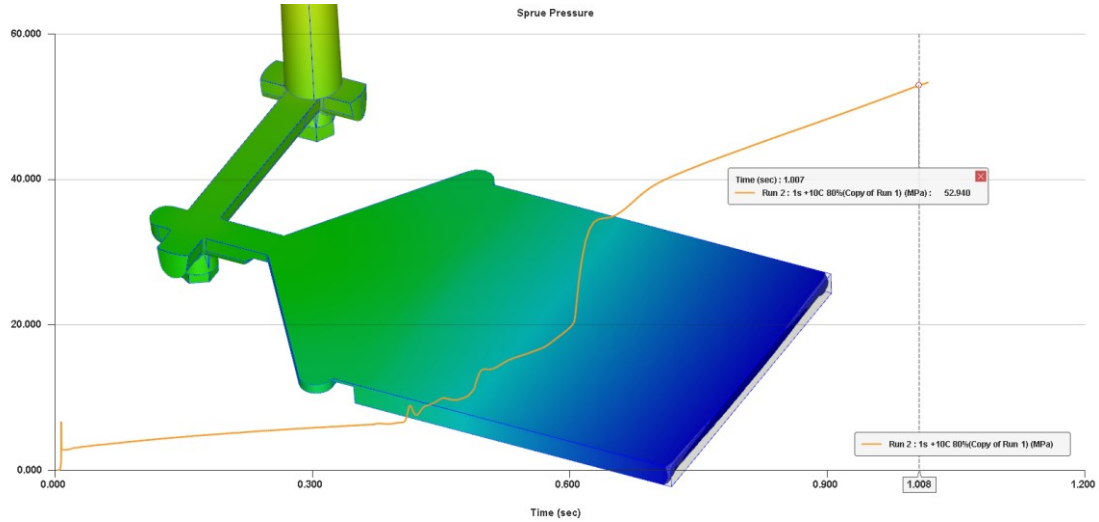

Figure 85 – One–cavity filling 99 %

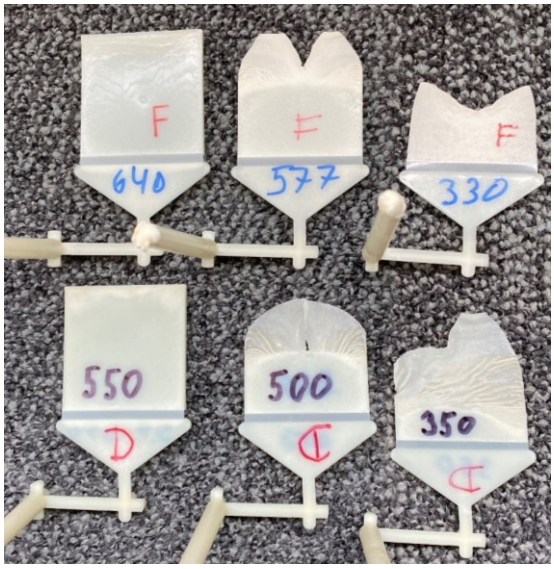

Figure 86 – Filling studies of one–cavity system from Demag and Ferromatik machine

11.5.1 Sprue pressure curve for one–cavity system

Figures 87 and 88 show the plotted pressure curves from the simulation and experimental parts. Figure 87 displays the pressure curve calculated from the simulation using Moldex3D with the injection pressure of 1 s and packing pressure of 80 %. Figure 88 shows two curves with the injection time of 1.4 s. The red curve expresses the injection pressure with the packing pressure of 80 %. The green curve presents the injection pressure from the previous cycle where the packing pressure was set to approximately 20 %. Both pressure curves show the filling similar in shape; however, considering the simulation at about 0.5 s the more detailed curve is monitored. The simulation injection time was 1 s whereas for the experiment it was 1.4 s. This difference may play a significant role in the cavity filling and shear rate. The difference in the injection time between the simulation and experimental part reflects the conditions that could not be set in Moldex3D, such as the machine and mold wear, product quality, and operator's experience.

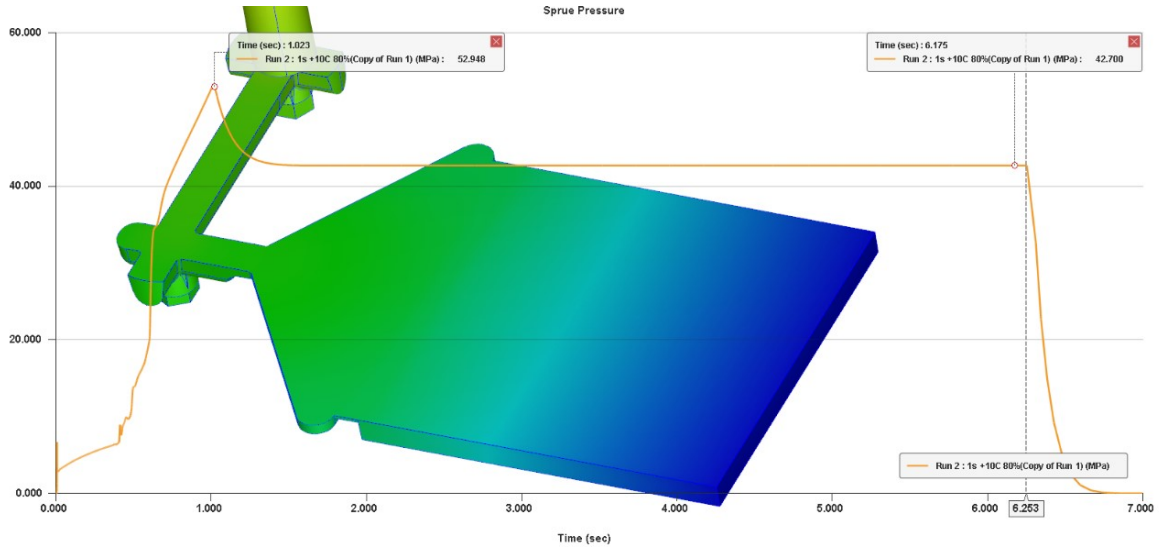

Figure 87 – Pressure curve of one–cavity system (Moldex3D)

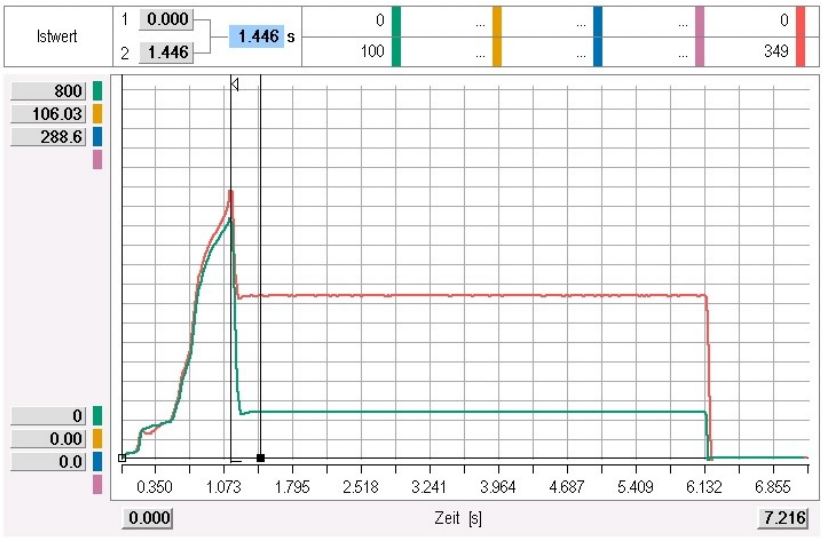

Figure 88 – Pressure curve of one–cavity system (Demag)

11.6 Two–cavity filling

Figures 89, 90, 91 and 92 illustrate the filling of the mold cavity for two cavities at 48 %, 60 %, 90 %, 99.5 %. At 48 % filling of the product, the injection pressure was 28.2 MPa in the simulation and the pressure was approximately 38 MPa in this area in the experimental part. At 60 % filling, the pressure was 41.3 MPa in the simulation and it was approximately 40 MPa in this area in the experiment. For 90 % filling, the pressure was 54.8 MPa in the simulation and the pressure determined by the experiment was 60 MPa in this area. At 99.5 % filling, the simulated pressure was 59.5 MPa and the experimental pressure in this area was 60.5 MPa. The inaccuracies may reflect may stem from different conditions which were ideal in the simulation, while the real conditions may be influenced by the actual

condition of the machine and its wear. Filling data gained from both machines were compared with the simulation data. The simulated filling % is similar to the results obtained in the experiment.

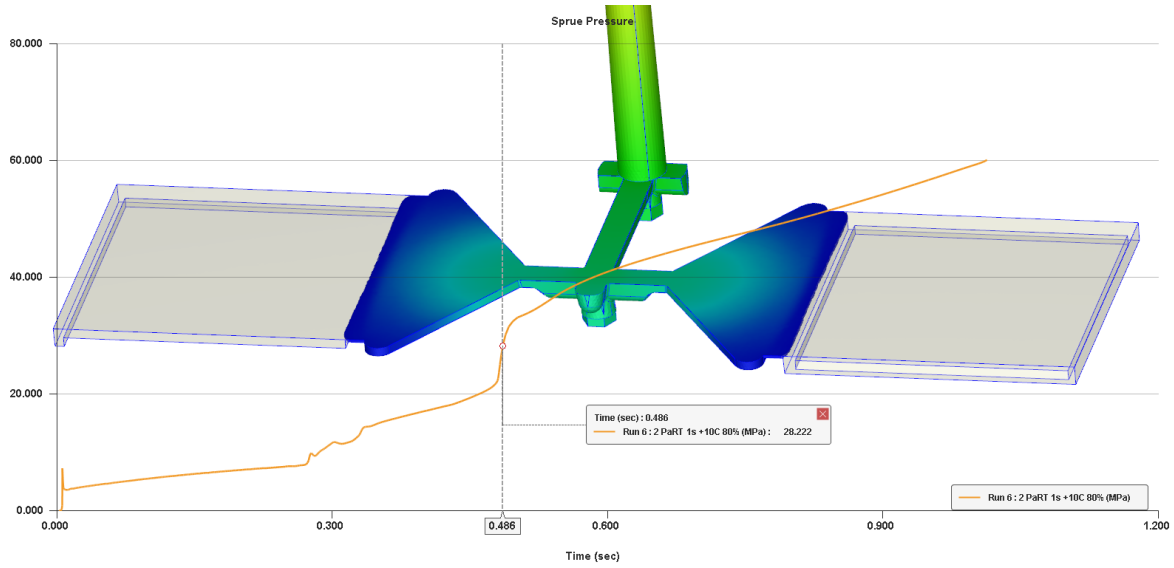

Figure 89 – Two–cavity filling 48 %

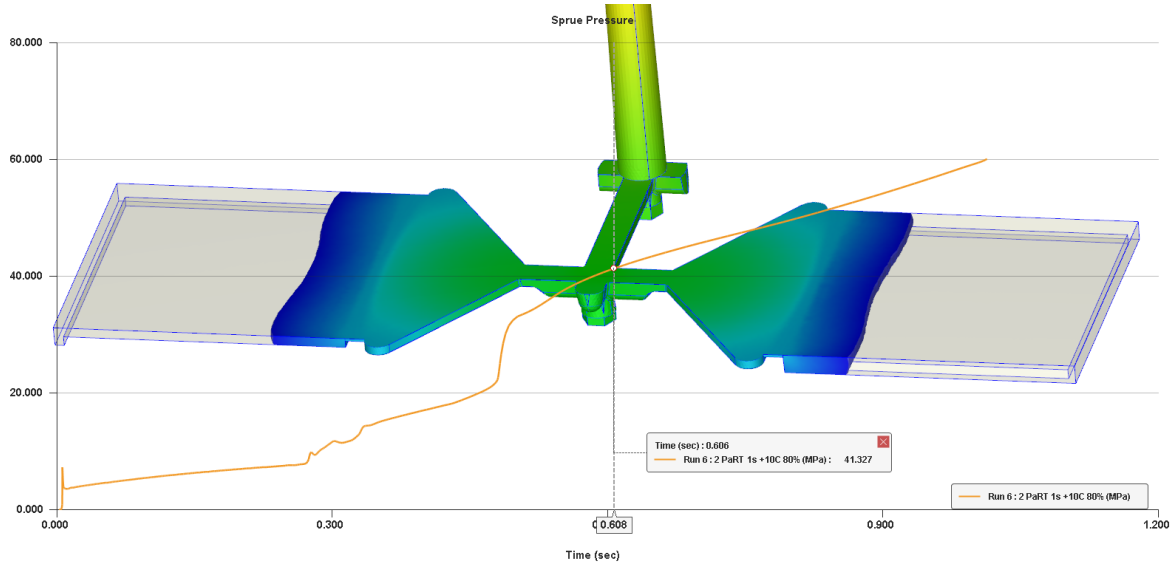

Figure 90 – Two–cavity filling 60 %

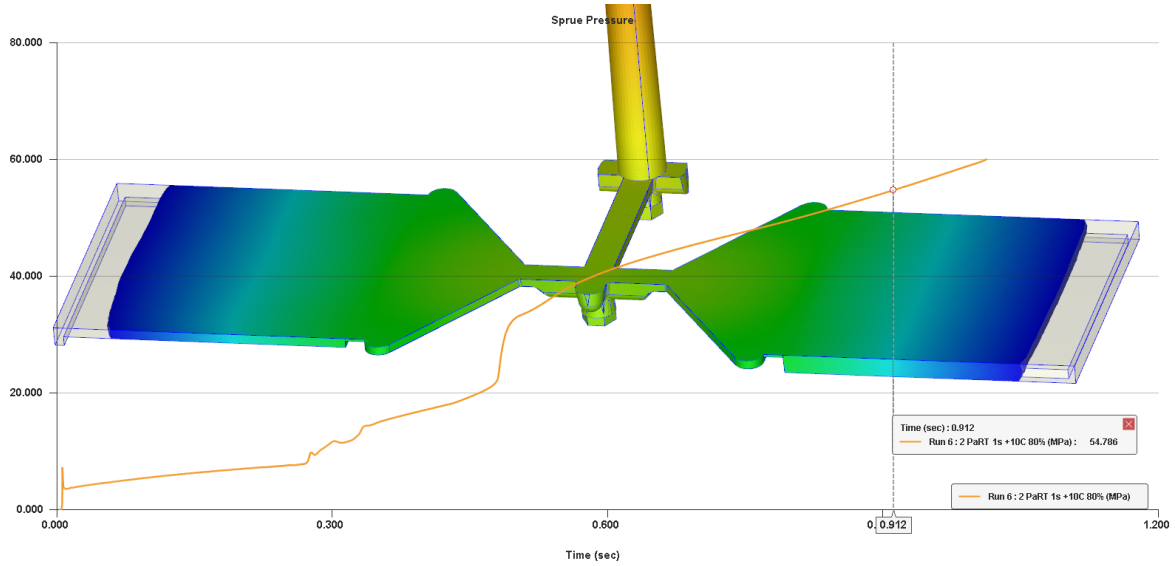

Figure 91 – Two–cavity filling 90 %

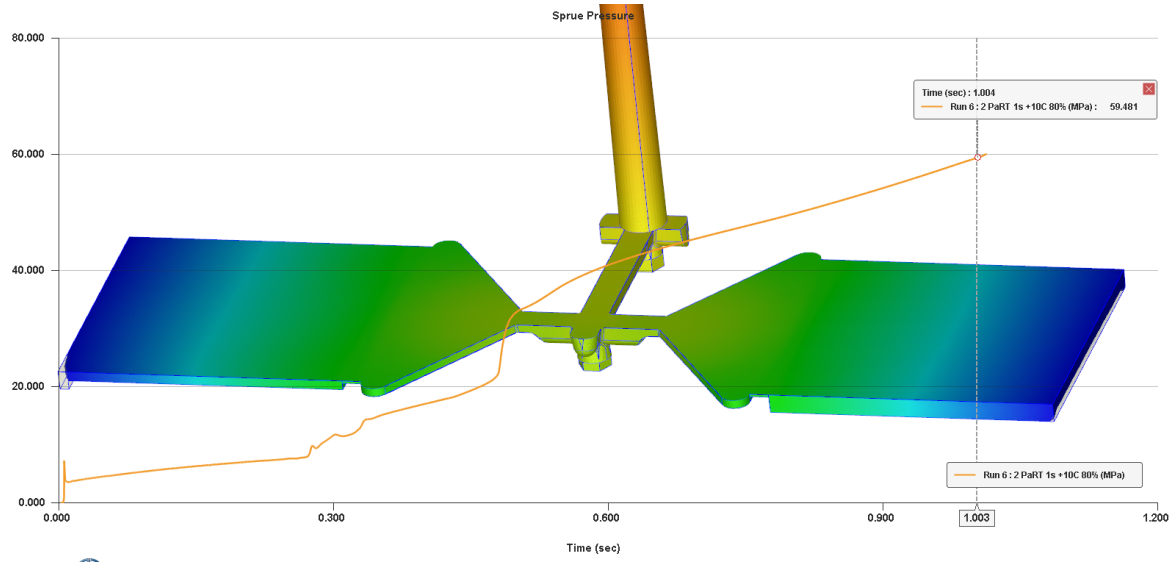

Figure 92 – Two–cavity filling 99.5 %

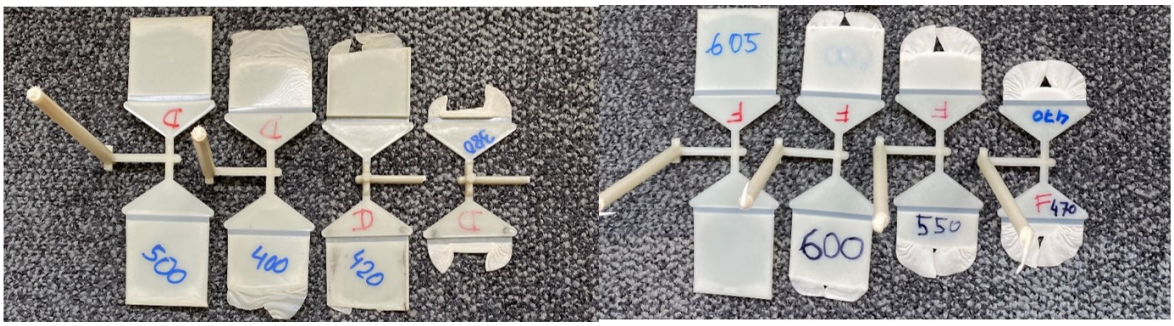

Figure 93 – Filling studies of two–cavity system from Demag and Ferromatik machine

11.6.1 Sprue pressure curve for two–cavity system

Figures 94 and 95 show the pressure curves from the simulation and experimental parts. Figure 94 depicts the pressure curve calculated from the simulation using Moldex3D with the injection pressure of 1 s and packing pressure of 80 %. Figure 95 shows two curves with the injection time of 1.4 s. The red curve expresses the injection pressure with the packing pressure of 80 %. The green curve shows the injection pressure from the previous cycle where the packing pressure was approximately 60 %. The simulation injection time was 1 s whereas the experimental time was 1.4 s. This difference may influence the cavity filling and shear rate. The diversity in the injection time in the simulation and experiment indicates the conditions that could not be set in Moldex3D, such as the machine and mold wear, product quality, and operator's experience.

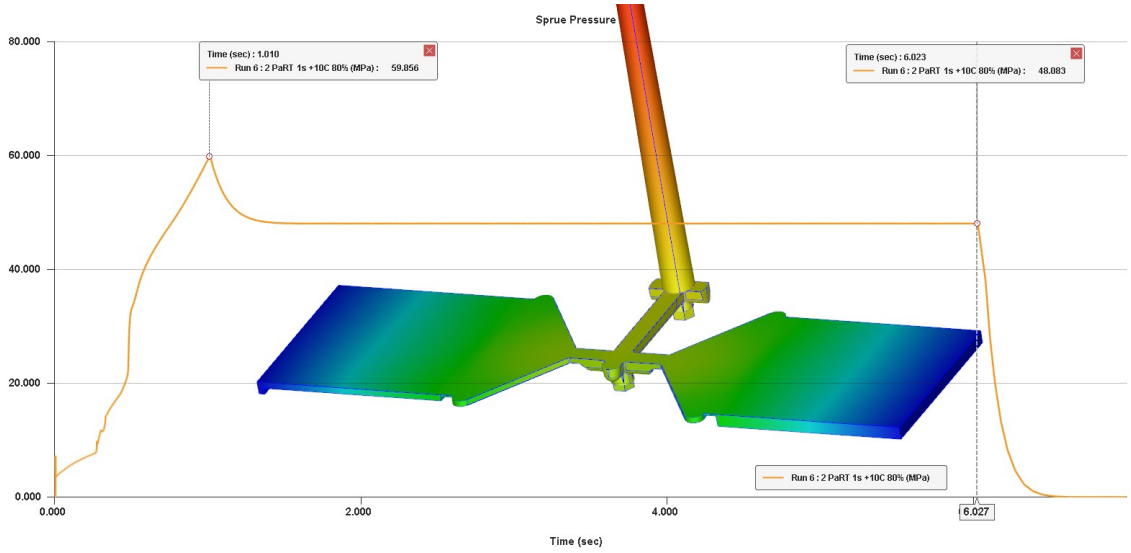

Figure 94 – Pressure curve of two–cavity system (Moldex3D)

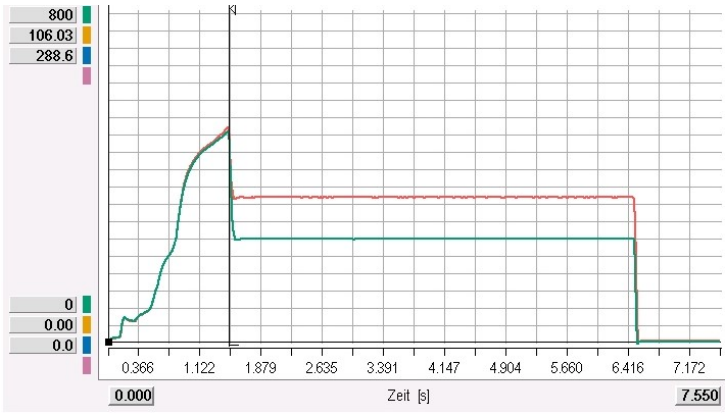

Figure 95 – Pressure curve of two–cavity system (Demag)

11.7 Three–cavity filling

Figures 96, 97, 98 and 99 depict the filling of the mold cavity for three cavities at 44.5 %, 60 %, 90 %, 99 %. At 44.5 % filling of the product, the simulated injection pressure was 33.8 MPa while the experimental pressure was approximately 42 MPa. At 60 % filling, the simulated pressure was 53.2 MPa and the experimental 45 MPa. For 90 % filling, the simulated pressure was 65.8 MPa and the experimental pressure was 60 MPa. At 99 % filling, the pressure was 67.6 MPa in the simulation and the experimental pressure was 65 MPa. These variations may be caused by different conditions in the simulation and real experiment. The data obtained from both machines were compared with the simulation data. In most of the cases, the pressure on the injection machine during the experiment was bigger than during the simulation.

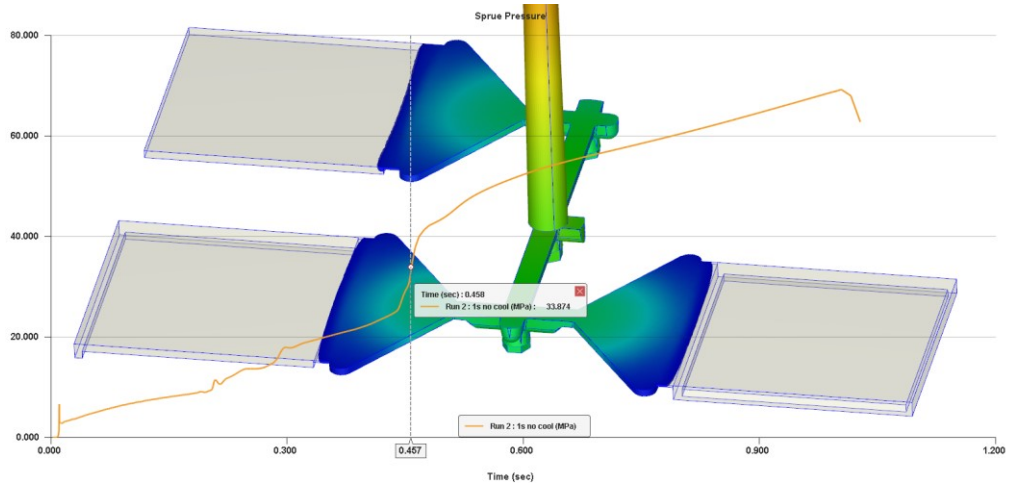

Figure 96 – Three–cavity filling 44.5 %

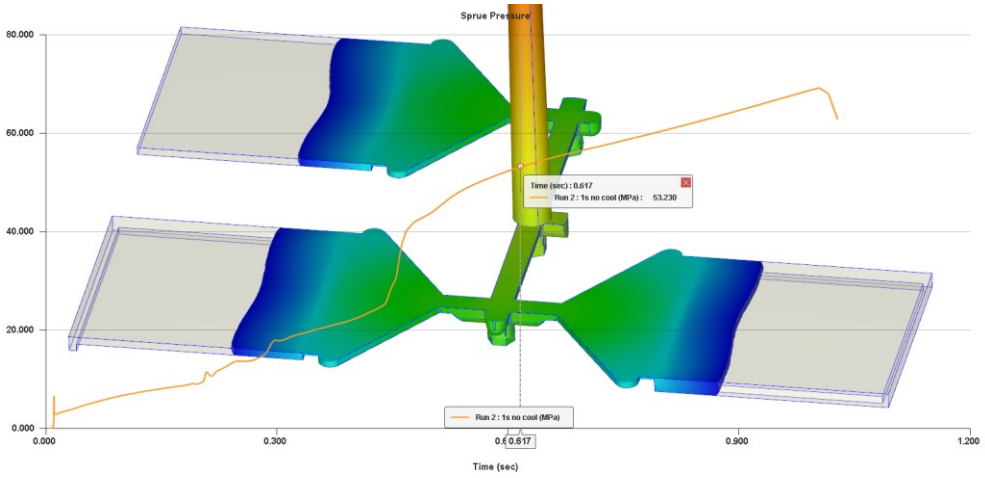

Figure 97 – Three–cavity filling 60 %

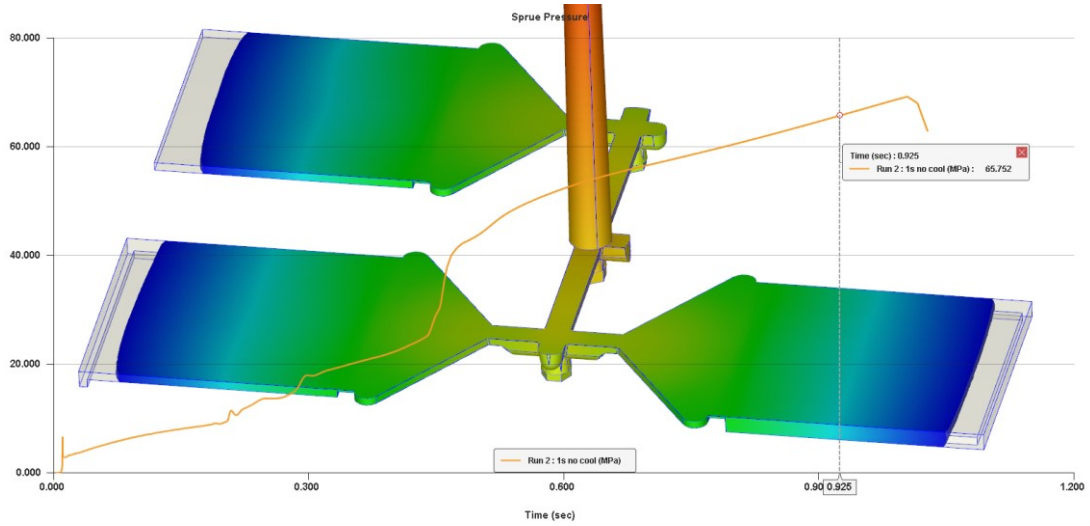

Figure 98 – Three–cavity filling 90 %

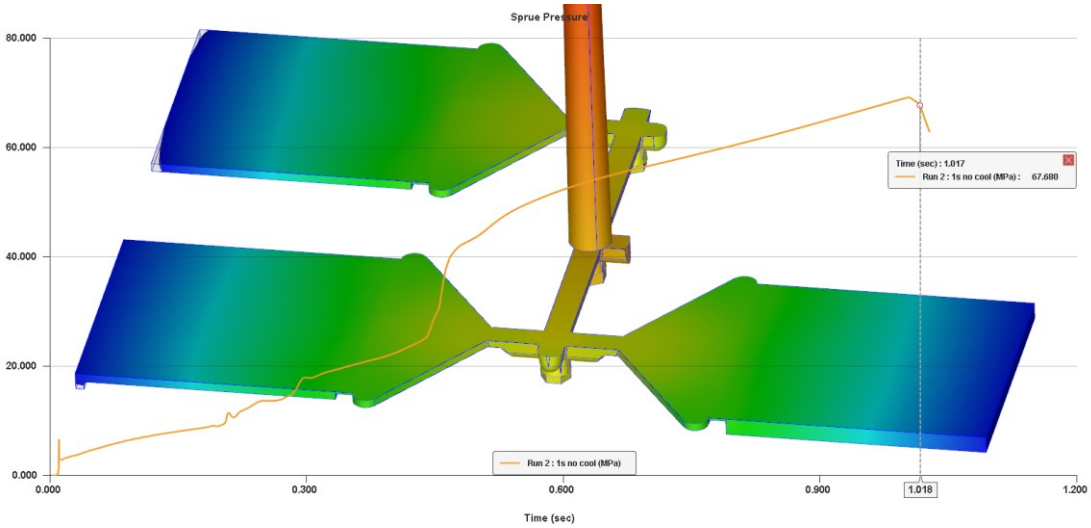

Figure 99 – Three–cavity filling 99 %

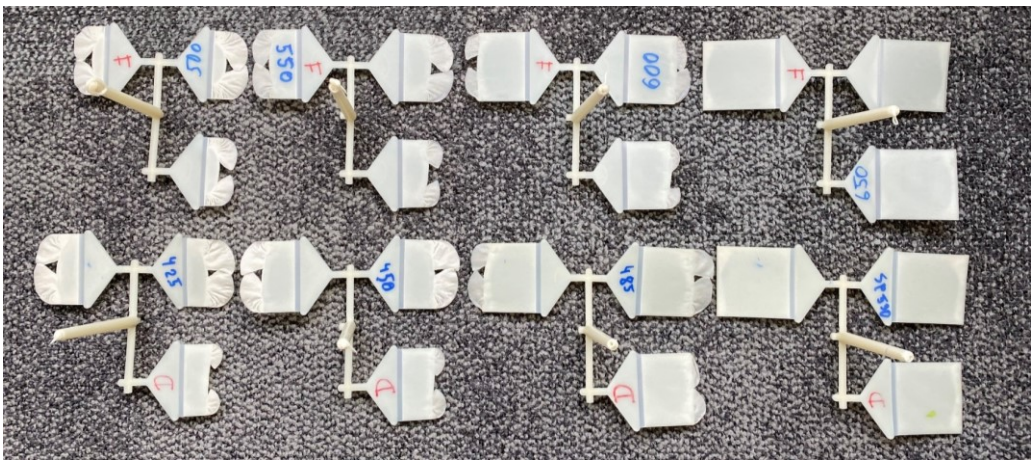

Figure 100 – Filling studies of three–cavity system using Demag and Ferromatik machine

11.7.1 Sprue pressure curve for three–cavity system

Figure 101 and 102 shows the pressure curves from the simulation and experimental parts. The pressure curve calculated from the simulation using Moldex3D with the injection pressure of 1 s and packing pressure of 80 % is in Figure 101. Two curves with the injection time of 2 s are shown in Figure 102. The red curve represents the injection pressure without any packing pressure. The green curve expresses the injection pressure from the previous cycle with the packing pressure of 20 %. The 20 % packing pressure in the green curve responds to the injection parameters that did not require high packing pressure while the ideal product quality was achieved. The simulation injection time was 1 s whereas the experimental time was 2 s. This difference may influence the cavity filling and shear rate. The difference in the injection time between the simulation and experimental part reflects the conditions that could not be set in Moldex3D, including the machine and mold wear, product quality, and operator's experience.

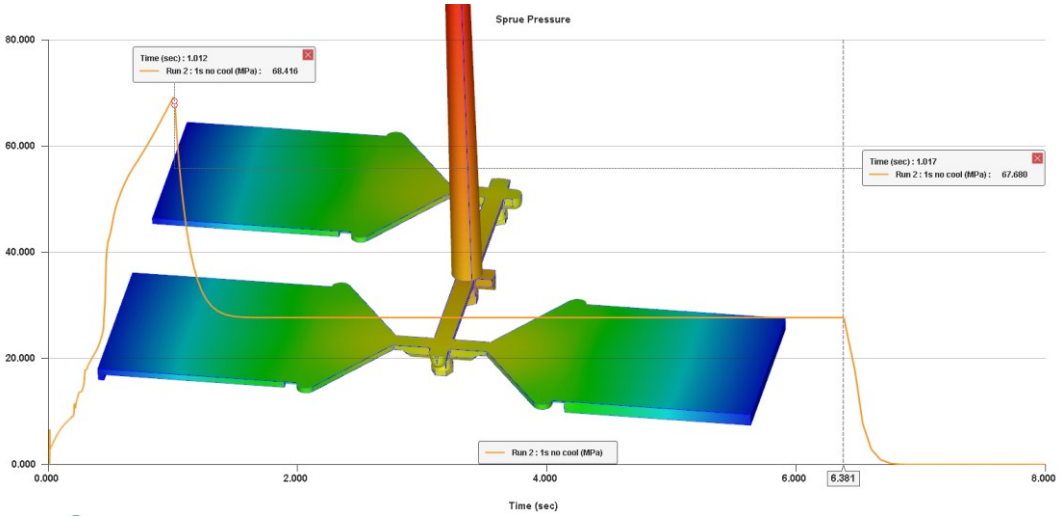

Figure 101 – Pressure curve of three–cavity system (Moldex3D)

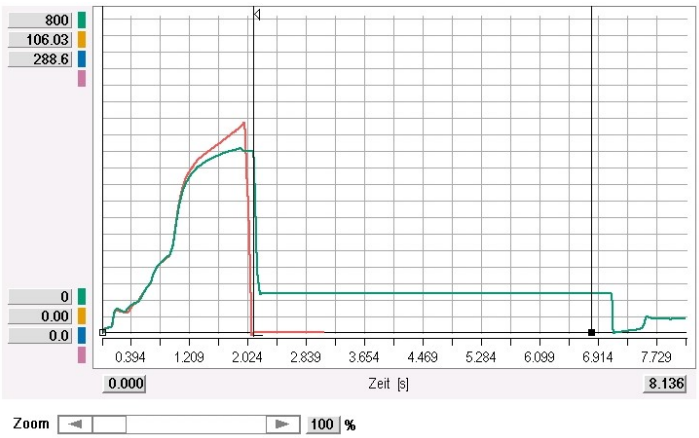

Figure 102 – Pressure curve of three–cavity system (Demag)

12 STRUCTURAL MECHANICAL ANALYSIS

In this thesis the finite element Analysis (FEA) is used to perform structural mechanical analysis with the program packet ANSYS 2020 R2.

The simulation focuses on the mold deformation during the injection cycle and mold opening during the application of pressure onto the mold cavity.

A parametrical FEA model was set up to simulate all cycles of the experiment using a set of parameters. After the setup of such a kind of model, a set of parameters can be passed automatically as input parameters. Then the FEA analysis is tarted with these parameters corresponding to one point of DOE. After the solution is obtained, ANSYS automatically reports the output as a numerical value. In this work the output is the mold opening.

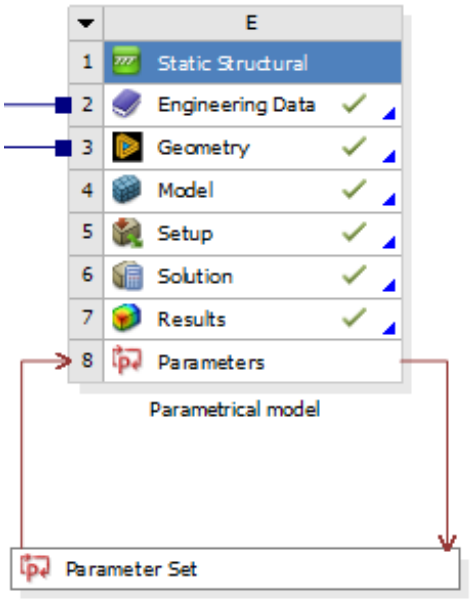

Figure 103 – Parametrical FEA model

The following setting has been established for all 20 cycles in the experiment, but the procedure and the results from each step will be discussed for only one cycle from the Demag machine (Run number 8). The results of the other runs can be found in the ANSYS project data because all FEA runs are retained and can be reviewed in ANSYS Workbench.

Table 13 – Run number 8 (Demag)

Run Order	Clamping force [kN]	Packing pressure [Bar]	Number of Cavities [-]	Machine type
8	10	400	3	Demag

12.1 Mesh preparation

First, the injection mold was simplified by removal of all minor details and holes to reduce the overall calculation time. Small gaps were removed to have continuous mesh with nodes shared over the borders of the parts.

With this continuous mesh there was no need to set up contacts or multipoint constrains to fix the parts together. This significantly reduces CPU time for the solution.

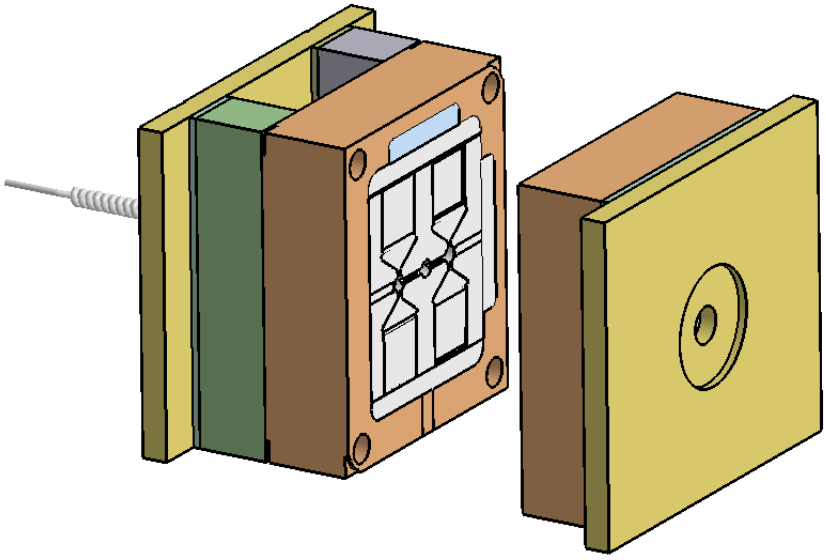

Figure 104 – Simplified injection mold assembly

Figure 104 shows a fully meshed injection mold assembly. The overall element size selected for this model was 20 mm. The whole model contains 75352 nodes and 46638 elements with paraboloid shape function (Solid 186/Solid 187).

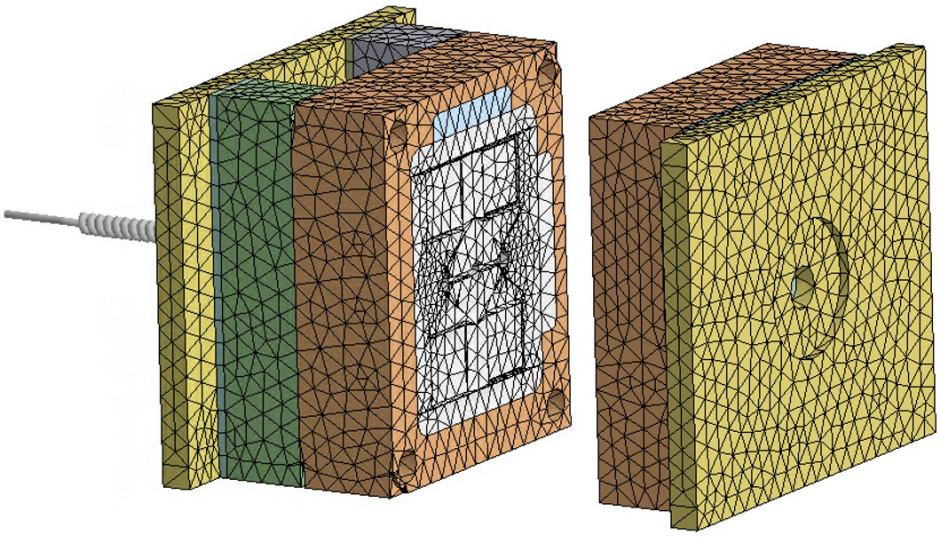

Figure 105 – Mold assembly meshing

12.2 Material properties

In this analysis, all parts follow the material definition of structural steel. As plastic deformations are not expected, the definition of elastic properties is sufficient.

Structural Steel

Fatigue Data at zero mean stress comes from 1998 ASME BPV Code, Section 8, Div 2, Table 5-110.1

Density	7,85e-09 tonne/mm³

Structural	
Isotropic Elasticity	
Derive from	Young's Modulus and Poisson's Ratio
Young's Modulus	2e+05 MPa
Poisson's Ratio	0,30000
Bulk Modulus	1,6667e+05 MPa
Shear Modulus	76923 MPa
Isotropic Secant Coefficient of Thermal Expansion	1,2e-05 1/°C
Compressive Ultimate Strength	0 MPa
Compressive Yield Strength	250,00 MPa

Figure 106 – Structural steel material properties

12.3 Boundary conditions

Figure 107 shows the boundary conditions for the injection side. A fixed support was used on the injection side in all sub-steps to prevent movement in all three axes as well as when clamping the injection mold to the injection machine.

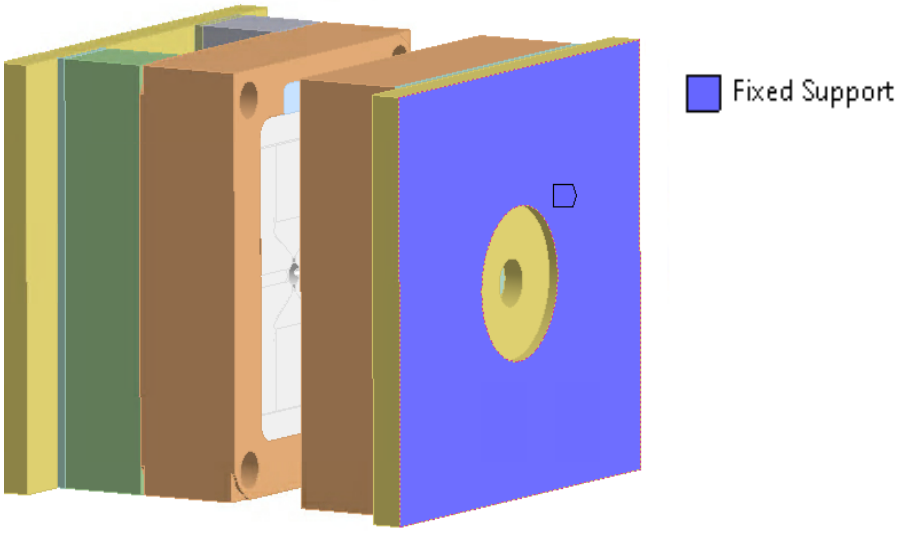

Figure 107 – Boundary conditions for the injection side

In loadstep 1 the clamping force rose over time as a preload on the spring system as a parameter.

The stiffness of the spring system corresponds with the stiffness of the Demag and Ferromatik machines used in the experimental part. Figure 108 includes table of machine stiffness shown as longitudinal stiffness. The values of the clamping force were taken from the table in the experimental part and the machine stiffness was calculated using Excel.

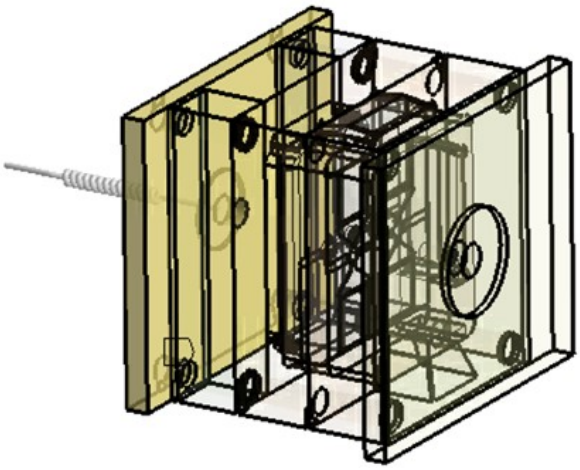

Definition	
Material	None
Type	Longitudinal
Spring Behavior	Both
P Longitudinal Stiffness	1,0174e+006 N/mm
Longitudinal Damping	0, N·s/mm
Preload	Load
P Load	-98100 N
Suppressed	No
Spring Length	278,97 mm
Element APDL Name	

Figure 108 – The stiffness of the machine

Figure 107 shows the fixation of mold movement in the X direction only. For this simulation, four translational joints were used for the best simulation of the movement of the four guide pillars during the mold opening and closing.

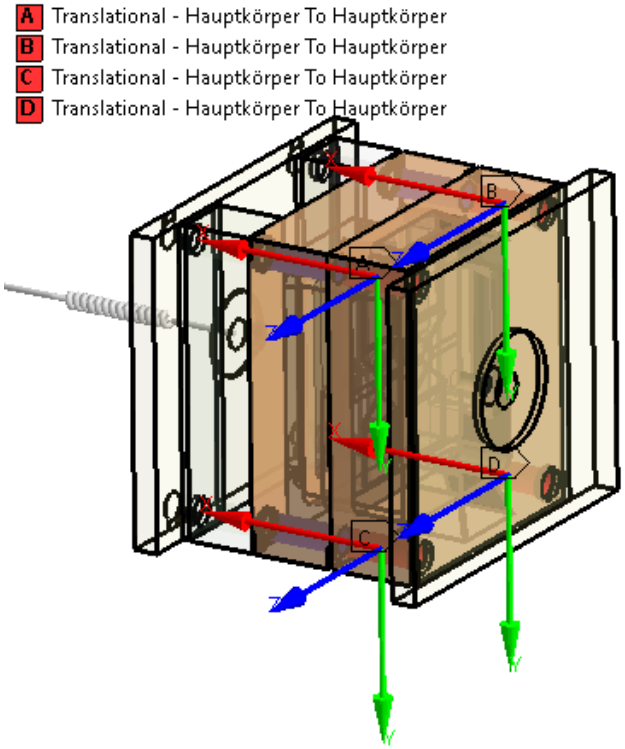

Figure 109 – Boundary conditions of guide pillars

Figure 110 depicts the surfaces in direct contact during the injection cycle. To simulate this contact pure penalty contact was employed.

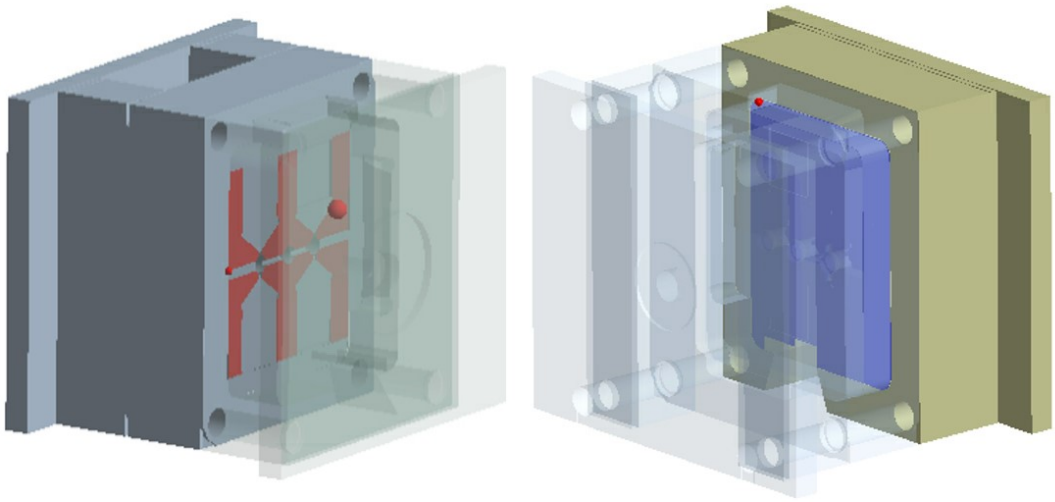

Figure 110 – Core and cavity contact

The clamping force is building up a contact pressure between both sides of the mold to prevent mold opening. In the loadstep 2 the internal load during packing is applied using 3 pressure boundary conditions for the cavities 1, 3 and 4. Figure 111 indicates the cavities subjected to a packing pressure of 40 MPa. In this case, pressure was applied to cavities 1, 3 and 4. The distribution of cavity numbers can be seen in Figure 44. n

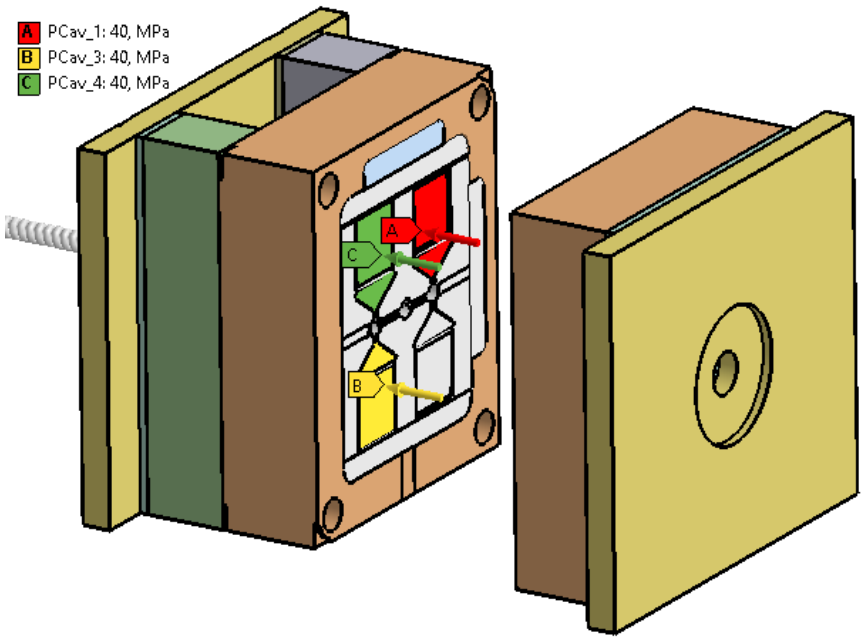

Figure 111 – Packing pressure area

12.4 FEA results clamping phase (Loadstep 1)

During the closing phase, the injection side is compressed against the injection side causing a displacement of about 0.013 mm. Figure 112 shows the greatest and the smallest displacement. The largest displacement is monitored at the clamping plate of the ejection side due to flexibility in the contact zone. A small amount of movement could also be seen in the experiment during clamping even though it was not measured.

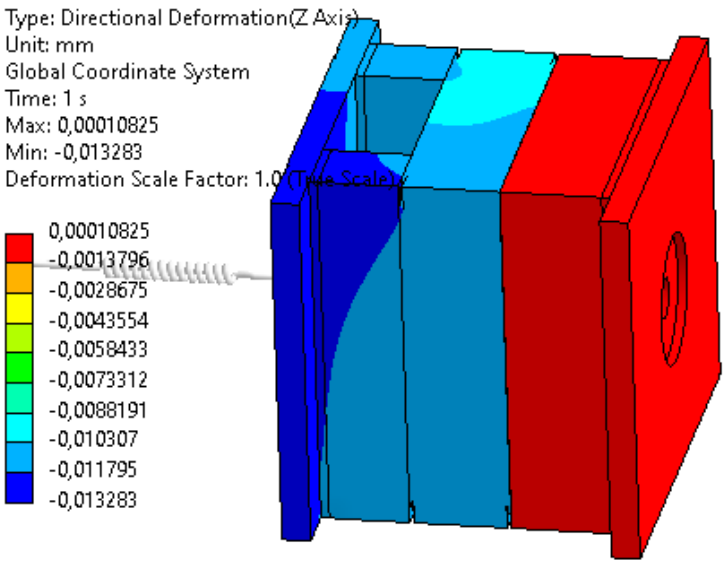

Figure 112 – Mold compressing during closing

Figure 113 displays simulated pressure of the contact between the core and cavity with the highest-pressure value of 31.5 MPa. The pressure level is not critical for steel mold as the maximum allowable pressure could be estimated with P_{max} = 0.8 yield stress.

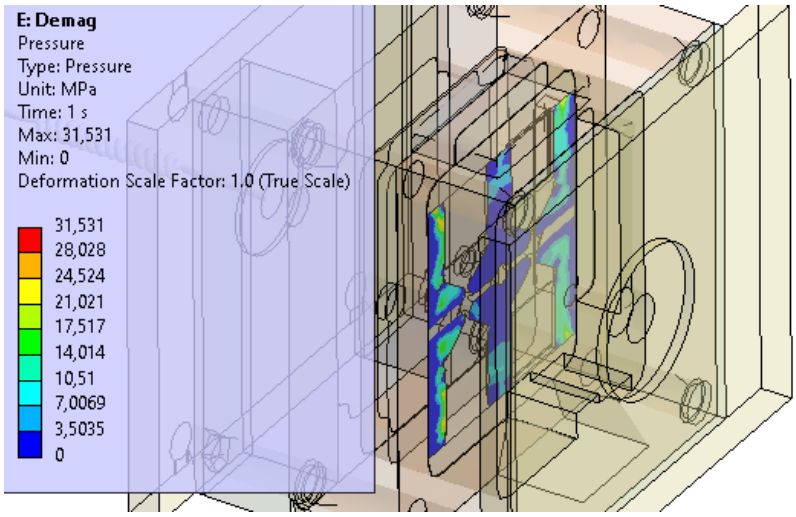

Figure 113 – Pressure between the core and cavity

12.5 Stress results (loadstep ½)

The part discusses the von Mises stress on the injection mold during the injection and packing phase. During these phases, the mold is loaded by the holding force and pressure in the cavity. These two forces act against each other. The stresses due to these loads are very low compared to the maximum stresses of the molding steel. All stresses are below the yield stress proving the behavior is fully elastic. Because the mold must withstand high-cycle numbers, failures occur mainly due to cyclic fatigue. Particularly for long thin cores, fatigue cracks represent a very common problem. Since fatigue occurs at high stress concentrations, sharp edges should be avoided in the design of long thin cores.

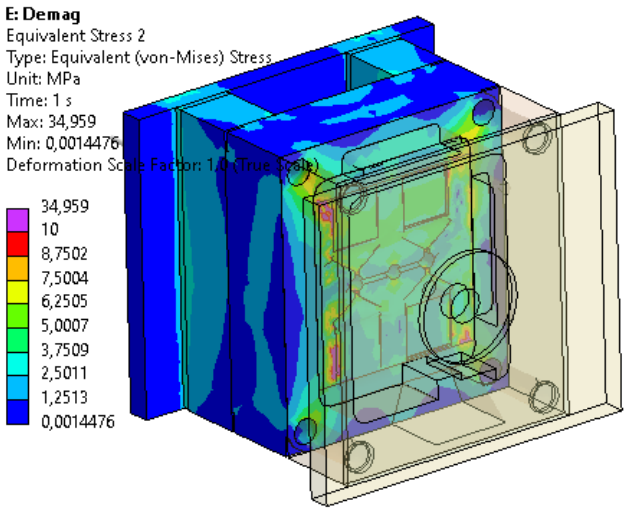

Figure 114 – Equivalent (von-Mises) stress on the ejection side during the clamping phase

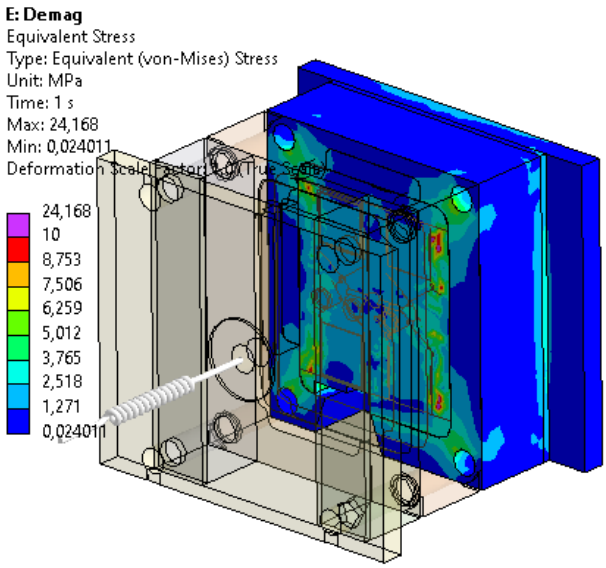

Figure 115 – Equivalent (von-Mises) stress on the injection side during the clamping phase

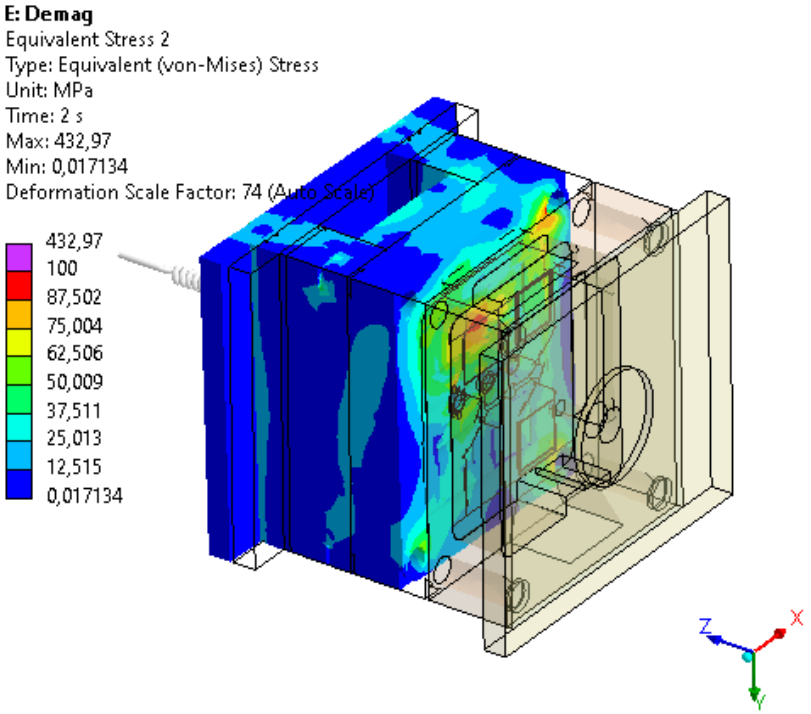

Figure 116 – Equivalent (von-Mises) stress on the ejection side during the packing phase

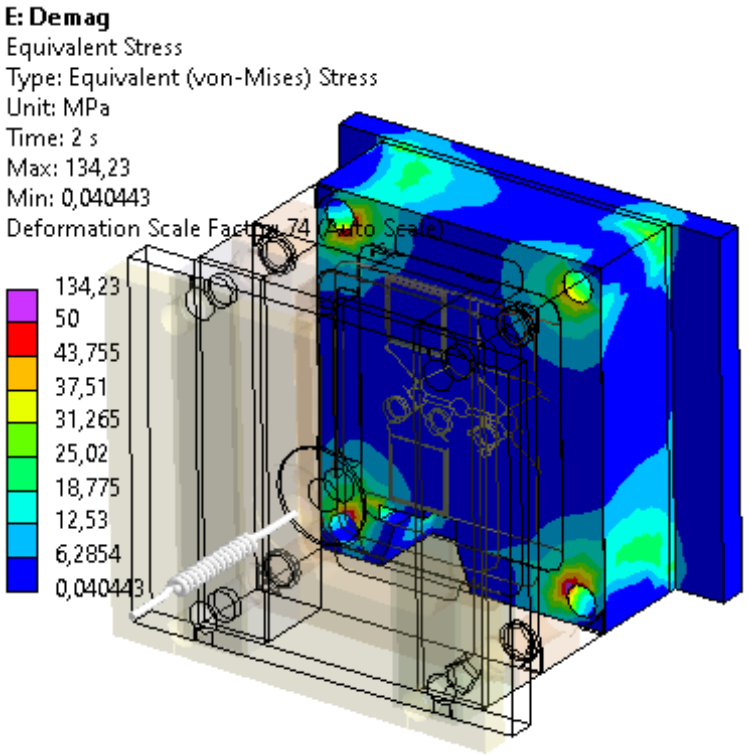

Figure 117 – Equivalent (von-Mises) stress on the injection side during the injection phase

12.6 Mold opening during the injection molding cycle

During the packing phase, high pressure is applied to the mold cavity. A clamping force is used to secure the mold against opening. If this force is exceeded during the packing, the mold tends to open. When the mold opens, burrs occur which affect the final quality of the product. As can be seen in Figure 118 and 119, the mold has been opened throughout the parting plane. Figure 118 shows at which point the mold is displaced (deformed). Figure 119 depicts at which point the mold opening occurs. The mold opening values are displayed on the side where the measuring device was placed during the experiment. The average mold opening on this side is 0.485 mm (Figure 120). In the upper half of the mold, where the two cavities are located, more pressure is applied causing larger mold opening in this area of the parting plane.

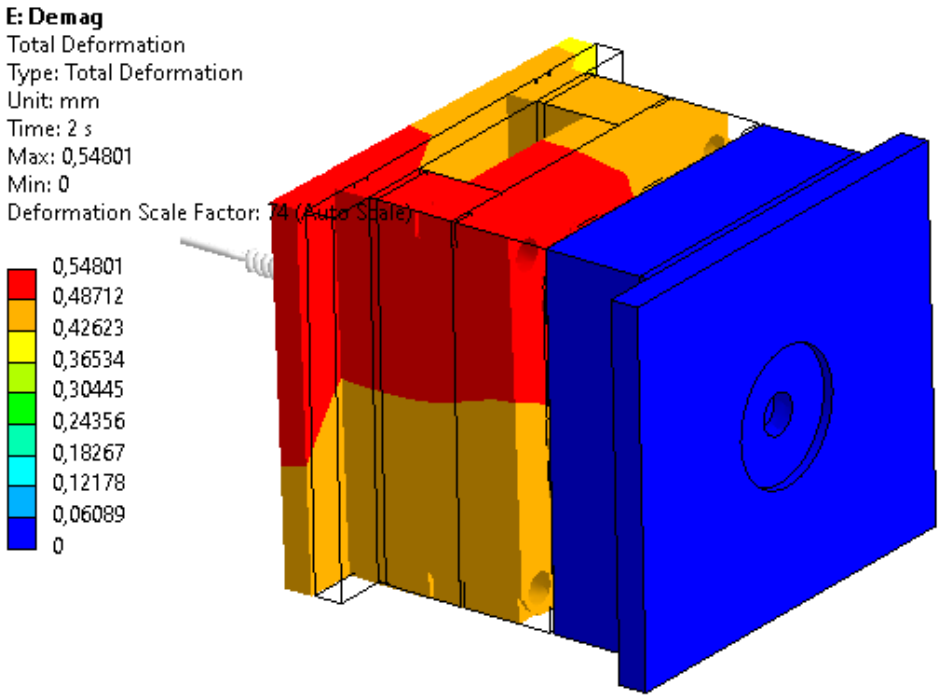

Figure 118 – Total deformation in millimeters

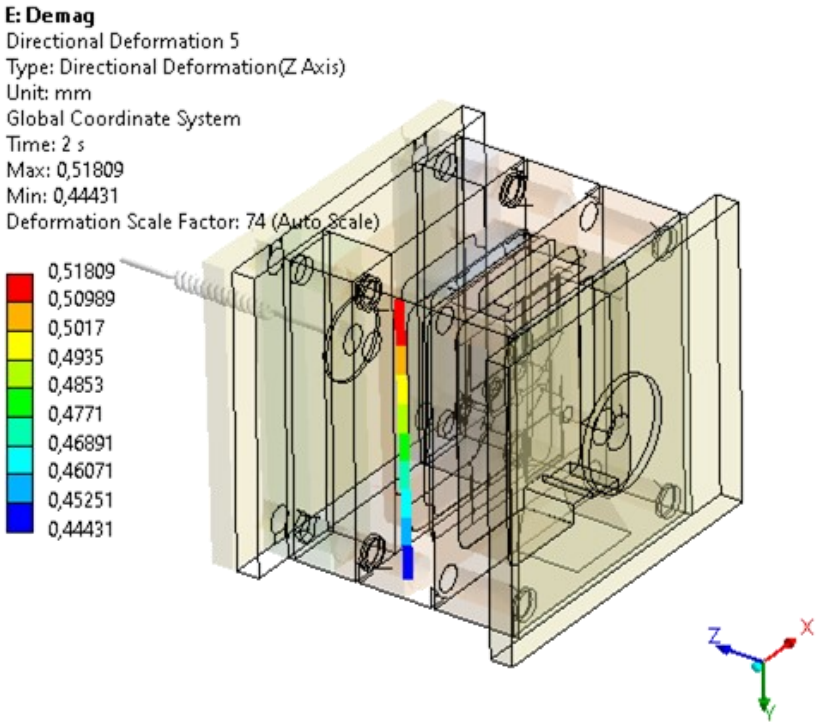

Figure 119 – Mold opening during the injection cycle

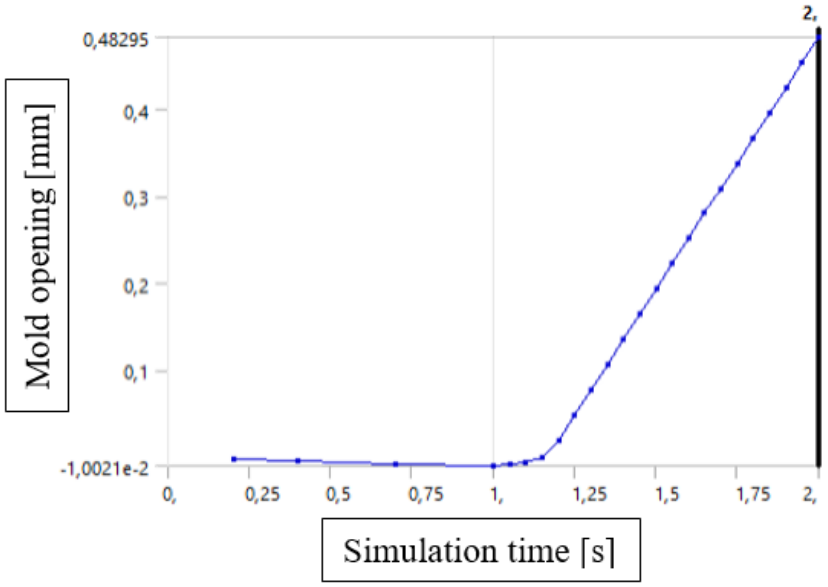

Figure 120 – Direction of deformation (ANSYS)

13 DOE AND FEA COMPARISON OF THE RESULTS

Figures 121 and 122 show a comparison of the results obtained using Demag and Ferromatik injection molding machines with the structural mechanical simulation including the mold opening values. Graphs in Figures 12 and 122 express the dependence of the mold opening on the run order. As can be seen, in most cases the simulation represented a larger mold opening than was actually observed in the experiment. The simulation assumes the ideal conditions while the experiment is influenced by the factors, such as the time of the injection molding machine use, machine wear, and time of the mold use. In simulation run 3, 5 and 7, negative values were recorded due to the pressure of the ejection side on the injection side.

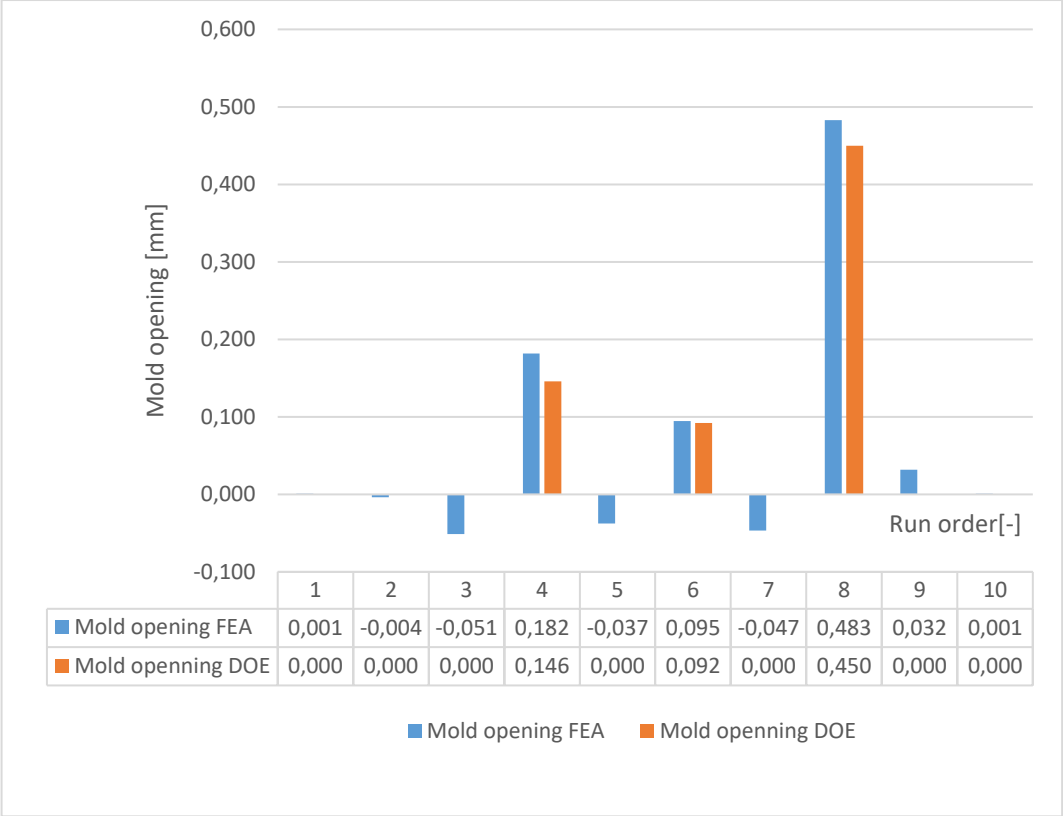

	1	2	3	4	5	6	7	8	9	10
Mold opening FEA	0,001	-0,004	-0,051	0,182	-0,037	0,095	-0,047	0,483	0,032	0,001
Mold openning DOE	0,000	0,000	0,000	0,146	0,000	0,092	0,000	0,450	0,000	0,000

Figure 121 – DOE and FEA mold opening comparison (Demag)

Figure 122 shows larger differences between measured and simulated values. Even though there was almost no opening in simulation run 1 and 2, the mold opened in the parting plane during the experiment. These differences are mainly due to the wear on the Ferromatik injection molding machine which was also shown in Chapter 10.

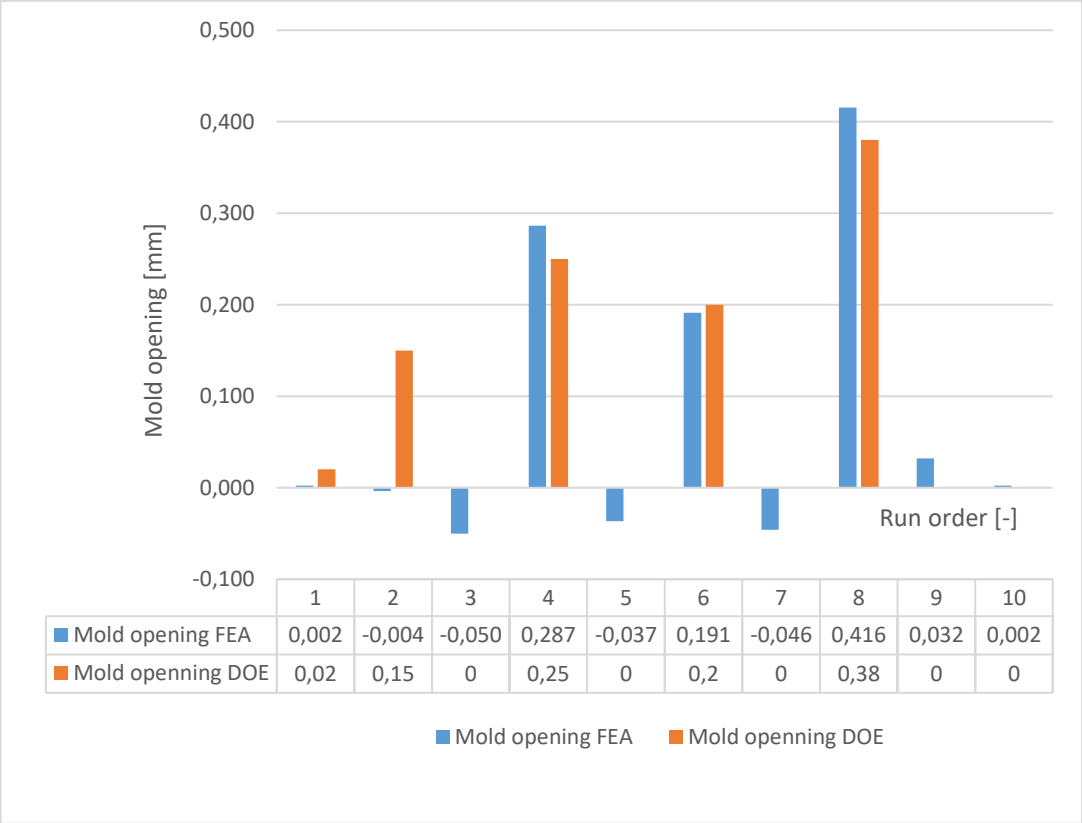

	1	2	3	4	5	6	7	8	9	10
Mold opening FEA	0,002	-0,004	-0,050	0,287	-0,037	0,191	-0,046	0,416	0,032	0,002
Mold openning DOE	0,02	0,15	0	0,25	0	0,2	0	0,38	0	0

Figure 122 – DOE and FEA mold opening comparison (Ferromatik)

14 DEMAG AND FERROMATIK MACHINE STIFFNESS

Figure 123 demonstrates dependence of the machine stiffness on the mold opening. The graph was created using Excel which was also applied to calculate the machine stiffness values. The points in the graph represent the values calculated from runs 4,6 and 8. This calculation was proceeded for both injection molding machines used in the experiment. At these points, the largest mold opening was measured.

Polynomial function was applied to obtain the curve. After the initial decline, the Ferromatik machine curve steeply rose. That shows that Ferromatik machine stiffness is significantly less stable than the Demag machine stiffness.

The stiffness of the injection molding machines can be estimated from DOE results showing the mold opening. By calculating the opening force, see formula 14.1 it was found that for different values of mold opening we get nonlinear behavior, which also causes a non-linear behaviour of the machine stiffness because the opening force is also used in the calculation of the machine stiffness 14.2.

$$\text{Opening force} = \text{Pressure force} - \text{Clamping force} \tag{14.1}$$

$$\text{Machine stiffness} = \frac{\text{Opening force}}{\text{Average of mold opening}} \tag{14.2}$$

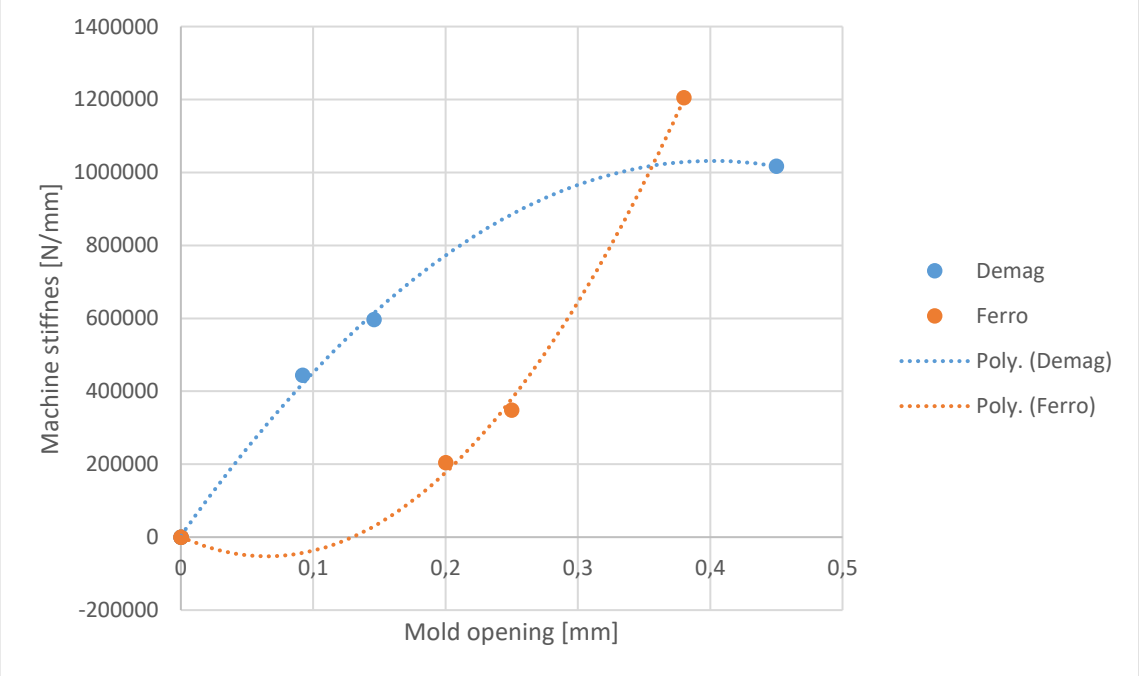

Figure 123 – Demag and Ferromatik machine stiffness

15 DISCUSSION OF RESULTS

The purpose of this thesis was to establish a systematic approach that would apply the information from the initial stages of the injection mold design and save any possible additional repairs and financial costs associated with the injection mold design. To achieve this, it was necessary to compare the systematic approach with the experimental part that confirmed the results obtained from the structural mechanical analysis.

The experimental part examines the mold opening and measures the burrs that occurred after the mold opening. Since these burrs could not be measured using a dimensional device, first, the weight of all parts was determined. Then, the weight of the part without the injection mold opening was compared with the part where the burrs occurred. The weight of the burrs equaled the difference. It was necessary to obtain all the values; however, during testing on the Ferromatik machine it was discovered that it was not appropriate to deal with the weight results during the experimental part. Although the initial idea was to incorporate the mass into the evaluation in MiniTab, it was found later that the results did not correspond to the correct value due to the problems with testing on the Ferromatik machine. As can be seen in Figure 68 and 69, a problem occurred in run 4 and 6 during testing on this machine. It was impossible to repeat this experiment more than once as the molten polymer penetrated into the area of the screws connecting the mold core with plate. This phenomenon did not occur on the Demag machine during the experimental testing. Therefore, it was needed to investigate why this error occurred on one machine and not on the other. Examining available results, the machine stiffness of the injection machine seems to be the main reason of this issue. The Ferromatik machine has been in operation longer than the Demag machine and this caused much of the problem. Nevertheless, the parameters associated with the setup of the machine also play an important role even though the initial basic process parameters were the same.

As no problems occurred during the mold opening measurements, the data obtained in this experiment could be used for the evaluation in MiniTab. Although the experiment was executed with limited process parameters of a clamping force (10 kN, 35 kN and 60 kN) with a combination of packing pressure (100 bar, 250 bar and 400 bar) using one to three cavities, it was possible to identify clearly which machine performed more frequent mold opening and which injection molding machine had less stiffness. Using MiniTab, it was established that the most frequent mold opening occurred during the application of the packing pressure of 400 bar with clamping force of 10 kN and the use of three cavities. In

this experiment, the largest mold opening was expected since the calculation (10.1) showed that the force applied during the packing exceeded the clamping force by several times. Using MiniTab and Excel it was also verified that the Ferromatik machine performed more frequent mold opening which corresponds to the fact it was older than the Demag machine. The evaluation was further determined using a pareto diagram which revealed that the clamping force has the greatest effect on the mold opening during the experiment. It is then followed by packing pressure, machine type and number of cavities. From graphs shown in Figure 73 and 74 can be determined that the combination of the parameters of 35 kN, 250 bar and the use of 2 cavities provides almost no mold opening. This was largely due to the failure to overcome the closing force by the force applied to the mold cavities. A minor opening on the Ferromatik machine was recorded once which may stem from the wear of the machine.

At the beginning of the experimental part, a filling study was used to set all necessary parameters which was then processed using Moldex3D software. The filling studies from the experimental and simulation part were compared and provided almost significantly similar results. They were not precisely the same which might be the consequence of the fact that the simulation does not consider factors, such as the machine wear, injection mold wear, and other factors related to the age. It assumes the ideal conditions. Another reason included the process parameters chosen for the simulation in general terms, whereas for the experimental part they were defined precisely.

In the mechanical simulations, it was necessary to establish the stiffness of the machine that would be used for the calculation. For this purpose, formula 14.2 was applied in the first steps for each experiment in which the mold was opened, then the average machine stiffness of the Ferromatik and Demag machines was obtained from these results. This value was used for the machine stiffness in the structural machine calculation. For the calculation regarding the Demag machine, there were no unexpected issues and the results were very close to the results from the experimental part. However, there was a problem with the calculation on the Ferromatik machine. The results were not in the alignment with the experimental values and therefore, a solution had to be discovered to avoid this problem in the future. After the investigation of the process, it was revealed that using the average stiffness values of the machine (Demag, Ferromatik) for all calculations did not provide correct results. By calculation of the opening we get non-linear behavior which causes non-linear behavior of the machine stiffness. For each calculation, the value gained from the formula 14.2 was

chosen and this step solved the problem on the Ferromatik machine while achieving more accurate results on both machines. The individual values obtained from these simulations including the comparisons are listed in Chapter 13. It can be concluded that in most cases the predicted value of mold opening in the simulation exceeded the experimental value. Yet again, it is due to the fact that the simulation supposes the ideal conditions, whereas the factors, including the machine wear, and mold wear, play a significant role in the experiment. The results showed that according to the simulation, the ejection side was shifted to negative values in some cases. This reflected the pressure of the ejection side on the injection side as section 12.4 explains. On the Ferromatik machine during run 1 and 2 mold opening occurred even though the simulation of these runs estimated that mold opening would not appear. The reason for this opening during the experiment was the level of the wear of the Ferromatik injection molding machine.

Graph in Figure 123 shows that the stiffness of the Demag machine is more stable than the stiffness of the Ferromatik machine. It was established by using polynomial function to obtain the curve by connecting the points calculated from obtaining the stiffness of the machine. The Ferromatik injection molding machine performed a low drop followed by a steep rise of the curve which determines the lower stability and stiffness of the machine than the properties of the Demag machine.

The results obtained in the practical part can be used as a systematic approach to solve issues related to the deformation of parts and burrs during the production. Furthermore, they can also be applied to compare stiffness of different injection molding machines.

CONCLUSION

The master's thesis aims to verify the design of the injection mold using moldflow and mechanical simulations. The theoretical part of the thesis discusses the injection molding. The information and knowledge obtained in the experimental part was further applied in the practical part.

The practical part provides the design of the injection mold for a special part in cooperation with Hirschmann Automotive GmbH and describes individual design ideas. Catia V5 R20 was used to design and work with the injection mold. The mold includes the possibility of altering the multiplicity of the injection mold. The injection mold was applied in the experimental part performed using Demag Intelect 180 – 450 and a Ferromatik Milacron Elektra 155 injection molding machines in Hirschmann Automotive GmbH Rankweil. In the course of the experiment, a filling study was proceeded and the injection mold opening and the part weight per cycle were measured using the measuring equipment obtained from TESA company. The material used for the experiment was RADILON A RV250W 100 NT. Examining the Ferromatik machine, due to large burrs it was impossible to complete experiment 4 and 6 as there was a risk of breaking the injection mold. Therefore, these data could not be applied afterwards. The mold opening data was processed using MiniTab 20 software. It has been determined that the clamping force influenced the mold opening during the injection molding cycle the most, however, the parameters determined prior to the experiment, such as the mold multiplicity and packing pressure, have been found to be significant as well. It could be summarized that all parameters have affected the course of the experiment. Furthermore, the results obtained from the MiniTab 20 clearly show that the Ferromatik injection molding machine performed more frequent mold opening, although the highest measured value was recorded on the Demag machine.

In this thesis, a simulation was created using Moldex 3D and compared with the filling study and the pressure curve from the experimental part. The results from the simulations were not precisely identical as the simulation calculated with the ideal conditions disregarding the factors, such as the mold wear.

ANSYS Mechanical 2021 R1 was employed for the simulations. The simulation results were almost identical to the experimental part in almost all points and the results of the comparison between the experimental and simulation parts can be evaluated as accurate.

The results of this thesis may be used to solve issues related to possible deformations and burrs occurring during the manufacturing processes and to enhance design of injection molds.

BIBLIOGRAPHY

[1] ZHOU, Huamin. Computer modeling for injection molding: simulation, optimization, and control. Hoboken, N.J.: Wiley, [2013]. ISBN 978-0-470-60299-7.

[2] WANG, Maw-Ling, Rong-Yeu CHANG a Chia-Hsiang HSU. Molding simulation: theory and practice. Cincinnati: Hanser Publishers/Munich Hanser Publications, [2018]. ISBN 978-1-56990-619-4.

[3] KAZMER, David. Injection mold design engineering. 2nd edition. Munich: Hanser Publishers, [2016]. ISBN 978-1-56990-570-8.

[4] -, M., By, -, Magazine.admin, & here, P. enter your name. (2018, April 22). 3 basic steps of the injection molding process " Injection Moulding World Magazine. Injection Moulding World Magazine.Retrieved March 2, 2022, from https://injectionmouldingworld.com/3-basic-steps-of-the-injection-molding-process/

[5] KG, A. R. B. U. R. G. G. H. + C. (n.d.). Search. ARBURG. Retrieved March 2, 2022, from https://www.arburg.com/en/search/?tx_solr%5Bq%5D=control%2Bsystem

[6] Group®, T. R. (n.d.). Hydraulic, electric, and hybrid plastic injection molding: Which process is right for you? The Rodon Group. Retrieved March 2, 2022, from https://www.rodongroup.com/blog/hydraulic-electric-and-hybrid-plastic-injection-molding-which-process-is-right-for-you

[7] KG, A. R. B. U. R. G. G. H. + C. (n.d.). Hydraulic Machines. ARBURG. Retrieved March 2, 2022, from https://www.arburg.com/en/products-and-services/injection-moulding/injection-moulding-machines/hydraulic-machines/

[8] KG, A. R. B. U. R. G. G. H. + C. (n.d.). Electric Machines. ARBURG. Retrieved March 2, 2022, from https://www.arburg.com/us/us/products-and-services/injection-molding/injection-molding-machines/electric-machines/

[9] Packaging. Plastix World. (n.d.). Retrieved March 2, 2022, from https://www.plastix-world.com/arburgs-challenging-solutions/packaging/

[10] Li, H. L., & Jia, Z. X. (2011). Study of the structural characteristics of mold for precise injection molding. Advanced Materials Research, 291-294, 610–613. https://doi.org/10.4028/www.scientific.net/amr.291-294.610

[11] DANGEL, Rainer. Injection moulds for beginners. Carl Hanser Verlag, Munich 2016: Hanser Publications, 2016. ISBN 978-1-56990-632-3.

[12] CRAWFORD, R. J. a James L. THRONE. Rotational molding technology. Norwich, N.Y.: Plastics Design Library/William Andrew Pub., c2002. ISBN 1-8z84207-85-5.

[13] REES, Herbert. Understanding injection mold design. Cincinnati, OH: Hanser Gardner Publications, 2001. ISBN 1569903115.

[14] MICHAELI, Walter. Training in injection molding: a text- and workbook. 2nd ed. Cincinnati: Hanser Gardner Publications, c2001. ISBN 1-56990-302-6.

[15] GASTROW, Hans a P. UNGER. Gastrow injection molds: 130 proven designs. 4th ed. Cincinnati: Hanser Gardner Publications, c2006. ISBN 3-446-40592-5.

[16] PAVLINA, E.J. a C.J. VAN TYNE. Correlation of Yield Strength and Tensile Strength with Hardness for Steels. Journal of Materials Engineering and Performance [online]. 2008, 17(6), 888-893 [cit. 2022-03-15]. ISSN 1059-9495. Available from: doi:10.1007/s11665-008-9225-5

[17] Bahri, A., Ellouz, M., Klöcker, M., Kordisch, T., & Elleuch, K. (2019). Brinell indentation behavior of the stainless steel X2CRNI18-9: Modeling and experiments. International Journal of Mechanical Sciences, 163, 105142. https://doi.org/10.1016/j.ijmecsci.2019.105142

[18] Tofail, S. A. M., Koumoulos, E. P., Bandyopadhyay, A., Bose, S., O'Donoghue, L., & Charitidis, C. (2018). Additive Manufacturing: Scientific and technological challenges, market uptake and opportunities. Materials Today, 21(1), 22–37. https://doi.org/10.1016/j.mattod.2017.07.001

[19] ASHBY, M. F. Materials selection in mechanical design. 4th ed. Amsterdam: Butterworth-Heinemann, c2011. ISBN 978-1-85617-663-7.

[20] Zhang, S., Wei, C., Yang, L., Lv, J., Zhang, H., Shi, Z., Zhang, X., & Ma, M. (2022). Formation ability, thermal stability, and mechanical properties of the ZR50CU34AL8AG8 amorphous alloys prepared by different mold materials. Materials Science and Engineering: A, 840, 142978. https://doi.org/10.1016/j.msea.2022.142978

[21] Mold makers and injection molders: 20 years of manufacturing experience. To be your molds team in China! (2021, October 8). Retrieved March 7, 2022, from https://www.spark-mould.com/

[22] BEAUMONT, John P. Runner and Gating Design Handbook: Tools for Seccessfull injection Molding. 3rd Edition. Munich: Hanser, 2019. ISBN 978-1-56990-591-3.

[23] CAMPO, E.Alfredo. The Complete Part Design Handbook: For Injection Molding of Thermoplastics. Munich: Hanser, 2006. ISBN 978-3-446-40309-3.

[24] MALLOY, Robert A. Plastic part design for injection molding: an introduction. 2nd ed. Cincinnati, Ohio: Distributed in the USA and in Canada by Hanser Publications, 2011. ISBN 978-1-56990-436-7.

[25] YANG, Yi, Xi CHEN, Ningyun LU a Furong GAO. Injection molding process control, monitoring, and optimization. Cincinnati: Hanser Publishers, [2017]. ISBN 978-1-56990-592-0.

[26] KENNEDY, Peter K. and Rong ZHENG. Flow Analysis of Injection Molds. 2nd Edition. Munich: Hanser Verlag, 2013. ISBN 978-1-56990-512-8.

[27] SHOEMAKER, Jay. Moldflow Design Guide: A Resource for Plastic Engineers. Framingham, Massachusetts, USA: Carl Hanser Verlag, 2006. ISBN 978-3-446-40640-7.

[28] MALKIN, Alexander Ya. a Avraam I. ISAYEV. Rheology: Concepts, Methods. and Application. ISBN 978-1895198331.

[29] Kazmer, D. O., Nageri, R., Kudchakar, V., Fan, B., & Gao, R. (2006). Validation of three on-line flow simulations for injection molding. Polymer Engineering & Science, 46(3), 274–288. https://doi.org/10.1002/pen.20463

[30] Guo, Z. Z., Li, Y., & Zhao, X. J. (2011). The analysis of core shift in injection mold and its optimization based on Ami. Advanced Materials Research, 189-193, 2879–2883. https://doi.org/10.4028/www.scientific.net/amr.189-193.2879

[31] Choi, J. H., Pyo, B. G., Tae, J. S., Park, H. P., & Rhee, B. O. (2014). Structural analysis examining the mold deformation behavior for the detection of the flash in the injection mold. International Polymer Processing, 29(4), 489–494. https://doi.org/10.3139/217.2891

[32] GĄSKA, D. a C. PYPNO. STRENGTH AND ELASTIC STABILITY OF CRANES IN ASPECT OF NEW AND OLD DESIGN STANDARDS. Mechanics [online]. 2011, 17(3), 226-231 [cit. 2022-04-07]. ISSN 1392-1207. Available from: doi: 10.5755/j01.mech.17.3.495

[33] Polyamide, high performance polymers, Advanced Textile Solutions. Polyamide, high performance polymers, advanced textile solutions. (n.d.). Retrieved April 11, 2022, from https://www.radicigroup.com/en

[34] Welcome to moldex3d support. Moldex3D Support. (n.d.). Retrieved April 26, 2022, from http://support.moldex3d.com/r15/

[35] LERMA VALERO, José R. Plastics injection molding: scientific molding, recommendations, and best practices. Munich: Hanser publications, [2020], xxiii, 400 s. ISBN 978-1-56990-689-7.

[36] CHEN, Shia-Chung a Lih-Sheng TURNG, ed. Advanced injection molding technologies. Munich: Hanser Publishers, [2019], xv, 426 s. Progress in polymer processing (PPP) series. ISBN 9781569906033.

[37] KERKSTRA, Randy a Steve BRAMMER. Injection molding advanced troubleshooting guide. Munich: Hanser Publishers, [2018], xx, 491 s. ISBN 9781569906453.

[38] KULKARNI, Suhas. Robust process development and scientific molding: theory and practice. Munich: Hanser Publications, c2010, xv, 256 s. ISBN 9781569905012.

[39] PÖTSCH, Gerd a Walter MICHAELI. Injection molding: an introduction. 2nd ed. Munich: Carl Hanser Publishers, c2008, x, 246 s. ISBN 9781569904190.

[40] LAWRENCE, Kent L. ANSYS tutorial release 2020R1: structural & thermal analysis using the ANSYS mechanical APDL 2020R1 environment. Mission, KS: SDC Publications, [2020], vi, 180 s. ISBN 978-1-63057-394-2

LIST OF ABBREVIATIONS

FEA	Finite element analysis
F	Force
D	Diameter
µm	Mikrometer
MPa	Megapascal
3D	Three-dimension
τ	Shear stress
η	Viscosity
$\dot{\gamma}$	Shear rate
h	Height between stationary and moving plate
v	speed of moving plate
CAE	Computer aided engineering
s	Second
°C	Celsia
GPa	Gigapascal
%	Percent
∅	Diameter
bar	Metric unit of pressure
kN	Kilos of newton
mm^2	Square millimeter
cm^3/s	Cubic centimeter per second
N/mm	Newton per millimeter
PA	Polyamide 66
DOE	Design of experiment
p_{max}	Maximum pressure

LIST OF FIGURES

LIST OF TABLES

APPENDICES

Appendix A: Mold Material Properties

- A I: Nonferrous Metals [3].

Mold material	Al 7075-T6	Al QC-10 Alloy	Cu 17200
Description	Aircraft grade aluminum alloy with high strength and corrosion resistance	Aluminum alloy developed for molds with higher strength, hardness, and conductivity	Beryllium-free copper alloy with high strength and thermal conductivity
Cost ($/kg)	26.9	20.7	61.2
Cost ($/cm^3)	0.076	0.058	0.531
Ultimate strength (MPa)	565	579	689
Modulus (MPa)	71,000	70,000	120,000
Yield stress (MPa)	421	525	517
Fatigue limit stress (MPa)	149	166	290
Hardness, Brinell (HB)	150	160	210
Feed per tooth (mm)	0.0762	0.0762	0.0762
Cutting speed (m/h)	23,600	23,600	3,600
Volume machine rate (m^3/h)	0.0091	0.0091	0.0014
Area machine rate (m^2/h)	0.225	0.225	0.034
Thermal expansion (°m/m°C)	24	24.7	18
Thermal conductivity (W/m°C)	130	160	259
Specific heat (J/kg°C)	960	879	506
Density (kg/m^3)	2,810	2,850	8,690
Thermal diffusivity (m^2/s)	4.82E-05	6.39E-05	5.89E-05

- A II: Common Mold Steels [3].

Mold material	1045	4140	P20
Description	High strength carbon steel, low cost but poor corrosion and wear resistance	Chrome alloyed steel with good fatigue, abrasion, and impact resistance	Common mold steel with good fatigue, abrasion, and impact resistance
Cost ($/kg)	4.8	10.3	11.6
Cost ($/m^3)	0.037	0.081	0.091
Ultimate strength (MPa)	752	778	965
Modulus (MPa)	207,000	200,000	205,000
Yield stress (MPa)	647	669	830
Fatigue limit stress (MPa)	291	412	456
Hardness, Brinell	225	259	300
Feed per tooth (mm)	0.0762	0.0508	0.0508
Cutting speed (m/h)	5600	4700	3800
Volume machine rate (m^3/h)	0.0021	0.0012	0.001
Area machine rate (m^2/h)	0.053	0.03	0.024
Thermal expansion (°m/m°C)	12.2	12.2	12.8
Thermal conductivity (W/m°C)	49.8	42.7	32
Specific heat (J/kg°C)	515	523	500
Density (kg/m^3)	7850	7850	7820
Thermal diffusivity (m^2/s)	1.23E-05	1.04E-05	8.18E-06

- A III: Other Mold Steels [3]

Mold material	A6	D2	H13	S7	SS420
Description	Heat treatable to be very hard with good wear resistance and fatigue life	High carbon/chrome steel for wear and abrasion resistance	Heavily alloyed, hard steel with excellent temperature and wear resistance	Excellent toughness and high strength but lower wear resistance	Excellent polishability and corrosion resistance with good hardness
Cost ($/kg)	20.6	19.7	46.7	25.5	63.6
Cost ($/m^3)	0.165	0.151	0.364	0.199	0.496
Ultimate strength (MPa)	2380	2200	1990	1620	655
Modulus (MPa)	203,000	210,000	210,000	207,000	207,000
Yield stress (MPa)	2100	1929	1650	1380	345
Fatigue limit stress (MPa)	834	755	760	528	190
Hardness, Brinell	650	685	528	369	195
Feed per tooth (mm)	0.0508	0.0508	0.0508	0.0508	0.0508
Cutting speed (m/h)	2900	2700	700	3900	5000
Volume machine rate (m^3/h)	0.0007	0.0007	0.0002	0.001	0.0013
Area machine rate (m^2/h)	0.018	0.017	0.004	0.025	0.032
Thermal expansion (°m/m°C)	11.8	11.8	11.5	12.1	10.8
Thermal conductivity (W/m°C)	27	21	24.3	29	24.9
Specific heat (J/kg°C)	460	460	460	460	460
Density (kg/m^3)	8030	7670	7800	7810	7800
Thermal diffusivity (m^2/s)	7.31E-06	5.95E-06	6.77E-06	8.07E-06	6.94E-06